CHARACTERIZATION OF PUTATIVE EFFECTOR PROTEINS FOR THE SMALL GTPASE, CDC42, DURING *DROSOPHILA* DEVELOPMENT

by

Baharak Zahedi
B.Sc., Simon Fraser University, 1999

THESIS
SUBMITTED IN PARTIAL FULFILLMENT OF
THE REQUIREMENTS FOR THE DEGREE OF

DOCTOR OF PHILOSOPHY

In the Department
of
Molecular Biology and Biochemistry

SIMON FRASER UNIVERSITY

Fall 2005

APPROVAL

Name: **Baharak Zahedi**

Degree: **Doctor of Philosophy**

Title of Thesis: **Characterization of Putative Effector Proteins for the Small GTPase, Cdc42, during *Drosophila* Development**

Examining Committee:

Chair: **Dr. Bruce Brandhorst, Professor**
Department of Molecular Biology and Biochemistry

Dr. Nicholas Harden, Associate Professor
Senior Supervisor
Department of Molecular Biology and Biochemistry

Dr. Esther Verheyen, Associate Professor
Supervisory Committee member
Department of Molecular Biology and Biochemistry

Dr. David Baillie, Professor
Supervisory Committee member
Department of Molecular Biology and Biochemistry

Dr. Nancy Hawkins, Assistant Professor
Internal Examiner
Department of Molecular Biology and Biochemistry

Dr. Susan Parkhurst, Senior Scientist
External Examiner
Fred Hutchinson Cancer Research Centre
Seattle, Washington, U.S.A.

Date Defended/Approved: November 22, 2005

ABSTRACT

The Rho subfamily GTPases (Rho, Rac, Cdc42) are small GTP-binding proteins that act as molecular switches, controlling many cellular functions. These GTPases fluctuate between a GTP-bound 'on' state and a GDP-bound 'off' state, and convey signals into the cell. Cdc42 has been implicated in a diverse array of processes, including vesicular trafficking, gene expression, formation of F-actin based membrane protrusions (filopodia), cell polarity, apoptosis, and cell cycle regulation.

Model systems such as *Drosophila* have furthered the understanding of the functional roles of Cdc42 in epithelial morphogenesis, establishment of cell polarity, and neuronal path finding and development. The use of model systems allows the study of molecular processes at levels not possible in cell culture. These include genetic approaches and the study of gene function at the level of tissue morphogenesis. Three putative downstream effectors for Cdc42, originally identified in mammals, were studied in *Drosophila*. DCIP4, a putative cytoskeletal regulator, is expressed in a dynamic pattern throughout development. DCIP4 is required during oogenesis and functions with Cdc42 in crossvein development. The two members of the *Drosophila* ACK non-receptor tyrosine kinase family, DACK and DPR2, are both expressed at the leading edge epidermis during the embryonic process of dorsal closure. DACK functions downstream of Cdc42 in dorsal closure, but is not required for JNK signalling during embryonic development. However, DACK may modulate signalling downstream of, or in parallel to, the Decapentaplegic pathway in this process.

This thesis is dedicated

to my family,

my friends, and my lab,

for giving me the motivation to go on

when times got rough!

ACKNOWLEDGEMENTS

There are many people that need to be acknowledged for help with the completion of this thesis. First and foremost, I would like to thank my senior supervisor for all of his encouragement, words of wisdom, and advice on many different topics. I am very glad that I stayed at SFU to do my PhD as I do not think I could have found a better supervisor at any other school. I would like to thank my lab mates, Kaiping Sem who started the ACK family project, Caillin Langmann, who taught me everything I needed to know in my first two years of grad school and who continues to be supportive from across the country, Justina Sanny, for keeping me sane (and crazy!), for her help in training me, supporting me, watching out for me, and of course for producing our transgenic flies, as well, embryonic RNAis and RNA *in situs* that were not shown in this thesis. You truly are the sister I never had! Ryan Conder for his, support, extreme and endless generosity, and for teaching me how to use the confocal microscope. I could not have asked for a better lab mate. I owe a great amount of thanks to an incredible research assistant, Meena Mahey, who has been a tremendous amount of help this past year with everything in the lab, but mainly with ovary dissection and characterization of *PBc02472*. I would like to thank my lab mate Barton Xu for his help on generating the DACK mutants and for his help on characterizing the DACK and DPR2 mutants, Weiping Shen, Simon Wang and Stephanie Vlachos for their continuing help, kindness and support.

I was lucky to be an honourary member of another lab during my PhD, the Verheyen lab, who strongly supported me and helped me extensively with ideas and

experiments. Specifically I would like to thank, Esther Verheyen, who I refer to as my other supervisor. Thank you for all of your support, help with my projects, and advice on being in science, throughout the years. I would like to thank Wendy Lee for taking the time to always find me anything I needed in her lab, helping me with difficult crossing schemes, and for going out of her way to make sure she is giving me the correct information. I would also like to thank Arial Zeng for her generosity in training me in cell culture and tissue dissections, as well for general, helpful discussions about research. I would like to thank Brian Andrews for helpful ideas and discussions and Sheila Andrews for providing us with a *dpp in situ* probe many years ago (!).

I would like to thank all of the undergraduates who have aided in the progression of this thesis, in particular Dan Jover who helped with the ACK family project, Stephanie Lamos, Rob Hollebacken and Bonny Tam who worked on both the ACK and the DCIP4 projects. I would like to especially thank all of the undergrads who worked on the deficiency screen, unfortunately there are too many of you to mention here!

Finally, there have been several people who have provided reagents, and advice on experiments and have been kind to allow me to use their equipment. In particular, I would like to thank, the Parkhurst lab, especially Craig and Susan for providing me with so much guidance and for training us in injections, Dr. Baillie for his advice, guidance, and for being a great and helpful thesis advisory member, the Hawkins/Beh lab, especially Nancy, Chris, Gabe, and my fly girl, Meena Roh, for advice and reagents, Muneer and Victor from the Leroux lab, the Scott lab, the Honda lab, Dr. Bechenbach for help with sequence alignments, and the Sen lab. Finally I would like to thank all of my friends and my fly girls (Arial, Justina, Meena, and Wendy) for all of their support.

TABLE OF CONTENTS

LIST OF FIGURES

LIST OF TABLES

1 INTRODUCTION

1.1 The Rho subfamily of Ras-related small GTPases and their regulators

The Rho subfamily is part of the large family of Ras-related small GTPases. Although there are over 20 members of this subfamily to date, the original and best characterized members are Rho, Rac and Cdc42. These proteins are of low molecular weights, ranging between 20-30 KDa in size, and contain a ~13 amino acid alpha helical domain that distinguishes them from Ras GTPases (Johnson, 1999).

Rho GTPases have the ability to bind to and hydrolyse GTP and this characteristic controls their activation states. Rho proteins are active when bound to GTP and become inactive once they hydrolyse this GTP into GDP. This "on"/"off" state is directly regulated by at least three different types of protein. First, proteins called GTPase Activating Proteins (GAPs) stimulate the relatively slow intrinsic GTPase activity of the Rho proteins to hydrolyse their bound GTP and thus become inactive. Second, Guanine nucleotide Exchange Factors (GEFs) bind to inactive Rho proteins and induce the exchange of GDP for GTP to activate the GTPase. And third, Guanine nucleotide Dissociation Inhibitors (GDIs) act to lock the GTPase in either its active or inactive state by inhibiting the exchange of GDP or GTP (Johnson, 1999). Although very little is known about GDIs in general, several studies have provided insight on how GAP and GEF proteins function to regulate GTPases.

Rho GAP proteins regulate Rho GTPases through the RhoGAP domain. The RhoGAP domain interacts with the two switch regions, switch I and II, of Rho GTPases. These regions constitute the Rho GTP-binding pocket. Interaction of the RhoGAP domain with these regions restricts the freedom of a water molecule required for GTP hydrolysis and thus may reduce the energy barrier needed for hydrolysing GTP (Moon and Zheng, 2003).

The second family of proteins that regulate Rho GTPases, GEFs, can catalyse the exchange of GDP for GTP within Rho proteins by stabilizing or promoting a nucleotide-free state. This leaves the nucleotide-binding pocket, the switch regions, completely solvent-exposed. As GTP is found at substantially higher concentrations than GDP within the cell, another GTP molecule is then loaded into the switch regions. Binding of GTP to the Rho proteins then causes further conformational changes that leads to dissociation of the GEF-GTPase complex (Rossman et al., 2005).

1.2 The Rho GTPase, Cdc42

Intensive efforts have been made to elucidate the cellular functions of Rho GTPases, including Cdc42. Much of the work on Cdc42 has been done in cultured mammalian cells with the use of constitutively active (CA) or dominant negative (DN) versions of this protein (Van Aelst and D'Souza-Schorey, 1997). Numerous studies using these constructs have demonstrated that Cdc42 is required for activation of cellular signals and for regulation of the actin cytoskeleton (Van Aelst and D'Souza-Schorey, 1997); (Johnson, 1999). In particular, Cdc42 can stimulate the formation of finger-like protrusions of the cell membrane, referred to as filopodia, at the leading edge of a migrating cell (Johnson, 1999). Filopodia formation is dependent on the formation of

long filamentous actin (F-actin) structures under the plasma membrane. In order to form such structures, Cdc42 relies on downstream effector proteins that directly regulate F-actin formation. Cdc42-mediated filopodia formation also requires other signalling components that lead to activation or expression of components required for regulation of the cytoskeleton (Johnson, 1999). Though it is not clear in each case, how, or even if, Cdc42 activation of a given pathway is directly linked to Cdc42-mediated regulation of the cytoskeleton, the mechanism or components required for Cdc42-mediated F-actin formation are known. Actin nucleation downstream of Cdc42 requires Cdc42 to bind to and activate a downstream effector protein called the Wiskott-Aldrich Syndrome Protein (WASP). Active WASP then recruits globular actin (G-actin), and a complex of actin nucleating proteins known as the Arp2/3 complex, to sites of filament assembly or branching on a previously existing actin filament-the mother filament (Carlier et al., 2003). A new daughter filament is then formed in the presence of G-actin from the pre-existing mother branch.

WASP binds to active or GTP-bound Cdc42 via a Cdc42 and Rac Interacting and Binding (CRIB) domain (Burbelo et al., 1995). Upon binding to Cdc42, WASP undergoes a conformational change that relieves the protein from an autoinhibited state (Pufall and Graves, 2002). The once-hindered domains within the WASP protein sequence become solvent-exposed and allow for actin nucleation to take place. WASP is not the only CRIB-containing Cdc42 effector protein. Members of the non-receptor serine/threonine p21-activated kinase (PAK) and the tyrosine activated Cdc42-associated tyrosine kinase (ACK) families also interact with Cdc42 via a CRIB domain. Similar to WASP, some PAK family members have been shown to be released from autoinhibition

by Cdc42 (Pufall and Graves, 2002). However, this has not been shown for any member of the ACK family to date.

1.2.1 The ACK family of non-receptor tyrosine kinases

The ACK family of non-receptor tyrosine kinases is comprised of four mammalian family members, ACK1, ACK2, Kos1, and TNK1 (Sem et al., 2002). There is also one *C. elegans* family member, ARK-1, and two *Drosophila* ACKs, DACK and DPR2 (Sem et al., 2002). Not all of these family members directly bind to Cdc42. In particular, DACK and TNK-1 lack CRIB domains and thus may not bind directly to Cdc42 (Sem et al., 2002). Very little is known about the cellular functions of this kinase family. However, a few key studies have implicated members of this family in both integrin signalling and clathrin-mediated endocytosis of the Epidermal Growth Factor Receptor (EGFR) (Yang et al., 2001b); (Lin et al., 2002).

Studies performed on ACK2 revealed that ACK tyrosine kinase activity was stimulated by cell attachment to plates coated with fibronectin or polylysine. This stimulation of ACK2 kinase activity was in part mediated by integrin β_1. ACK2 co-immunoprecipitates with the integrin β_1 complex (Yang et al., 1999). As this complex is a part of a large group of proteins that give rise to the focal adhesion (FA) complexes, which are responsible for the docking and maintenance of actin stress fibres, ACK2 may have a regulatory role in the assembly or disassembly of FA complexes. To further support this hypothesis, ACK2 was shown to co-immunoprecipitate with the FA proteins vinculin and the integrin-associated protein, talin. Also, cells expressing ACK2 showed loss of vinculin from FAs and consistently inhibited activation of the Focal Adhesion Kinase (FAK). It was hypothesized that ACK2 binds to integrin and/or vinculin and

talin, leading to a change in FAK activity and cytoskeletal alterations that lead to cellular extentions (Yang et al., 2001a). Activation of ACK2 tyrosine kinase activity was then proposed to lead to FA disassembly and the dissolution of acin stress fibres, mediated by the phosphorylation of a focal contact or of cytoskeletal-associated components (Yang et al., 2001a)

Integrins and focal adhesion assembly are known to be required for invasion and uptake of bacterial pathogens by the host cell. The process of invasion involves the pathogen's induced uptake of itself into the host cell, and therefore manipulation of the host cell endocytic machinery. Interestingly, in addition to ACK2's association with Focal adhesion complexes, both ACK1 and ACK2 directly bind to the clathrin heavy chain, a component of the clathrin coat that encapsulates forming vesicles (Teo et al., 2001); (Yang et al., 2001b). Overexpression of ACK seemed to enhance clathrin coat formation suggesting that ACK overexpression results in an increase in endocytosis, possibly through stablilization of the clathrin coat (Lin et al., 2002; Yang et al., 2001b).

One function for ACK2-mediated endocytosis may be to regulate EGFR levels at the cell surface (Lin et al., 2002). ACK2 accomplishes this with the aid of another protein required for endocytosis, Sorting Nexin 9 (SH3PX1). ACK2, SH3PX1 and clathrin heavy chain form a complex and promote the uptake of EGFR, leading to down regulation of EFGR from the cell surface. Interestingly, this may be a negative feedback loop, as EGF stimulation activates ACK2 in a Cdc42-dependent manner; ACK2, in turn, binds to and phosphorylates SH3PX1 (Lin et al., 2002). The *Drosophila* ACK, DACK, has also been shown to bind to and phosphorylate the *Drosophila* homologue of

SH3PX1, DSH3PX1 (Worby et al., 2002), implying that the role of ACKs in EGFR recycling or endocytosis might be conserved.

Aside from CRIB-containing Cdc42 effector proteins such as the ACKs, there is also an emerging group of proteins that bind to Cdc42 with another GTPase effector domain, the HR1 domain. One member of this protein family is the Cdc42 Interacting Protein 4 (CIP4). Interestingly, CIP4 belongs to a larger family of proteins, the Pombe Cdc15 Homology (PCH) family, in which only certain members contain an HR1 domain and hence act as effectors for GTPases such as Cdc42.

1.2.2 Cdc42 interacting protein 4 (CIP4) is a member of the *Pombe* Cdc15 Homology (PCH) family of proteins

The first mammalian CIP4 protein was isolated in a yeast two hybrid screen for interactors of GTP-bound Cdc42 (Aspenstrom, 1997). The Cdc42 construct used in the screen, Cdc42L61, contained a Gln to Leu substitution in the GTP binding and hydrolysis domain and results in a decrease in the level of intrinsic Cdc42 GTPase activity. This mutation thereby generates a constitutively active protein that remains bound to GTP (Johnson, 1999). CIP4-related proteins make up a unique group of Cdc42 effectors, in that they bind to Cdc42 via a PRK1/PNK homology region 1 (HR1) domain. HR1 domains, also known as Rho Effector Motifs (REMs), were first characterized as the PRK1/PKN effector domain for Rho binding (Flynn et al., 1998). The CIP4 HR1 domain was the first HR1 domain shown to bind Cdc42 (Aspenstrom, 1997).

Besides an HR1 domain, CIP4 also contains an N-terminal Fer/CIP4 Homology (FCH) domain, implicated in microtubule binding (Fankhauser et al., 1995; Tian et al., 2000), a coiled-coil region that can result in self assembly or oligomerization (Kessels

and Qualmann, 2004), proline-glutamic acid-serine-threonine rich (PEST) sequences, characterised as motifs that are recognized by the degradation machinery (Blondel et al., 2005; Rechsteiner and Rogers, 1996), and a C-terminal Src Homology 3 (SH3) domain shown to interact with several proline-rich domain-containing proteins such as WASP and Huntingtin (Holbert et al., 2003; Tian et al., 2000). This arrangement of domains places CIP4 into the Pombe Cdc15 Homology (PCH) family of proteins (Lippincott and Li, 2000).

PCH family proteins bear greater resemblance in the organization of their predicted structural domains than they do at the level of their primary sequence (Lippincott and Li, 2000). Similar to CIP4, most PCH family proteins contain an FCH domain, one or two coiled-coil domains close to their amino terminus, one or two SH3 domains at their carboxyl terminus, and one or more PEST sequences. Some family members such as Felic and MAYP/PSTPIP2 lack the SH3 domain, while some members also contain additional domains. For example, CIP4, Rapostlin/FBP17 and TOCA-1 contain HR1 domains for GTPase binding (Aspenstrom, 1997; Fujita et al., 2002).

One function that PCH family members have in common is that they regulate the organization of the actin cytoskeleton. For example, overexpression of CIP4 in Swiss 3T3 fibroblasts led to a decrease in F-actin and stress fibre content, while the remaining actin filaments appeared thinner and less organised than control cells (Aspenstrom, 1997). This suggested that CIP4 either caused breakdown of the pre-existing stress fibres or interfered with their formation and organization. In addition, other PCH family members, such as different Syndapins/FAP52/Pacsin isoforms and Raposltin/FBP17 can induce filopodia and localise to these sites of high actin turnover (Kessels and Qualmann,

2004). The yeast PCH family members, Cdc15p, Bzz1p, Hof1p/Cyk2p, and Imp2, all localize to actin structures and are required for either maintenance or formation of an acto-myosin contractile ring required during cytokinesis (Lippincott and Li, 2000).

The majority of PCH family members probably induce these effects on the actin cytoskeleton through their association with WASP. Many PCH family members, including CIP4, bind to a proline-rich region of WASP via their SH3 domains (Aspenstrom, 1997). Biochemical studies have shown that, through their association with WASP, the PCH family members TOCA-1 and Bzz1p can recruit the actin polymerization machinery *in vitro* to form actin fibres (Ho et al., 2004; Soulard et al., 2002). TOCA-1, a close homologue of CIP4, is specifically required for Cdc42-mediated activation of N-WASP, and hence actin nucleation. The presence of TOCA-1 was shown to be essential for Cdc42 dependent N-WASP mediated actin nucleation in cell extracts prepared from calf brains. However, Rohatgi et al. had previously reported that Cdc42-mediated actin nucleation could occur in a purified system consisting only of Cdc42-GTPγS, recombinant N-WASP, the Arp2/3 complex, and Rhodamine-labeled actin, suggesting that no other components were required (Rohatgi et al., 2000). In calf cell lysates, N-WASP was predominantly found in a complex with Verprolin/WASP interacting protein (WIP) (Rohatgi et al., 2000). This suggested that the importance of TOCA-1 for Cdc42-mediated N-WASP activation may be through relieving N-WASP of a preexisting inhibitor such as WIP. In the revised model, Cdc42 interacts with TOCA-1 and the N-WASP/WIP complex, and these interactions lead to the activation of N-WASP, which in turn stimulates actin nucleation through the Arp2/3 complex (Ho et al., 2004). Interestingly, the *S. cerevisiae* PCH protein, Hof1p, has been shown to interact with the

S. cerevisiae WIP, verprolin, via its SH3 domain and is required for Hof1p localization during cytokinesis (Naqvi et al., 2001).

Similar to TOCA-1, the *S. cerevisiae* Bzz1p can only polymerize actin in the presence of yeast cell extracts (Soulard et al., 2002). Cell extracts prepared from yeast mutants in several of the polymerization machinery proteins such as the *S. cerevisiae* WASP, *las17*, verprolin, *vrp1*, and *arp2* of the Arp2/3 complex, could not induce Bzz1p-mediated actin polymerization. When purified Las17p was introduced back into *las17*-deficient cell extracts, Bzz1p-mediated nucleation occurred. This polymerization required the Bzz1p C-terminal SH3 domain, which interacts with Las17p. Unlike TOCA-1, which is probably an orthologue of CIP4, Bzz1p does not contain an HR1 domain and thus its directed actin polymerization via WASP may not be dependent on Cdc42p.

The functional studies of TOCA-1 and Bzz1p define a clear requirement for WASP in the association of PCH family members with the actin cytoskeleton. However, other studies suggest that WASP may not be the only component linking these proteins to actin. For example, the *S. pombe* Cdc15 does not rely on Wsp1p directly for its effects on actin dynamics. Instead, it interacts with the Type I myosin, Myo1p, which binds to and activates the Arp2/3 complex (Lee et al., 2000); (Carnahan and Gould, 2003). The interaction of Cdc15p with Myo1p requires the N-terminal domains, and not the SH3 domain, of Cdc15p. Cdc15p also interacts directly with an actin nucleator, the formin Cdc12p (Carnahan and Gould, 2003). In *S. pombe*, Cdc12p, like Cdc15p, is required for the formation of the cytokinetic actin ring (Arai and Mabuchi, 2002) and its localization is lost in *cdc15* mutants (Carnahan and Gould, 2003).

MAYP is another PCH protein that regulates the actin cytoskeleton in an SH3/WASP-independent manner. MAYP does not contain an SH3 domain and hence cannot bind WASP. However, expression of MAYP in macrophages can induce filopodia but inhibits membrane ruffling in response to colony stimulating factor-1, CSF-1 (Yeung et al., 1998). Further analysis showed that MAYP functions as an actin filament bundling protein, producing flexible actin structures, both *in vitro* and *in vivo* (Chitu et al., 2005). MAYP does not directly bind to actin to perform this function. However, MAYP aggregates in the presence of the actin polymerization machinery and this aggregation may lead to its actin-bundling function (Chitu et al., 2005).

MAYP is not the only PCH family member that has been shown to aggregate/oligomerize *in vitro* and *in vivo*. Different PCH family members, such as Syndapins/Focal adhesion protein 52 (FAP52)/Pacsins, can self-assemble via their coiled-coil domains and, in particular, different Pacsin isoforms can hetero-oligomerize (Kessels and Qualmann, 2004). The coiled-coil domain present in all PCH family proteins may be an integral component for their role in actin cytoskeleton reorganization.

The association of PCH family members with other signalling molecules has provided a bridge between the actin cytoskeleton and many different signals and cellular processes. For example, Syndapins are PCH family members that link the actin cytoskeleton to vesicle trafficking (Kessels and Qualmann, 2002). Syndapins arise at this function through binding, via their SH3 domains, to N-WASP and different proteins required for vesicle trafficking, such as the GTPase Dynamin, the phosphatidyl 5-phosphatase, Synaptojanin (a protein essential for uncoating of clathrin coated vesicles) and Synapsin I (a protein that associates with the pool of synaptic vesicles that are in

reserve) (Kessels and Qualmann, 2004). It is not clear whether Syndapins function to inhibit or promote vesicle trafficking; however, it is clear that Syndapin can recuit N-WASP to membranes and trigger local actin polymerization *in vivo* in an SH3-domain and Arp2/3 complex-dependent manner (Kessels and Qualmann, 2004). This cytoskeletal role of Syndapins is reflected by the fact that these proteins are enriched at sites of high actin turnover such as lamellipodia and neuronal growth cones (Kessels and Qualmann, 2004). Another PCH family member, FBP17, has been shown to bind to Sorting Nexin 2 (SNX2) and Dynamin, indicating that FBP17, similar to Syndapins, functions in vesicle trafficking (Fuchs et al., 2001); (Kamioka et al., 2004).

FBP17 contains an HR1 domain; however, it does not bind to Cdc42 or other members of the Rho GTPase family such as RhoA, RhoB, RhoC, RhoG, TTF, Rac1 or Rac2 (Fuchs et al., 2001). The rat homologue of FBP17, Rapostlin, also does not bind to Cdc42 (Fujita et al., 2002). Rapostlin is 93% identical to FBP17 yet only 47% identical to CIP4 (Fuchs et al., 2001; Fujita et al., 2002). Though Rapostlin and FBP17 have a similar domain arrangement to CIP4, they contain an insert region prior to their HR1 domains. In Rapostlin, this domain is essential for interaction with the GTPase, Rnd2/Rho7 (Fujita et al., 2002). Given the level of homology between Rapostlin and FBP17, it is possible that FBP17 may also function as an effector for Rho7.

Members of the mammalian PCH family seem to be required in neuronal development and have been implicated in neurodegenerative disease. Rapostlin and its associated GTPase, Rnd2, are highly expressed in neurons in the brain and can induce neurite branching in neuronal PC12 cells (Fujita et al., 2002). CIP4 and different Syndapin isoforms are also expressed in brain tissue (Holbert et al., 2003; Kessels and

Qualmann, 2004). Two *Drosophila* PCH family members, Nervous Wreck (Nwk) and *Drosophila* Syndapin, are enriched at the larval neuromuscular junctions (Drysdale, 2005); (Coyle et al., 2004). *Drosophila Syndapin* mutants show severe locomotive defects, whereas in *nwk* mutants, motor neurons contain an excess of synaptic boutons.

Two PCH family members, Pacsin I and CIP4, have been shown to interact with the Huntingtin (Htt) protein, which is associated with Huntington's Disease (HD), a neurodegenerative disorder caused by polyglutamine expansion (PGE) of Htt (Modregger et al., 2002). Although these proteins both bind to Htt, their role in development of HD may differ from one another. First, the interaction between Pacsin I and Huntingtin is enhanced by the presence of PGE within Htt (Modregger et al., 2002). Unlike Pacsin I, CIP4 bound equally to normal and mutated Htt from HD patients (Holbert et al., 2003). Second, these proteins show distinct distributions during development of HD. Pacsin I, which is normally found within synaptic boutons, is found mostly in the cytoplasm of HD patient neurons. This relocalization of Pacsin I is seen early in HD development as brain tissue of presymptomatic patients show Pacsin I redistribution. Further, Pacsin I immunostaining of HD patient tissue reveals concentration of Pacsin I in perinuclear regions, coincident with mutant Htt (Modregger et al., 2002). In tissues of later stage HD, Pacsin I staining is almost completely lost, though analysis of normal and HD brain homogenates suggest that Pacsin I is not degraded, but rather delocalised in the cytoplasm of HD neurons. In contrast, elevated CIP4 protein levels were observed in human brain tissue of HD brain striatum and in neostriatum of HD patients. CIP4 accumulation was increased in patients with later stages of HD. Furthermore, CIP4

localised to inclusions that form in neurons of HD patients and overexpression of CIP4 induced death of striatal neurons in normal brain cells (Holbert et al., 2003).

As mentioned above, Pacsin I concentrated to perinuclear regions in HD neurons. Perinuclear staining can often include the Golgi apparatus (Larocca et al., 2004). Pacsin I localization at perinuclear regions is a result of a biological pathway gone wrong and may not represent its true biological localization (Modregger et al., 2002). However, CIP4 does localise to the Golgi apparatus and is required for the maintenance of the Golgi apparatus through its association with cyclic AMP-dependent protein kinase A (AKAP) 350 (Larocca et al., 2004). AKAP350 is a large anchoring protein that is found at the Golgi apparatus and the centrosomes, where it interacts with Protein Kinase A (PKA), in epithelial cells (Larocca et al., 2004). Both FBP17 and CIP4 bind to AKAP350. Thus far, CIP4 is the only AKAP350 binding partner that is also a substrate for PKA. CIP4 localization at the Golgi does not require of the presence of Cdc42. AKAP350 and CIP4 are necessary for maintenance of normal Golgi structure (Larocca et al., 2004). CIP4 may be modulating the Golgi actin cytoskeleton by interacting with cytoskeletal regulators. This hypothesis is supported by the fact that an inhibitor of actin nucleation, latrunculin B, induced similar morphological changes on the Golgi as observed with displacement of CIP4 from the Golgi (Larocca et al., 2004). Interestingly, the PCH protein PSTPIP localizes to the cytoplasm and perinuclear regions when it is bound to the protein tyrosine phosphatase, PTP-PEST (Cote et al., 2002).

In addition to being phosphorylated by PKA, CIP4 has also been shown to be phosphorylated by Src kinase (Abram and Courtneidge, 2000). Though the ramifications of these phosphorylations on CIP4 function are unknown, it is likely that phosphorylation

is one mechanism of regulation of PCH family proteins. The murine PSTPIP is hyperphosphorylated in cells lacking the tyrosine phospatase, PTP-PEST (Cote et al., 2002). PSTPIP phosphorylation can also be induced in mouse fibroblasts that have been treated with EGF or PDGF. Interestingly, this phosphorylation seems to be independent of Src kinases as treatment of fibroblasts with the Src inhibitor, PP2, did not affect PSTPIP phosphorylation. The phosphorylation of PSTPIP allows it to interact with various phosho-tyrosine binding domains, named Src Homology 2 (SH2) domains. In particular, tyrosine-phosphorylated PSTPIP interacted with SH2 domains of Crk, Fyn, Abl and Src tyrosine kinases. However, phosphorylation of PSTPIP in its SH3 domain blocks its binding to WASP.

Many PCH family members are phosphorylated and this phosphorylation can lead to changes in their localization and function, as described above. In the case of *S. cerivisiae* Hof1p, regulation by phosphorylation can lead to its degradation. Hof1p is hyperphosphorylated in its PEST domain at the end of mitosis. Interestingly, Hof1p is degraded at this time, most likely by the ubiquitin ligase, SCF^{Grr1}. SCF^{Grr1} binds to the PEST domain of Hof1p; Hof1p without its PEST domain is stable in cells and leads to severe cytokinesis defects due to a delay in contraction and subsequent ingression of the actomyosin ring (Blondel et al., 2005). Interestingly, comprehensive yeast two hybrid analysis has also identified Bzz1p as a binding partner for SCF^{Grr1} suggesting that degradation may be a common mechanism for regulation of yeast, and perhaps other, PCH family members, as most members contain PEST sequences (personal observation).

Very little is known about the function of the FCH domain of PCH family proteins. However, a few experiments have shown that it may be required for

microtubule binding: murine CIP4 and rat Rapostlin were shown to cosediment with microtubules unless the FCH domains were not present (Tian et al., 2000); (Fujita et al., 2002). Overexpression of CIP4 leads to translocation of WASP from actin filaments to the cellular microtubular array (Tian et al., 2000). Whether the translocation of WASP to microtubules was an artifact of overwhelming the system with CIP4 or if it provides insight to methods of regulation or other functions of WASP remains to be seen.

1.2.3 Cdc42 is required for cytoskeletal regulation downstream of the Transforming Growth Factor-β (TGF-β) family of cytokines

As more Cdc42-interacting proteins become known, it is necessary to begin deciphering which upstream signals lead to activation of each set of downstream components by finding interactions between growth factors/receptors and effector proteins of Cdc42. One example of a signal in which researchers are beginning to establish such connections is the TGF-β pathway.

In the most recent model, the TGF signal is transduced by the binding of TGF-β/Activin/BMP family of ligands to different receptor complexes, which always consist of one member of a Type-I and one member of a Type-II receptor family. Ligand binding results in the phosphorylation and subsequent activation of the receptors. At this stage it is proposed that the active receptor-ligand complex is endocytosed (Gonzalez-Gaitan, 2003). Within early endosomes the activated Type-I receptor protein phosphorylates the transcription factor Smad (Smad2/3 for TGF-β and Smad1/5 for BMP2/4; (Newfeld et al., 1999), which is recruited to the endosome by an adaptor protein called SARA (Smad Anchor for Receptor Activation). SARA itself is recruited to the endosome by binding to phosphotidylinositol-3-phosphate (PtdIns(3)P). The activation

of the Smad protein by the receptor is thus dependant on SARA and endosome formation. Phosphorylated Smad protein then interacts with a co-transcription factor, Smad4, and enters the nucleus to regulate gene expression (Gonzalez-Gaitan, 2003).

TGF-β has also been shown to induce responses independent of Smad-related transcription. TGF-β-induced filopodia formation requires the activation of Cdc42 and Cdc42 downstream targets, the p38 MAPK and PAK2, but does not require Smad-related transcription (Edlund et al., 2002; Wilkes et al., 2003). Recently, PAK1 was shown to co-immunoprecipitate with the TGF-β receptor and it is possible that PAK1 is required for TGF-β induced downregulation of tight junctions (Barrios-Rodiles et al., 2005; Ozdamar et al., 2005). In addition, it has been suggested that Rho GTPases may also contribute to TGF-β induced gene expression in a long range response to TGF-β signalling (Derynck and Zhang, 2003; Edlund et al., 2002).

1.3 Cdc42 is required for the development of *Drosophila melanogaster*

As many of the cellular processes that require Cdc42 function, such as cell migration, endocytosis, and cell adhesion, are required for morphogenesis of tissues, it is not surprising that Cdc42 is an important component of several developmental processes. In particular, *Drosophila* Cdc42 has been shown to be required for several aspects of *Drosophila* development. The developmental processes requiring Cdc42 that are relevant to this thesis will be introduced below, followed by discussion of the role of Cdc42 in each process.

1.3.1 The role of Cdc42 during *Drosophila* oogenesis

A *Drosophila* ovary consists of roughly 16 ovarioles (Figure 1.1). Each ovariole represents an independent egg assembly line, containing a single germarium that gives rise to multiple future eggs (Spradling, 1993). The germarium is made up of two kinds of cells, germ cells and somatic epithelial cells. Each germ cell divides to produce a cyst of 16 cells that stay connected to each other via an actin-rich cytoplasmic bridge referred to as a ring canal. One of the 16 cells differentiates to become the oocyte, while the other 15 cells, the nurse cells, provide nutrients to the oocyte as it develops. The 16-cell cyst becomes encapsulated by the somatic epithelia and forms a round shaped egg chamber, or follicle. This follicle buds off from the germarium but stays connected to the next developing egg chamber by a string of epithelial cells referred to as stalk cells. A healthy germarium typically contains 12 forming cysts at different stages of their development, with the most developed cyst becoming encapsulated at the posterior end of the germarium (Spradling, 1993). The most developed egg chamber is at stage one of its development at this time and continues through a total of 14 developmental stages before it becomes a mature egg.

The actin cytoskeleton is essential for *Drosophila* oogenesis (Cooley and Theurkauf, 1994) which makes this an excellent system to study cytoskeletal regulators such as Cdc42. Both the germ cells and the follicle cells are large, allowing the visualization of different types of F-actin present in each cell type. As in many cell types, subcortical F-actin outlines both the germ cells and the follicular epithelium (FE) that surrounds them (Figure 1.1 C). Expression of CA or DN Cdc42 mutant transgenes in the germ cells disrupts this subcortical F-actin causing it to become discontinuous. The

Figure 1.1 An ovariole in the *Drosophila* ovary.

(A-P) axis is oriented left to right in this and subsequent figures. (A) Schematic diagram of an ovariole from a wild-type ovary. An ovary typically contains about 16 ovarioles. At the anterior end of the ovariole the progeny of germline and somatic stem cells are assembled into egg chambers in the germarium. Egg chambers exit the germarium and move posteriorly as they develop; each ovariole consists of a chain of progressively older egg chambers. The FE shown in green surrounds the germline cells of each egg chamber. Germline cells consist of 15 nurse cells and the oocyte, which is at the posterior end of the egg chamber and increases in size as it ages. The boundary between nurse cells and the oocyte is depicted with a vertical line in each egg chamber. Staging is according to Spradling (1993). (B) Schematic diagram showing apical-basal organization of the FE. Apical membrane is shown in green, lateral membrane in yellow and basal membrane in blue. za, zonula adherens. (C) Phalloidin-stained ovariole, extending from germarium through to stage 9 chamber.

This figure was kindly donated by R. Conder (unpublished).

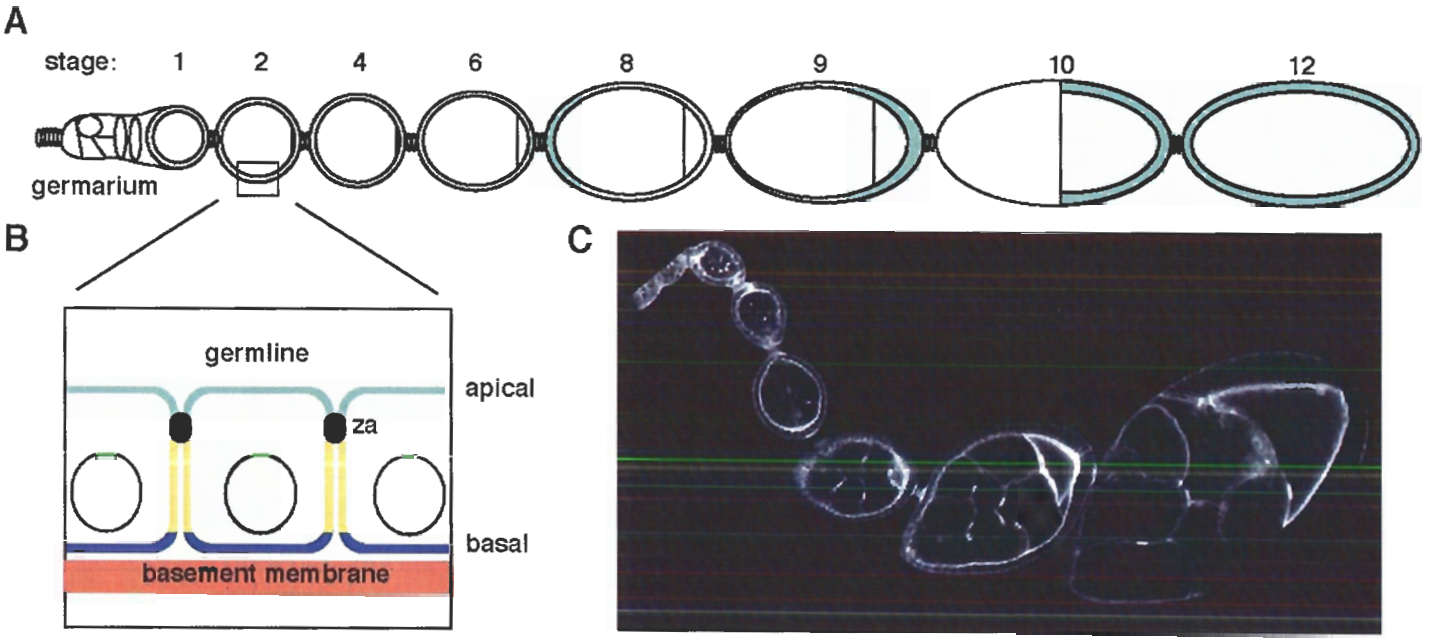
A
stage: 1 2 4 6 8 9 10 12
germarium
B
germline
apical
za
basal
basement membrane
C

specialized actin structures, the ring canals, that allow the germ cell cyst to exist as a syncitium, are released from the membrane in Cdc42 mutant egg chambers, resulting in germ cell fusion and the formation of multinucleated cells (Murphy and Montell, 1996). Though expression of both types of Cdc42 mutant transgenes cause release of ring canals into the germ cytoplasm, this phenotype is more severe in the presence of CA Cdc42 (Murphy and Montell, 1996).

Another germ cell-specific actin structure that requires Cdc42 function begins forming in stage 10 within the nurse cells. Extensive actin bundles form radially around each nurse cell nucleus at this stage (Cooley and Theurkauf, 1994). The bundles begin at the plasma membrane and extend to the nuclear membrane, where they bend to form a large cage around the nucleus (Cooley and Theurkauf, 1994). At the plasma membrane, actin bundles of neighbouring cells intercalate, suggesting that the membrane insertion sites protrude into their neighbours (Cooley and Theurkauf, 1994). It is hypothesized that these actin cages secure the nurse cell nuclei in place before the nurse cells contract to rapidly transfer their cytoplasmic contents to the oocyte in stage 11. This hypothesis is based on the phenotypes observed in egg chamber mutants such as *Drosophila* profilin, *chickadee,* that do not form these specialized nurse cell actin structures (Verheyen and Cooley, 1994b); (Cooley and Theurkauf, 1994). When nurse cells contract in such mutants, the nurse cell nuclei become lodged into the ring canals, blocking transfer of the nurse cell cytoplasm into the oocyte. Egg chambers of heteroallelic combinations of different Cdc42 mutations appear to have fewer nurse cell cytoplasmic actin filaments and improper transfer of the nurse cell cytoplasm to the oocyte (Genova et al., 2000).

Besides the cortical F-actin that outlines the follicle cells, one other specialized F-actin distribution can be found in the developing egg chamber. Beginning in early egg chamber development (stages 4-7), F-actin fibres assemble in polarized bundles at the basal surface of the FE, perpendicular to the anterior-posterior (A/P) axis. These polarised actin bundles may act as a molecular corset to promote elongation of the oocyte in the A/P axis (Gutzeit and Haas-Assenbaum, 1991). As the egg chamber develops, the FE reorganises from a cuboidal to a columnar epithelium that migrates over the oocyte and leaves behind a thin sheet of squamous epithelium to cover the nurse cells. As this process is occuring, the basal F-actin also becomes less organised and no longer lies perpendicular to the A/P axis. Instead, the actin bundles seem more randomly distributed. Though it is unclear if Cdc42 is required for the change in basal F-actin distribution during egg chamber development, it has been shown that Cdc42 mutant egg chambers remain cuboidal during stage 9 when the wild-type FE has begun to take on a more columnar appearance (Genova et al., 2000).

1.3.2 The role of Cdc42 in cellularization of the *Drosophila* syncitial embryo

In *Drosophila*, embryogenesis begins by a series of nuclear divisions occuring in a common syncitium; that is, the nuclei divide in a common cytoplasm in the absence of cytokinesis. After the 9^{th} division, nuclei begin to migrate to an area just below the embryonic membrane where they continue to divide to complete the last set of syncitial nuclear divisions. During the final division cycle, cycle 14, the plasma membrane invaginates between the blastoderm nuclei, creating an epithelial monolayer of approximately 6000 blastodermal cells (Foe, 1993). This process, whereby the formation of the membrane cleavage furrows leads to eventual encompassing of each nucleus, is

referred to as cellularization. Cellularization is dependent on the acto-myosin and microtubule cytoskeletons as well as the donation of new membrane via vesicles from internal cellular compartments (Mazumdar and Mazumdar, 2002). The requirement of both the actin and microtubule cytoskeletons in cellularization is supported by the fact that treatment of a pre-cellularization stage embryo with inhibitors of microtubule formation, such as cholchicine, or of F-actin formation, such as cytochalasin-D, block cleavage furrow formation (Foe, 1993). Similarly, the importance of new membrane addition to the growing cleavage furrow was demonstrated by the finding that cellularization is blocked in mutants for endocytic proteins such as the GTPases, Dynamin and Rab11 (Strickland and Burgess, 2004).

Injection of cellularization stage embryos with CA Cdc42 also disrupted cellularization (Crawford et al., 1998). In these embryos, progression of cellularization halted, leading to collapse of the cleavage furrow and further arrest in embryonic development. The nuclei that had migrated to the egg membrane began to fall away from the embryo surface and were no longer found in a regular array at the cortex. These phenotypes correlate with disruption of the F-actin and myosin localization in these embryos and most likely occur a result of actin and myosin disruption (Crawford et al., 1998).

1.3.3 The function of Cdcd42 in the context of other signalling components required in dorsal closure of the *Drosophila* embryo

Dorsal closure (DC) refers to a process that occurs late in embryogenesis where the lateral epidermis migrates from both sides of the embryo over a dorsally localised tissue called the amnioserosa. During stage 12 of embryogenesis, at the beginning of

DC, the epidermis consists of two types of epithelial tissues (Figures 1.2 and 1.3). A sheet of unified polygonal-cell epithelium covers the ventral and lateral sides of the embryo. The dorsal surface of the embryo at this stage is occupied by the amnioserosa, which is an epithelium comprised of large, flat cells (Harden, 2002). Morphogenetic cues signal the lateral epidermis from each side of the embryo to migrate over the amnioserosa. The opposing lateral epithelia meet at the dorsal midline where they adhere to one another, forming a seamless embryo. The amnioserosa, which then lies underneath this epithelium, undergoes cell death.

The process of DC begins with the dorsalward elongation of the first row of lateral epidermal cells on each side of the embryo, known as the leading edge (LE) cells. This elongation occurs as a result of a polarised accumulation of F-actin and myosin at the dorsal end of each LE cell, leading to its constriction in an A/P direction (Harden, 2002). This elongation is first seen in the LE cells; however, it subsequently occurs in the more ventrally located epidermal cells as well. Accompanying LE elongation is the formation of filopodia at the apical surface of each LE cell and the cells of the amnioserosa (Harden, 2002). Loss of the LE cell filopodia leads to failure to close the dorsal hole (Jacinto et al., 2002). Live imaging of developing *Drosophila* embryos has demonstrated that at the final stages of DC, filopodia of LE cells on one side of the epidermis seek out filopodia of LE cells from the opposing side, leading to adhesion of the once-lateral surfaces at the dosal midline (Jacinto et al., 2002).

Many signalling cues are required for DC to occur. The c-Jun N-terminal Kinase (JNK) cascade has been found to be a central component of the signalling driving DC (Harden, 2002). The JNK cascade is a Mitogen-activated Protein Kinase (MAPK)

Figure 1.2 Dorsal closure is a model for epithelial movement in the Drosophila embryo.

(A – D) Panels show dorsal views of progressively older embryos stained with anti-phosphotyrosine antibodies to show closure of the epidermis over the large flat cells of the amnioserosa.

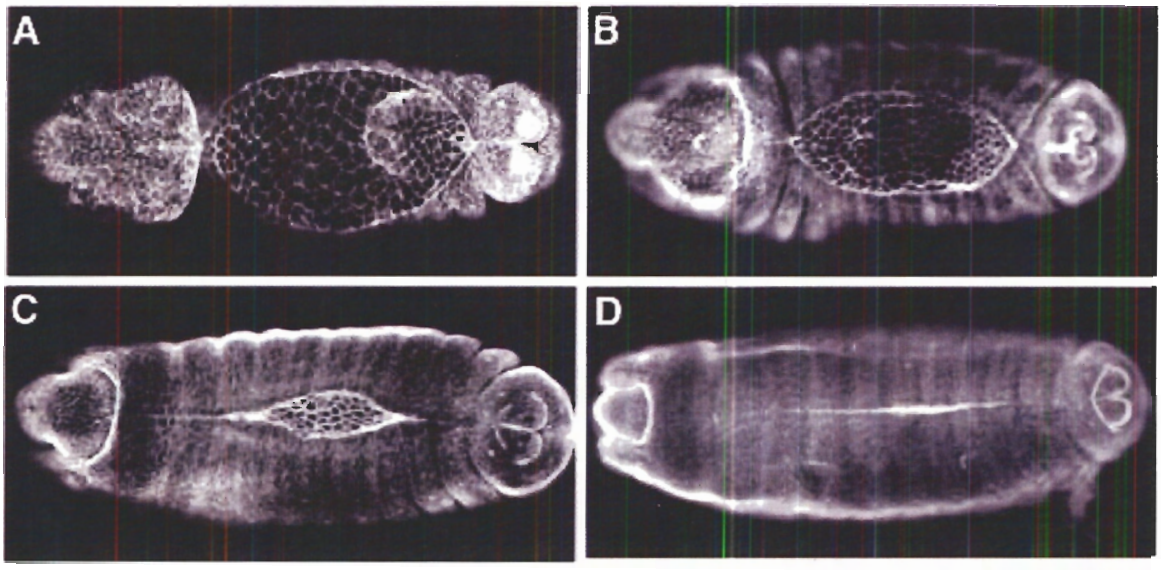
A
B
C
D

cascade that is required for epithelial morphogenesis in many different developmental processes (Xia and Karin, 2004). MAPK cascades consist of a string of kinases that activate each other via phosphorylation leading to the eventual phosphorylation, of their downstream non-kinase substrates, which, in most cases, are transcription factors. Therefore, target transcription factors are phosphorylated and activated by a MAPK that was itself activated by a MAPK kinase (MAPKK) that was activated by a MAPKK kinase (MAPKKK). The first gene cloned encoding a JNK component that affected DC was *hemipterous* (*hep*), a MAPKK most similar to JNKK (Glise et al., 1995). Following this, *Drosophila* JNK (DJNK) was shown to be encoded by *basket* (*bsk*) and *Drosophila* JNKKK (DJNKKK) encoded by a MLK gene, *slipper* (*slpr*) (Harden, 2002). Mutations in the *Drosophila* JNK cascade produce non-constricted LE cells, disruption of F-actin and myosin at the LE, and the failure of DC to complete. A downstream substrate of the JNK cascade is c-Jun, which, with c-Fos, forms the AP-1 complex of transcription factors. The *Drosophila* homologues of these proteins are Djun and Dfos, encoded by the genes, *l(2)A109* and *kayak* (*kay*), respectively (Harden, 2002). *l(2)A109* and *kay* mutants exhibit the same DC defects as seen for mutants in the other JNK components.

Activation of the AP-1 complex leads to transcriptional activation of several target genes. Two of these genes have been well characterised with respect to their AP-1 dependent expression in the LE cells during DC. The first gene, *puckered* (*puc*), encodes the *Drosophila* homolog of a VH-1 family MAPK phosphatase for DJNK (Harden, 2002). This is a demonstration of a negative feedback loop present during DC to regulate JNK activity. Overexpression of Puc resembles the loss-of-function phenotypes of JNK pathway components, and a reduction of *puc* can partially rescue the DC defects

associated with reduction of Hep/DJNKK (Martin-Blanco et al., 1998). The second gene whose transcription is activated by the JNK cascade in the LE cells is *decapentaplegic* (*dpp*). Dpp is the *Drosophila* homologue of the Bone Morphogenetic Protein 2 (BMP2) and BMP4 proteins, which are members of the TGF-β family of cytokines (Martin-Blanco et al., 1998; Ring and Martinez Arias, 1993). Embryos mutant for various combinations of *dpp* alleles die before DC due to an earlier requirement for Dpp in embryogenesis (Morisato and Anderson, 1995).

Although the role of Dpp cannot be directly assessed during DC with loss-of-function *dpp* alleles, mutations exist for several components of Dpp signalling, some of which do show DC defects. Loss-of-function mutations in either of the Type-I and Type-II Dpp receptors, *thick veins* (*tkv*) and *punt* (*put*), or a transcription factor required for Dpp signalling, *schnurri* (*shn*), cause DC defects (Harden, 2002). Moreover, the overexpression of Dpp or expression of an activated version of Tkv can rescue DC defects caused by mutations of the JNK pathway (Ip and Davis, 1998). This clearly demonstrates that Dpp signalling is required during DC, but the exact mechanisms of action have not yet been resolved. However, it has been observed that the transcript levels of the *Drosophila* non-muscle myosin heavy chain, *zipper* (*zip*), are reduced in LE cells deficient in *tkv* (Arquier et al., 2001).

Several studies have indicated that Cdc42 is also required for DC (Harden, 2002). Although it is not possible to produce embryos completely devoid of both maternal and zygotic Cdc42 function due to a requirement for Cdc42 during oogenesis, females bearing heteroallelic combinations of weak and strong Cdc42 alleles can be used to produce Cdc42 mutant embryos severely lacking in Cdc42 function (Genova et al.,

2000). These mutant embryos display DC defects (Genova et al., 2000). In addition, expression of DN Cdc42, Cdc42N17, during DC results in holes in the dorsal surface (Harden et al., 1999). Expression of Cdc42N17 at the LE results in loss of filopodia of the LE cells, leading to failure to seek out and adhere to the opposing epidermis (Jacinto et al., 2000).

The involvement of Cdc42 in DC with regard to JNK and Dpp signalling has also been addressed. It was initially observed that overexpression of CA Rac1 or Cdc42 during DC results in ectopic activation of the JNK cascade, suggesting that these GTPases contribute to DC by acting as upstream activators of this MAPK cascade (Glise and Noselli, 1997). However, several studies indicate that Cdc42 may act largely downstream of JNK. First, Cdc42 mutants and expression of DN Cdc42 produce DC defects where by the epidermis looks bunched at the LE (Harden et al., 1999). This phenotype is similar to that seen in embryos of Dpp pathway mutants (Ricos et al., 1999). Second, overexpression of CA Cdc42 can suppress the DC defects associated with loss of Tkv function (Ricos et al., 1999). Finally, Cdc42 mutant embryos display wild-type Dpp transcript levels at the LE during DC, suggesting that Cdc42 does not signal through the JNK pathway during DC (Genova et al., 2000). The ectopic expression of Dpp seen in embryos expressing CA Cdc42 may have been an artifact of overexpression, leading to "bleedthrough" activation of the JNK cascade, which may normally be only regulated by Rac.

The research described above demonstrates that Cdc42 is required for Dpp signalling and regulation of the actin cytoskeleton during DC. However, the components required for Cdc42 to relay its signal during DC have not been well characterised. As an

effort to characterise downstream effectors for Cdc42 during DC, we decided to characterise *Drosophila* homologues of two mammalian proteins that had been identified as effectors for Cdc42. These two proteins were CIP4 and ACK. We chose to name the *Drosophila* homologues of these proteins after their mammalian counterparts, and thus called them *Drosophila* CIP4 (DCIP4) and *Drosophila* ACK (DACK). As previously mentioned, there are two *Drosophila* ACKs, and during the course of our research we found it necessary to begin characterising both ACKs in order to define the function of DACK. Our aim was to characterize the function of these genes with respect to Cdc42 signalling in DC. However, we found that although all three genes are expressed at the LE during DC, embryos mutant in either of these genes do not display DC defects. We were, however, able to establish a role for DACK in Dpp signalling during DC. We also identified the possibility of a role for DCIP4 in several other tissues/processes that have been shown to require Cdc42 signalling, such as cellularization, nervous system development, wing development, and oogenesis.

2 MATERIALS AND METHODS

2.1 Fly Stocks

Unless otherwise stated, all stocks were obtained from the *Drosophila* Stock Centre at Bloomington, Indiana. Unless otherwise stated, all crosses were raised at 25°C. w^{1118} was used as a wild-type control strain. *DACK* mutations were generated by imprecise excisions of the P element, *KG00869*, kindly provided by H. Bellen. *UAS-*tkv^{Q199D} (*TAJ3*) was a gift from M. O'Connor, $GAL4^{332.2}$ from B. Giebel, *Hs-*$Gal4^{M-4}$ from J. Roote, kay^{2} from D. Bohmann, dpp^{hr27} from K. Wharton, and Med^{23} from R. Padgett. *UAS-DACK* and *UAS-KD-DACK* transgenes were described previously (Sem et al., 2002). *PBc02472* was obtained from S. Artavanis-Tsakonas. *Cdc42* mutants *1-6* were obtained from R. Fehon, wsp^{1} and wsp^{3} mutants from E. Schejter, and nwk^{1} and nwk^{2} alleles were obtained from T. Littleton.

2.2 cDNAs

All cDNA were produced by the Berkeley *Drosophila* Genome Project. *LD14951* and the *zip (LD21871)* cDNA can be currently obtained from Open Biosystems (http://www.openbiosystems.com/*drosophila*_gene_collection_2.php). Ribosomal protein 49 (rp49) cDNA used as a loading control was provided by D. Sinclair (O'Connell and Rosbash, 1984). cDNAs for *CG15014 (GH15813), DPR2 (LD28966), CapG (LD22256), TppII (LD 24257),* and *Dfos (SD04477)* were obtained from the Canadian *Drosophila* Microarray Centre.

2.3 Standard molecular techniques

Routine techniques such as restriction digestion, cloning, agarose gels, and Polymerase Chain Reaction (PCR) were performed as described in Sambrook et al. (1989) or according to manufacturer's instructions.

PCR reactions where high fidelity was required, such as generating cDNA constructs for protein expression, were carried out using Vent DNA polymerase obtained from New England Biolabs and used according to manufacturer's instructions. Screening and analytical PCR were carried out using Taq polymerase from Qiagen according to manufacturer's instructions.

cDNA constructs were transformed into DH5-alpha or XL1-Blue bacterial competent cells for amplification and general maintenance. The cells were obtained from Stratagene and used according to manufacturer's instructions. cDNAs in pGEX5X-3 or pMAL-c2, for generation of GST- or MBP-fusion proteins required JM109 or BL21 bacterial competent cells obtained from Stratagene and used according to manufacturer's instructions. JM109 was used as it is *recA-* and therefore prevents recombination commonly experienced with pGEX5X-3, while being an efficient competent cell. BL21 was used for enhanced expression of GST- or MBP-fusion proteins, and prevention of protein degradation or formation of inclusion bodies.

2.4 Sequencing

To obtain the sequence of *LD14951*, a restriction map was built and identified overlapping *Eco*RI and *Pst*I fragments were cut, subcloned into pBS and sequenced using the Sanger chain termination method with T7 and T3 primers. The Sanger method was

carried out using either the T7 Sequenase version 2.0 DNA sequencing kit or the Thermo Sequenase radiolabeled terminator cycle sequencing kit following manufacturer's instructions (Amersham Life Science).

2.5 Generation of Transgenic *Drosophila* lines

Components:

Injection buffer: 5mM KCl, 0.1mM sodium phosphate pH 6.8. Filter sterilized using 0.2 micron filter.

The pUAST construct has two P-element ends necessary for insertion into chromosomes and contains a marker, the *white* (*w*) gene, which enables visualization of the presence of an insert in w^- flies (Brand and Perrimon, 1993). The gene of interest is placed under the control of a pre-engineered *UAS* promoter. This, along with another plasmid encoding a transposase, is injected into the pre-blastoderm of an embryo, and should invoke a random insertion into a chromosome resulting in progeny containing transgenic DNA (Ashburner, 1989).

Preblastoderm w^{1118} embryos obtained from a 30 minute collection at room temperature were put onto a wet piece of Whatmann filter paper using a wet paint brush. Excess water was removed and the embryos were transferred onto double sided sticky tape by inverting the Whatmann paper onto a piece of tape attached to a glass slide and brushing the back of it with a paint brush. The embryonic chorion, or egg shell, was removed by putting another glass slide with double sided sticky tape on top of the embryos and subsequently pulling the slides apart. This tears apart the chorion but does

not harm the vitelline membrane still covering and protecting the embryo. The embryos were then lifted from within their torn egg shells and transferred to double sided sticky tape attached to a cover slip, with their posterior ends facing the edge of the coverslip. Embryos were desiccated at room temperature and immersed in halocarbon oil (Voltalef). After immersion in halocarbon oil, embryos were injected in their posterior ends with 400μg/mL of pUAST + transgene construct mixed with 200μg/mL of pUChsΔ2-3, as a transposase source, in injection buffer.

Plasmid DNA to be used for injection was prepared using the Qiagen MidiPrep kit and quantified by absorbance spectroscopy at 260nm and by comparison with standards on a 1% agarose/TAE gel. The microinjection system used was as described in O'Connor and Chia (O'Connor and Chia, 1993). Injected embryos were allowed to develop at room temperature and surviving adults were individually mated to w^{1118} flies. Progeny with eye colour were mated to *yw;Gla/Cyo* and *w;Tm3Ser/Tm6Tb* to capture and balance insertions on the second or third chromosome. First chromosome insertions were easily identifiable by following the migration of the X chromosome in male and female progeny and were left unbalanced.

The ability of the transformants to express cDNA from the *UAS* promoter was verified using Northern blot analysis. Transgenic flies were crossed to a heat shock inducible Gal4 driver on the second or third chromosome. Progeny carrying both the *UAS*-insertion and the Gal4 driver were then heat shocked 1-2 hours at 37°C, to induce expression of Gal4 and thus transcription of the cDNA in front of the *UAS* promoter. Subsequently the flies were incubated for 1 hour at room temperature to allow

transcription to continue. RNA was then collected from these flies and Northern blot analysis was performed as described below.

2.6 Generation of *Drosophila* mutations by P element mobilization

The *EP* element is a nonautonomous P element, meaning that it does not contain an active transposase necessary for its mobilization and consequent transposition within the genome (Rorth, 1996). Introduction of a source of transposase allows for the re-mobilization of a nonautonomous P element in the germ line. The re-mobilization of a P element often results in an imprecise excision event, resulting in random deletions about its insertion point and consequently a mosaic reflecting this in the germ line (Preston et al., 1996). The progeny of the mosaic will bear the resulting genotype. Monitoring the generation of mosaics is made simple by the presence of a marker gene engineered into the P element, which produces a visible phenotype such as eye or body colour in the adult fly. Cells lacking the P element will also lack the phenotype of the marker gene, thus making it easy to spot a mosaic fly.

EP elements contain a *mini-white* marker gene, which codes for a transmembrane transporter required for the transport of pigment precursors into pigment cells in the fly eye. The presence/absence of eye colour confirms the presence/absence of the *EP* element and thus allows the identification of mosaic flies as their eyes will be mosaic in their pigmentation. As WT flies already contain a functional *white* (*W*) gene on their first chromosome, the *EP* collection was generated in a *w* background to allow detection of the *EP* element through eye colour produced from expression of the *mini-white* gene.

The *EP* elements that were mobilized to generate mutations in *DCIP4, EP(3)0671* and *EP(3)3507,* were mated *en masse* to transposase-containing flies of the genotype *w;Δ2-3Sb/TM3Ser.* 200 and 60 mosaic F1 males of the genotype *EP(3))0671/Δ2-3Sb* and *EP(3)3507,* respectively, were selected, and each was mated individually to 6 *w;TM3Sb/TM6Tb* females. Non-Sb, white eyed male progeny isolated from these crosses were assumed to have lost their *EP* element-and associated mini-white gene in an excision event. These males were mated individually to 6 *w;TM3Sb/TM6Tb* females to generate further progeny bearing the excised chromosomes, and subsequently brother-sister crossing was completed to establish individual lines. Homozygous viability of each line was assessed by the loss of the balancer chromosome marker in the stock. Molecular analysis of the excision events were carried out using Northern blotting to screen for loss of *DCIP4* transcript and PCR of the genomic region where the *EP* element was previously inserted. If a resulting PCR fragment was shorter or longer than one obtained from wild-type flies, the PCR fragment was sent for sequencing using the primers used to generate the fragment. Lethal lines or lines that failed to produce PCR products were screened by Southern blotting, using cDNAs for *DCIP4* and *CG15014* as probes.

2.7 Northern hybridization

Total RNA from embryos or adult flies was prepared using the TRIzol reagent (Life Technologies) according to manufacturer's instructions. 20mg of tissue or 20 adult flies was homogenized in 400μl of TRIzol.

Formaldehyde-agarose gels were prepared according to Sambrook et al. (1989). Northern analysis was done using the protocol of Virca et al. with staining of the gels with Acridine Orange omitted (Virca et al., 1990). RNA in the gel was transferred to the

Hybond N membranes using capillary action and hybridized as described by Virca *et al.* Probes for Northern hybridization were generated as described in section 2.9.

2.8 Southern hybridization

Genomic DNA was prepared as described by Roberts (Roberts, 1998) and digested with the appropriate restriction endonuclease for ~12 hours at 37°C. Samples were run on 0.7% agarose gels and treated as described in Sambrook et al. (1989). Denatured DNA was transferred onto Hybond N membranes using capillary action and hybridized as described in Sambrook et al. (1989), except that the last 2 washes were done at 80°C. Probes for Southern hybridization were generated as described in section 2.9.

2.9 Generation of radiolabeled probes for Northern and Southern blotting

DNA fragments to be used as probes for Northern or Southern blotting were purified from agarose gels using QIAquick gel extraction kit. The DNA fragments were amplified in the presence of 50μCi of {α-^{32}P}dCTP using the Rediprime™II random prime labelling system (Amersham Pharmacia biotech, RPN 1633). Unincorporated radionucleotides were removed using MicroSpin™ S-200 HR columns (Amersham Pharmacia biotech, 27-5120-01) according to manufacturer's instructions. Probe made from a 600 bp *Eco*RI-*Hind*III *rp49* fragment was used as a loading control for Northern blot.

2.10 Generation of DCIP4 polyclonal antibodies

DCIP4 polyclonal antibodies were generated by immunizing hens with purified DCIP4 conjugated to a 6xhistidine epitope tag. The recombinant DCIP4 protein was made by our collaborator, Dr. Avital Rodal from Dr. Troy Littleton's lab at Massachusetts Institute of Technology (MIT), and sent to Aves Labs Inc for immunization of chickens, and subsequent egg and serum collection. Avital cloned *RE39037* into pTRCHISA (Invitrogen) and transformed this construct into BL21 DE3 RP cells (Invitrogen). She grew 2L of this culture and induced it with 40μM IPTG for 2 hours at 37°C. Cells were spun down and resuspended in 20ml of 20mM NaPO4 pH 8.0, 20mM imidazole, 500mM NaCl and complete protease inhibitors (Roche, 1 tablet/50ml buffer) and sonicated 3x30 seconds at high voltage or until the cell suspension cleared. TritonX-100 was added to a final concentration of 0.5%, to aid in solubilization of protein. Cell debris was pelleted and the supernatant was filtered through a 0.45μm syringe filter. The filtrate was applied to a prepared HiTrap chelating HP column (Amersham) and eluted according to manufacturer's instruction. The eluted protein was further purified by running it through an FPLC, and concentrated using Amicon Ultra 10 KDa MWCO (Millipore) concentration devices to 4mL in PBS (roughly 1.2mg of protein per mL). The concentrated protein was sent to Aves labs as 500μl aliquots.

2.11 Affinity purification of the DCIP4 antibody

Components:

GLB: LB + 0.2% glucose

LB: 5g bactotryptone, 5g NaCl, 2.5g bacto-yeast extract in 500 mL of water. Autoclaved.

LB agar: LB + 7.5g agar. Autoclaved. Cooled to 55°C and ampicillin added to 50μg/mL. Poured on plates.

LB + ampicillin: LB. Autoclaved. Cooled to 55°C and ampicillin added to 50μg/mL.

PBS: as per Sambrook et al. (1989).

PBT: PBS + 0.5% TritonX-100

TritonX-100

RE39037 was cloned into pMALc-2 to generate RE39037p-Maltose binding protein (MBP) fusion proteins. This construct was transformed into BL21 cells (Invitrogen) and a single bacterial colony of BL21 harbouring the appropriate MBP-fusion construct was inoculated into 50mL of GLB + ampicillin and cultured at 37°C overnight (O/N). This O/N culture was diluted 1/50 and added to 4L of GLB + ampicillin and grown at 37°C until the OD600 reached ~0.5. Alternatively, a single bacterial colony of BL21 harbouring the appropriate MBP-fusion construct was streaked onto an LB agar plate and incubated O/N at 37°C. The following morning, cells were scraped off the agar plate, inoculated into 4L of GLB + ampicillin and grown at 37°C until OD600 reached ~0.5. The culture was induced with 0.5mM IPTG at 37°C for 3-4 hours, and then spun at 4000 rpm for 10 minutes repeatedly in 4 X 50mL Falcon tubes (BD Falcon). Each Falcon tube thus contained cells from approximately 1 L of culture. Pellets were washed with 20mL of cold PBT and spun down at 4000rpm for 10 minutes

in a table-top centrifuge. The supernatant was removed and the cell pellet was stored at -70°C. On the next day, pellets were thawed, and resuspended in 15mL of Column buffer by vortexing. The suspension was sonicated until the viscous solution appeared fluid. The debris was spun down and supernatant passed through a 0.45μm filter. The filtrate was supplemented with 1mL of 80% glycerol, mixed and aliquots of 2 mL each were flash frozen and stored at -70°C or put through the purification process.

The MBP fusion protein was purified as described in pMAL™ Protein Fusion and Purification System (Expression and Purification of Proteins and Cloned Genes) manual (PFPSM) (New England Biolabs). The purified protein was then desalted 2X with Coupling buffer, using Amicon Ultra 10 or 30 kDa MWCO (Millipore) concentration devices. Roughly, 7-10 mg of fusion protein in coupling buffer was cross-linked to a HiTrap NHS column (Amersham) according to manufacturer's instructions and the affinity columns were kept at 4°C until use. The efficiency of the coupling or crosslinking reaction was determined according to manufacturer's instructions.

The affinity column was put through a series of washes at 0.5mL/min. First, it was washed with 5mL 0.1M glycine pH 2.8 to remove noncovalently bound protein from the column. This wash was followed by 20mL of PBS, 5mM PBS + 1mg/mL BSA, and 10ml PBS washes. The DCIP4 antibody was diluted 1/10 in PBS and applied to the column and the flow thorough was reapplied to the column once more. For every 10ml of diluted antibody, the column was washed with 20mL of PBS, and the bound antibody was eluted with 5mL 0.2M glycine pH 2.8 or 3.5M $MgCl_2$. The eluted antibody was desalted 1 X with PBS and once with PBS + 0.02% sodium azide using Amicon Ultra 10 or 30 KDa MWCO (Millipore) concentration devices. The antibody was concentrated to

its original volume (1mL) or to half its original volume and tested for reactivity against lysates from wild-type and mutant *DCIP4* flies and recombinant purified MBP-DCIP4 at 1/20,000-1/1000 dilutions.

2.12 Embryo fixation

Components:

20% paraformaldehyde: 10g of paraformaldehyde was added to a 50mL Falcon tube. 35mL of water and 0.5mL of 1M NaOH was added and the tube was heated at 65°C until the paraformaldehyde dissolved. 10mL of 5X phosphate buffered saline (PBS) was added.

PBS: as per Sambrook et al. (1989).

Heptane

Methanol or 80% Ethanol

0.01% Triton-X

Household Bleach

Embryos were fixed as described in Ashburner (1989). Embryos were allowed to develop as indicated and dechorionated using 50% household bleach: 0.01% Triton-X, for 3 minutes and rinsed with 0.01% Triton-X. Removal of the protective chorion is required to allow the diffusion of molecular probes into the embryo.

Embryos were fixed in a solution containing 1mL 20% paraformaldehyde, 4mL 1X phosphate buffered saline (PBS), and 5mL heptane. Vigorous shaking was performed

for 25 minutes and the bottom aqueous layer was removed. 5mL methanol was added and the tube was shaken vigorously for one minute and the embryos were allowed to settle. Embryos were removed and washed with methanol three times. Some antibodies are sensitive to methanol fixation therefore some embryos were fixed by substituting 80% ethanol for methanol.

2.13 Cuticle preparations

Components:

Hoyer's medium: 30g of gum arabic was added to 50mL of water. Once dissolved, 200g of chloral hydrate was added sparingly while stirring. 20g of glycerol was introduced, mix and centrifuged at 5000rpm to 10000rpm for 20 minutes to separate and remove the sediment. Medium was stored in the dark.

Household Bleach

0.01% Triton-X

Cuticle preparations were performed as described by Ashburner (1989). Embryos were allowed to develop a full 24 hours AEL in order to allow for the secretion of the cuticle. Embryos were dechorionated using 50% household bleach : 50% 0.01% Triton-X for three minutes and rinsed with 0.01% Triton-X.

Hoyer's medium was placed upon glass slides and dechorionated embryos were added to the medium. A glass coverslip was used to cover the medium and the slides were incubated at 65°C until the embryos cleared, leaving the cuticle.

2.14 RNA *in situ* hybridization

Components:

4% paraformaldehyde

Methanol

PBSTw: PBS with 0.1% Tween-20

Bovine Serum Albumin (BSA)

Hybridization buffer: 50% deionized formamide, 4X SSC (as per Sambrook et al. (1989), 1X Denharts (as per Sambrook et al., 1989), 0.1% Tween-20, 5% dextran sulphate, 250μg/mL salmon sperm DNA, 50μg/mL heparin. Stored at -20°C.

Wash buffer: 50% formamide, 2X SSC (as per Sambrook et al., 1989), 0.1% Tween-20.

Ashburner Wash Buffer: 100mM NaCl, 50mM $MgCl_2$, 100mM Tris, pH 9.5, 0.1% Tween-20. As described by Ashburner (1989).

NBT: 4-nitro blue tetrazolium chloride at 100μg/μL (Roche, 92451026)

BCIP: 5-bromo-4-chloro-3-indolyl-phosphate at 50μg/μL (Roche, 1383221)

RNA *in situs* were performed as described in Sem et al. (2002). Digoxigenin-labelled (DIG) RNA probes were generated by *in vitro* transcription of the antisense strand of the cDNA clones using the DIG RNA labelling kit from Roche Molecular Biochemicals according to manufacturer's instructions. Unincorporated nucleotides were

then removed using MicroSpin S-200 HR columns. One microlitre of the probe was run on a 1% DNA agarose gel to quantitate the concentration of RNA. The intensity of the RNA band was compared to the intensity of the 1.6 kb band from a 1 kb DNA ladder (Invitrogen, 0.5μg loaded). As a general rule, the amount of probe added to each hybridization reaction was two times the intensity of the 1.6 kb DNA marker. Fixed embryos stored in either methanol or 80% ethanol were serially rehydrated for two minutes in 3:1, 1:1, 1:3 methanol : 4% paraformaldehyde. The embryos were then fixed in 4% paraformaldehyde for ten minutes, followed by three rinses in PBSTw. 0.5mL of hybridization buffer (boiled for ten minutes and put on ice) was added to the embryos and prehybridized for one hour at 52°C. The probe was then added and incubation was allowed to proceed at 52°C overnight without agitation. Following overnight incubation, the probe was removed and stored at -20°C for reuse. Before reuse, the probe was heated at 65°C for 10-15 minutes to denature the RNA. After removal of probe, the embryos were then washed in wash buffer at 52°C for at least four times, with the last wash allowed to proceed overnight. Room temperature rinses were done 3X with PBSTw followed by washing for 30 minutes in PBSTw. PBSTw was removed and anti-digoxigenin-alkaline phosphatase (Roche Molecular Biochemicals), diluted 1,000X in 1mL PBSTw + 5% BSA, was added. Samples were incubated for 90 minutes at room temperature. The antibody solution was discarded. Embryos were washed 3 X 10 minutes in PBSTw followed by 3 X 5 minutes in alkaline phosphatase wash buffer. The last wash was not removed and 3.4μL of NBT and 3.5μL of BCIP were added. Colour development was allowed to proceed under dissection microscope and halted when the desired resolution was obtained. The colour reaction was stopped by rinsing embryos 3X

in PBSTw. Embryos were rotated in 70% glycerol for 30 minutes at room temperature to allow clearing of embryonic tissue and subsequently stored at 4°C or mounted for visualization. Embryos were observed using differential interference contrast (DIC) microscopy on a Zeiss Axioplan microscope.

2.15 Immunostaining of *Drosophila* embryos

Components:

PBT: PBS + 0.1% Triton-X

BSA

PBB: PBT + 1% BSA

Nickel solution: 2.5% Nickel ammonium sulphate, 0.1% sodium acetate buffer pH 6.

DAB reaction mix: 50µL of 5mg/mL DAB, 10µL of 0.2 g/mL glucose, 2µL of 0.2g/mL NH_4Cl, 1mL of Nickel solution, and 3µL of 2mg/mL glucose oxidase (Sigma, G2133, 250000U).

Immunostaining was performed as described by (Harden et al., 1996). Fixed embryos were rehydrated in 1mL PBT for 3 X 10 minutes on a Nutator. All incubation and wash steps were performed at room temperature while rotating, unless otherwise stated. Embryos were blocked in PBB for one hour. An appropriate concentration of primary antibodies diluted in PBB was introduced to the embryos and incubated at 4°C overnight. Concentrations of antibodies were as follows: Hts, 1/5; DCIP4, 1/20,000-

1/1000; pMad 1/10,000-1/7,500. Solution was then removed, followed by washing 3 X 10 minutes in PBT. The last PBT wash was then removed and embryos were exposed to the appropriate PBB diluted secondary antibody conjugate to Horseradish peroxidase (HRP), Fluorescein (FITC), or biotin.

HRP-mediated visualization of antibody staining using DAB was performed using a secondary antibody directly conjugated to HRP or a biotinylated secondary antibody which was then subsequently exposed to streptavidin conjugated-HRP to amplify the signal. HRP or biotin conjugated goat anti-rabbit or goat anti-mouse secondary antibodies were added in a 1/200 dilution (Vector Laboratories). HRP or biotin conjugated donkey anti-chicken was used in a 1/500 dilution (Jackson Immunoresearch). Incubation was done for two hours at room temperature. Embryos were then washed 3 X 10 minutes in PBT. If a biotinylated secondary was used, the embryos were then incubated with 1/1000-2000 streptavidin-HRP in PBB for 30 minutes, followed by 3 X 10 minute washes with PBT. Colour development proceeded in the presence of DAB reaction mix and staining was stopped by rinsing 3X with PBT. PBT was then substituted with 70% glycerol and embryos equilibrated for 30 minutes. Samples were stored at 4°C or mounted for observation. Embryos were observed using differential interference contrast (DIC) microscopy.

Fluorescent detection of antibody staining was conducted using goat anti-mouse or goat anti-rabbit antibodies conjugated to FITC or biotin, or with donkey anti-chicken-HRP and subsequent Cyanine 3 (Cy-3)-tyramide (Renaissance, Perkin Elmer). Biotinylated secondaries were subsequently exposed to streptavidin conjugated Texas Red (TRITC) (Vector Laboratories). All steps were perfomed in the dark following the addition of the fluorophore conjugates to embryos. FITC- or biotin-conjugated anti-mouse or anti-rabbit secondary

antibodies were added in a 1/200 dilution (Vector Laboratories). Incubation was done for two hours at room temperature. Embryos were washed 3 X 10 minutes in PBT. If a biotinylated secondary antibody was used, the embryos were then incubated with 1/1000 TRITC in PBB for one hour and subsequently washed 3 X 10 minutes in PBT. If anti- chicken-HRP was used, the embryos were subjected to 1/400 Cy3-tyramide in Amplification buffer for 30 minutes and subsequently rinsed 3X with PBT. Following the removal of the last wash/rinse, Vectashield mountant (Vector Laboratories) was added and embryos equilibrated for 30 minutes at room temperature or overnight at 4°C in the dark. Embryos were observed using confocal microscopy.

Unless otherwise stated all primary antibodies were obtained from the Developmental Studies Hybridoma Bank. The p-Mad antibody was obtained from P. ten Dijke. DNA was stained with 1/10,000 Propidium Iodide (Molecular probes), or 1/10,000 SYBR GREEN (Molecular Probes).

2.16 Generation of mutations in *Drosophila* using Ethyl Methyl Sulphonate (EMS)

Flies homozygous for the ebony marker, e^1, which produces black body colour, were fed media that contained 50 μM EMS in 1% sucrose as described in (Greenspan, 1997). 500 EMS-exposed chromosomes were isolated as described in (Greenspan, 1997) and screened for lethality when in combination with the deficiency, *Df(3L)C175*. All lines that complemented *Df(3L)C175* were identified by the presence of brown bodied F1 progeny as *Df(3L)C175* does not carry the e^1 marker.

2.17 Generation of *Drosophila* mosaics

The generation of genetic mosaics or 'clones' has been shown to be an important tool for the analysis of the maternal effect of recessive zygotic mutations as well as the examination of the tissue specific roles of a gene. This method takes advantage of the site-specific recombination activity of the FLP recombinase, which can direct recombination between homologous chromosomes at FRT sequences during mitosis.

Alleles of the gene of interest are recombined onto chromosomes containing FRT sequences near the centromere. FLP-mediated recombination allows the creation of clones of cells homozygous for the allele in a heterozygous individual.

FLP is placed under the control of a heat shock promoter, hsp70, and is therefore induced, usually at 37°C. The scheme for the duration and repetition of heat shock is determined experimentally by the investigator. In this way, specific tissues can be targeted by heat shock inductions at the desired developmental stage.

To generate follicle cell clones lacking *DCIP4*, *hsFLP;TM3Sb/TM6Tb* females were crossed to *FRT79D, GFP* males. The ubi-GFP transgene is a reporter that allows visualization of cells that are not homozygous mutant clones. The *hsFLP; FRT79D, ubi-GFP/TM3Sb* males from the F1 progeny were mated to *FRT79D, DCIP4$^{34-1}$/TM3Sb* females. F2 progeny were heat shocked for 2 hours at 37°C, in order to drive genetic recombination in follicle cells undergoing mitosis. This was done for 4 consecutive days to ensure younger larva that were emerging at later times were also exposed to the same heat shock regiment at the proper developmental stage. Female progeny, of the genotype *hsFLP;FRT79D, ubi-GFP/FRT79D, DCIP4$^{34-1}$*, were grown on media containing yeast

for a couple of days to allow for development of healthy ovaries. The females' ovaries were dissected and stained as described in section 2.15 to retrieve the egg chambers.

2.18 Fixation of *Drosophila* egg chambers

Components:

EBR buffer: 130mM NaCl, 4.7mM KCl, 1.9mM $CaCl_2$, 10mM H*EP*ES pH 6.9 as per Sambrook et al. (1989).

Buffer B: 100mM potassium phosphate pH 6.8 as per Sambrook et al. (1989), 450mM KCl, 150mM NaCl, 20mM MgCl2.

Devitellinizing buffer: 1 vol buffer B, 1 vol formaldehyde 36%, 4 vol water.

Formaldehyde 36%

BSA

PBS

PBO: 1 X PBS, 0.3% Triton-X, 0.5% BSA.

Heptane

Ovary fixation and staining was performed as described by (Verheyen and Cooley, 1994a). Ovaries were dissected in cold EBR and transferred to a microfuge tube containing cold EBR on ice. EBR was removed and 100μL devitellinizing buffer and 600μL heptane was added. The sample was vigorously agitated to be sure that the buffer was saturated with heptane and then was rotated for 10 minutes at room temperature. The solution was removed with a pipette and rinsed with PBS three times. The ovaries

were washed 3 X in PBS for 10 minutes each. If F-actin was being visualised, the egg chambers were subjected to 1:1000 phalloidin-FITC or TRITC conjugate (Sigma) for 30 minutes while rotating. The sample was then rinsed 3X with PBS and the last rinse was replaced with Vectashield. If DNA was being visualised, ovaries were treated as described by Orsulic and Peifer (1994). Briefly, dissected ovaries were fixed and incubated with Ribonuclease A for 2 hours at 37°C. The sample was then rinsed 3X with PBS and treated with either 1/10,000 Propidium Iodide (Molecular Probes) or 1/10,000 SYBR Green (Molecular Probes) for 20 minutes. The egg chambers were then rinsed 3X with PBS.

If ovaries were stained for a specific protein, after the 3 X 10 minute washes with PBS, the ovaries were blocked for 10 minutes in PBO and then primary antibody was added. Sample were treated the same as embryos from this point on. If doing antibody staining and visualising F-actin or DNA, after the last wash, F-actin staining or DNA staining was completed as described above and Vectashield was added. Ovaries were viewed with a confocal microscope.

2.19 Western analysis

Components:

Protein sample buffer: 0.01% mercaptoethanol, 2% SDS, 0.01% bromophenol blue, 6% glycerol, 25mM Tris pH 6.8.

Running buffer: 2.5mM Tris pH 8.3, 19.2mM glycine, 0.01%SDS.

Transfer buffer: 2.5mM Tris pH 8.3, 19.2mM glycine, 0.01% SDS, 20% methanol.

Protein samples were separated on 8-12% polyacrylamide gels using the BioRad Mini-Protean II Electrophoresis Cell and transferred to nitrocellulose membrane using the BioRad Trans-Blot Semi Dry following manufacturer's instructions. Gels were prepared as in Sambrook et al. (1989). Protein samples were loaded with sample buffer and electrophoresis carried out in running buffer. The Trans-Blot was run at 15V for one hour using the transfer buffer to transfer the proteins from the gel to the nitrocellulose membrane.

Western blotting was performed as per manufacturer's instructions using reagents from the Western Blotting Chemiluminescence Kit obtained from Roche. Concentrations of primary antibodies as follows: affinity purified chicken polyclonal anti-DCIP4 1:5-10,000 or 1:5000 rabbit polyclonal DPAK. Secondary antibody was a 1:2000-5000 dilution of an anti-rabbit or anti-chicken coupled HRP antibody. Visualization was performed using the luminal reagent from the Western Blotting Chemiluminescence kit (Roche).

2.20 Transgene expression using heat shock inducible GAL4 lines during embryogenesis.

For heat shock induction of transgenes, embryos were collected and aged at 25 °C for the appropriate stage. They were then placed in vials and heat shocked in a water bath set at 37°C. Following heat-shock, embryos were aged at 21°C for at least 48 h and

subjected to cuticle preparation, or aged for 7 h at 21°C and fixed for RNA *in situ* hybridization.

3 RESULTS PART 1: *DROSOPHILA* CDC42 INTERACTING PROTEIN 4 (DCIP4)

3.1 Identification of the *DCIP4* gene and cDNA

As part of our effort to better understand Cdc42 signalling in *Drosophila*, we decided to characterize the *Drosophila* homologue of the Cdc42 effector protein, CIP4. Expressed Sequence Tags (ESTs) were identified that represented candidate full-length cDNAs of *DCIP4* (Rubin et al., 2000). This was accomplished by performing a tBLASTn search, using the human CIP4 protein sequence and the six-frame translation of all known *Drosophila* ESTs. We identified *LD14951* as the longest cDNA with a translation that bore homology to CIP4. Overlapping *Eco*RI and *Pst* I fragments of this cDNA were subcloned and sequenced. Figure 3.1 shows the alignment of the cDNA sequence of *LD14951* with its corresponding translated protein product. We named the gene encoding *LD14951*, *Drosophila CIP4* (*DCIP4*), after its mammalian homologue.

Following the completion of this work, the *Drosophila* genome was sequenced (Adams et al., 2000). Blast searches against the six-frame translation of the *Drosophila* genome with both the CIP4 protein sequence and the translation of the *DCIP4* cDNA sequence returned two predicted genes, *CG15015* and *CG11341*. After completion of the Release 3 annotation of the *Drosophila* euchromatic genome (Misra et al., 2002), these two predicted genes were combined to form the complete *DCIP4* gene, which was assigned the prediction name, *CG15015*. *DCIP4* is 39654 nucleotides in length and physically maps to bases 4307066-4346719 on the left arm of the third chromosome,

Figure 3.1 Nucleotide sequence and conceptual translation of the *DCIP4* cDNA, *LD14951.*

Shaded regions outline the different domains present in the protein sequence.

Purple: FCH, red: Coiled-coil, orange: HR1, green: PEST and blue: SH3.

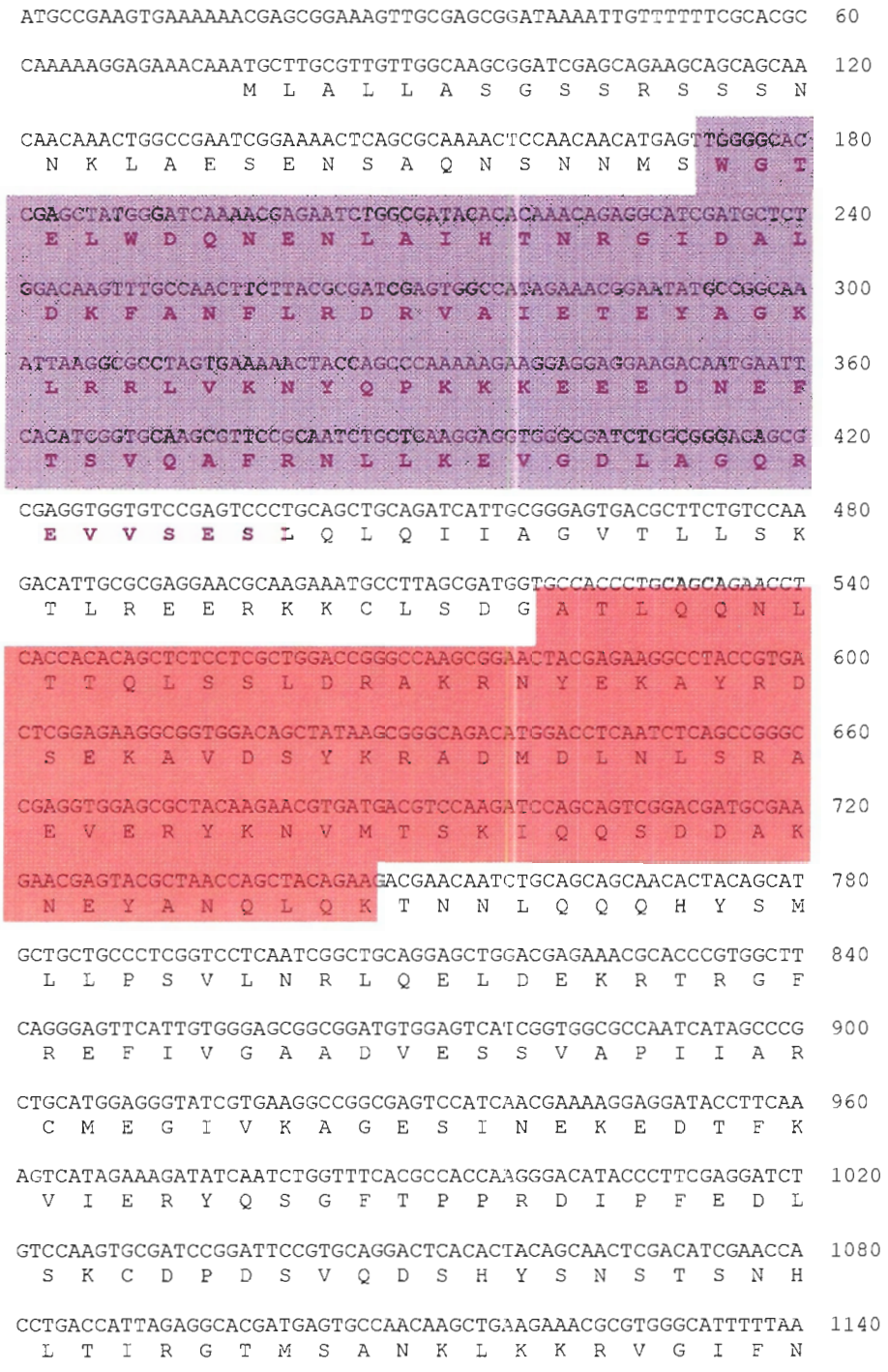
ATGCCGAAGTGAAAAAACGAGCGGAAAGTTGCGAGCGGATAAAATTGTTTTTTCGCACGC 60
CAAAAAGGAGAAACAAATGCTTGCGTTGTTGGCAAGCGGATCGAGCAGAAGCAGCAGCAA 120
M L A L L A S G S S R S S S N
CAACAAACTGGCCGAATCGGAAAACTCAGCGCAAAACTCCAACAACATGAGTTGGGGCAC 180
N K L A E S E N S A Q N S N N M S W G T
CGAGCTATGGGATCAAAACGAGAATCTGGCGATACACACAACAGAGGCATCGATGCTCT 240
E L W D Q N E N L A I H T N R G I D A L
GGACAAGTTTGCCAACTTCTTACGCGATCGAGTGGCCATAGAAACGGAATATGCCGGCAA 300
D K F A N F L R D R V A I E T E Y A G K
ATTAAGGCGCCTAGTGAAAAACTACCAGCCCAAAAAGAAGGAGGAGGAAGACAATGAATT 360
L R R L V K N Y Q P K K K E E E D N E F
CACATCGGTGCAAGCGTTCCGCAATCTGCTCAAGGAGGTGGCGATCTGGCGGGACAGCG 420
T S V Q A F R N L L K E V G D L A G Q R
CGAGGTGGTGTCCGAGTCCCTGCAGCTGCAGATCATTGCGGGAGTGACGCTTCTGTCCAA 480
E V V S E S L Q L Q I I A G V T L L S K
GACATTGCGCGAGGAACGCAAGAAATGCCTTAGCGATGGTGCCACCCTGCAGCAGAACCT 540
T L R E E R K K C L S D G A T L Q Q N L
CACCACACAGCTCTCCTCGCTGGACCGGGCCAAGCGGAACTACGAGAAGGCCTACCGTGA 600
T T Q L S S L D R A K R N Y E K A Y R D
CTCGGAGAAGGCGGTGGACAGCTATAAGCGGGCAGACATGGACCTCAATCTCAGCCGGGC 660
S E K A V D S Y K R A D M D L N L S R A
CGAGGTGGAGCGCTACAAGAACGTGATGACGTCCAAGATCCAGCAGTCGGACGATGCGAA 720
E V E R Y K N V M T S K I Q Q S D D A K
GAACGAGTACGCTAACCAGCTACAGAAGACGAACAATCTGCAGCAGCAACACTACAGCAT 780
N E Y A N Q L Q K T N N L Q Q Q H Y S M
GCTGCTGCCCTCGGTCCTCAATCGGCTGCAGGAGCTGGACGAGAAACGCACCCGTGGCTT 840
L L P S V L N R L Q E L D E K R T R G F
CAGGGAGTTCATTGTGGGAGCGGCGGATGTGGAGTCATCGGTGGCGCCAATCATAGCCCG 900
R E F I V G A A D V E S S V A P I I A R
CTGCATGGAGGGTATCGTGAAGGCCGGCGAGTCCATCAACGAAAAGGAGGATACCTTCAA 960
C M E G I V K A G E S I N E K E D T F K
AGTCATAGAAAGATATCAATCTGGTTTCACGCCACCAAGGGACATACCCTTCGAGGATCT 1020
V I E R Y Q S G F T P P R D I P F E D L
GTCCAAGTGCGATCCGGATTCCGTGCAGGACTCACACTACAGCAACTCGACATCGAACCA 1080
S K C D P D S V Q D S H Y S N S T S N H
CCTGACCATTAGAGGCACGATGAGTGCCAACAAGCTGAAGAAACGCGTGGGCATTTTTAA 1140
L T I R G T M S A N K L K K R V G I F N

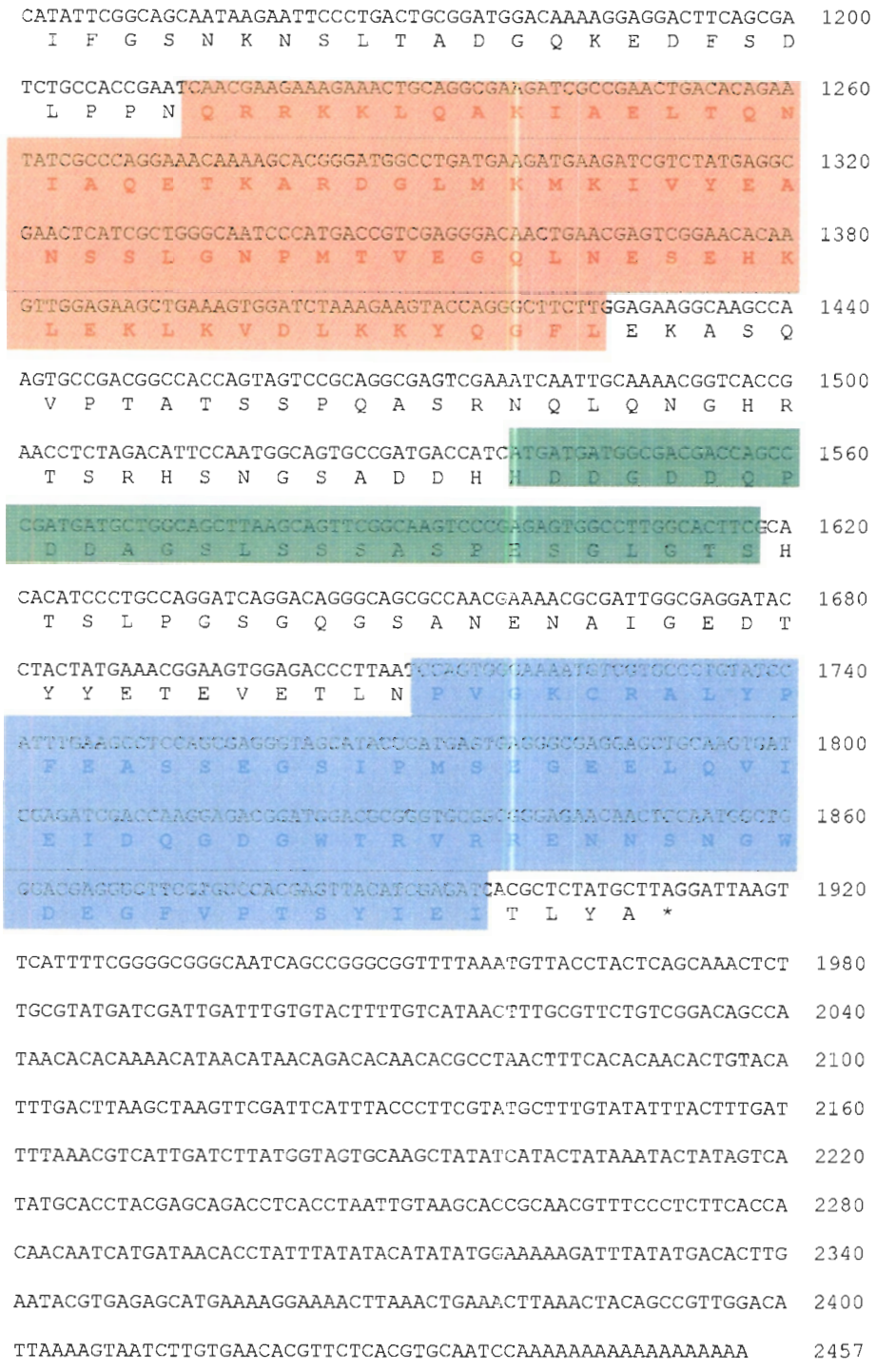
CATATTCGGCAGCAATAAGAATTCCCTGACTGCGGATGGACAAAAGGAGGACTTCAGCGA 1200
I F G S N K N S L T A D G Q K E D F S D
TCTGCCACCGAATCAACGAAGAAAGAAACTGCAGGCGAAGATCGCCGAACTGACACAGAA 1260
L P P N Q R R K K L Q A K I A E L T Q N
TATCGCCCAGGAAACAAAAGCACGGGATGGCCTGATGAAGATGAAGATCGTCTATGAGGC 1320
I A Q E T K A R D G L M K M K I V Y E A
GAACTCATCGCTGGGCAATCCCATGACCGTCGAGGGACAACTGAACGAGTCGGAACACAA 1380
N S S L G N P M T V E G Q L N E S E H K
GTTGGAGAAGCTGAAAGTGGATCTAAAGAAGTACCAGGGCTTCTTGGAGAAGGCAAGCCA 1440
L E K L K V D L K K Y Q G F L E K A S Q
AGTGCCGACGGCCACCAGTAGTCCGCAGGCGAGTCGAAATCAATTGCAAAACGGTCACCG 1500
V P T A T S S P Q A S R N Q L Q N G H R
AACCTCTAGACATTCCAATGGCAGTGCCGATGACCATCATGATGATGGCGACGACCAGCC 1560
T S R H S N G S A D D H H D D G D D Q P
CGATGATGCTGGCAGCTTAAGCAGTTCGGCAAGTCCCGAGAGTGGCCTTGGCACTTCGCA 1620
D D A G S L S S S A S P E S G L G T S H
CACATCCCTGCCAGGATCAGGACAGGGCAGCGCCAACGAAAACGCGATTGGCGAGGATAC 1680
T S L P G S G Q G S A N E N A I G E D T
CTACTATGAAACGGAAGTGGAGACCCTTAATCCAGTGCCAAAATGTCCGTGCCCTCTATCC 1740
Y Y E T E V E T L N P V G K C R A L Y P
ATTTGAAGCCTCCAGCGAGGGTAGCATACCCATGAGTCAGGGCGAGCAGCTGCAAGTGAT 1800
F E A S S E G S I P M S Q G E Q L Q V I
CGAGATCGACCAAGGAGACGGATGGACGCGGTGCGGCCGGAGAACAACTCCAATGCCTG 1860
E I D Q G D G W T R V R R E N N S N G W
GCACGAGGCTTCGTGCCACGAGTTACATCGAGATCACGCTCTATGCTTAGGATTAAGT 1920
D E G F V P T S Y I E I T L Y A *
TCATTTTCGGGGCGGGCAATCAGCCGGGCGGTTTTAAATGTTACCTACTCAGCAAACTCT 1980
TGCGTATGATCGATTGATTTGTGTACTTTTGTCATAACTTTGCGTTCTGTCGGACAGCCA 2040
TAACACACAAAACATAACATAACAGACACAACACGCCTAACTTTCACACAACACTGTACA 2100
TTTGACTTAAGCTAAGTTCGATTCATTTACCCTTCGTATGCTTTGTATATTTACTTTGAT 2160
TTTAAACGTCATTGATCTTATGGTAGTGCAAGCTATATCATACTATAAATACTATAGTCA 2220
TATGCACCTACGAGCAGACCTCACCTAATTGTAAGCACCGCAACGTTTCCCTCTTCACCA 2280
CAACAATCATGATAACACCTATTTATATACATATATGGAAAAAGATTTATATGACACTTG 2340
AATACGTGAGAGCATGAAAAGGAAAACTTAAACTGAAACTTAAACTACAGCCGTTGGACA 2400
TTAAAAGTAATCTTGTGAACACGTTCTCACGTGCAATCCAAAAAAAAAAAAAAAAAA 2457

according to release 4.1 of the *Drosophila* annotated genome sequence (Drysdale, 2005). This region corresponds to the cytological location *64B2-4*. The *DCIP4* gene is transcribed on the minus strand of the third chromosome.

As more cDNA libraries were generated by the *Drosophila* Gene Collection (DGC) (Stapleton et al., 2002), another *DCIP4* full-length cDNA, *RE39037*, was identified. The DGC and Flybase recognise this cDNA as the longest cDNA corresponding to the predicted gene, *CG15015*. *RE39037* was isolated from the RIKEN 0-22 hour embryonic cDNA library and is 60 bases longer than *LD14951*. The difference between the two cDNAs results from alternate splicing of the 9th intron where the splice donor site (GT), used to generate *RE39037,* is 60 bases downstream from that used to generate *LD14951* (Figure 3.2 B).

3.2 The *DCIP4* transcript and protein

The *DCIP4* transcript, isolated from adult flies, is roughly 2.4 Kb in length, as determined by Northern blot analysis with a labelled *DCIP4* cDNA probe and comparison with RNA standards (Figure 3.4 I). This is comparable to the lengths of RE39037 and LD14951 cDNAs (roughly 2.5 and 2.45 Kb, respectively). This transcript makes a protein that migrates at an estimated molecular weight of 100 kDa as detected from Western blot analysis using an antibody made against recombinant DCIP4 protein made from the *RE39037* cDNA (Figure 3.5 I). A 75 kDa band is also seen (data not shown). The predicted RE39037 protein has a molecular weight of about 70 kDa.

The DCIP4 protein (the translation of the *RE39037* cDNA sequence), has three known domains and one putative motif (Figure 3.1 and 3.2). At its amino (N)-terminus

Figure 3.2 *LD14951* and *RE39037* may be splice variants of *DCIP4*.

Alignment of the translated sequences of *DCIP4* cDNAs, *LD14951* and *RE39037*. (A) Schematic showing that *LD14951* and *RE39037* differ by alternate in-frame splicing of an exon (shaded in red) near the 3' end of the *DCIP4* gene. This results in a smaller exon in *LD14951*. (B) Bases 4308379-4308559 of the minus strand of chromosome 3L, within the *DCIP4* gene, showing the different splice donor sequence (GT) used by each variant. Sequence in red outlines the exon shaded in red in (A). Sequences in black represent introns. The splice acceptor site is shown in bold black. The donor site in green is used to generate *LD14951* and the donor site in blue is used to generate *RE39037*. (C) Alignment of the translated products of *LD14951* and *RE39037*. Shaded regions outline the different domains present in the protein sequence. Purple: FCH, red coiled-coil, orange: HR1, green: PEST and light blue: SH3.

A

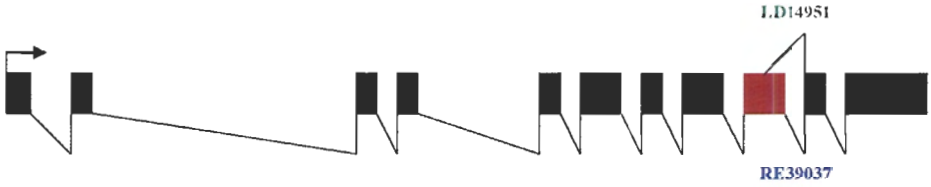

B

```
4308559 ACAATCTAAT AACTGAATAC CCCCACTTTA GACATTCCAA TGGCAGTGCC GATGACCATC
4308499 ATGATGATGG CGACGACCAG CCCGATGATG CTGGCAGCTT AAGCAGGTCA GATTCTGAGG
4308439 ATAATGTGGC GCAAATACAA AATGGGCATA ATAATAACAA TAACGGGTAC ACTCATAAGT
```

C

```
1   MLALLASGSSRSSSNNKLAESENSAQNSNNMSWGTELWDQNENLAIHTNRGIDALDKFAN RE39037
1   MLALLASGSSRSSSNNKLAESENSAQNSNNMSWGTELWDQNENLAIHTNRGIDALDKFAN LD14951

61  FLRDRVAIETEYAGKLRRLVKNYQPKKKEEEDNEFTSVQAFRNLLKEVGDLAGQREVVSE RE39037
61  FLRDRVAIETEYAGKLRRLVKNYQPKKKEEEDNEFTSVQAFRNLLKEVGDLAGQREVVSE LD14951

121 SLQLQIIAGVTLLSKTLREERKKCLSDGATLQQNLTTQLSSLDRAKRNYEKAYRDSEKAV RE39037
121 SLQLQIIAGVTLLSKTLREERKKCLSDGATLQQNLTTQLSSLDRAKRNYEKAYRDSEKAV LD14951

181 DSYKRADMDLNLSRAEVERYKNVMTSKIQQSDDAKNEYANQLQKTNNLQQQHYSMLLPSV RE39037
181 DSYKRADMDLNLSRAEVERYKNVMTSKIQQSDDAKNEYANQLQKTNNLQQQHYSMLLPSV LD14951

241 LNRLQELDEKRTRGFREFIVGAADVESSVAPIIARCMEGIVKAGESINEKEDTFKVIERY RE39037
241 LNRLQELDEKRTRGFREFIVGAADVESSVAPIIARCMEGIVKAGESINEKEDTFKVIERY LD14951

301 QSGFTPPRDIPFEDLSKCDPDSVQDSHYSNSTSNHLTIRGTMSANKLKKRVGIFNIFGSN RE39037
301 QSGFTPPRDIPFEDLSKCDPDSVQDSHYSNSTSNHLTIRGTMSANKLKKRVGIFNIFGSN LD14951

361 KNSLTADGQKEDFSDLPPNQRRKKLQAKIAELTQNIAQETKARDGLMKMKIVYEANSSLG RE39037
361 KNSLTADGQKEDFSDLPPNQRRKKLQAKIAELTQNIAQETKARDGLMKMKIVYEANSSLG LD14951

421 NPMTVEGQLNESEHKLEKLKVDLKKYQGFLEKASQVPTATSSPQASRNQLQNGHRTSSHS RE39037
421 NPMTVEGQLNESEHKLEKLKVDLKKYQGFLEKASQVPTATSSPQASRNQLQNGHRTSRHS LD14951

481 NGSADDHHDDGDDQPDDAGSLSRSDSEDNVAQIQNGHNNNNNGSASPESGLGTSHTSLPG RE39037
481 NGSADDHHDDGDDQPDDAGSLS----------------------SSASPESGLGTSHTSLPG LD14951

541 SGQGSANENAIGEDTYYETEVETLNPVGKCRALYPFEASSEGSIPMSEGEELQVIEIDQG RE39037
521 SGQGSANENAIGEDTYYETEVETLNPVGKCRALYPFEASSEGSIPMSEGEELQVIEIDQG LD14951

601 DGWTRVRRENNSNGWDEGFVPTSYIEITLYA                                RE39037
581 DGWTRVRRENNSNGWDEGFVPTSYIEITLYA                                LD14951
```

there is an FCH domain, which has been implicated in actin polymerization and direct microtubule binding (Fankhauser et al., 1995; Tian et al., 2000). This domain is followed by an alpha helical region that is predicted to form a coiled-coil domain. This domain is used for self assembly for other members of the PCH family (Kessels and Qualmann, 2004). Following the coiled-coil region, there is an HR-1 domain which is required by mammalian CIP4 proteins for binding to Cdc42 (Aspenstrom, 1997; Tian et al., 2000). Following the HR1 domain, there is a putative PEST motif. PEST motifs are characterised as motifs that are recognized by the degradation machinery (Blondel et al., 2005; Rechsteiner and Rogers, 1996). It is interesting to note that the translations of *RE39037* and *LD14951* differ only in the composition of their PEST domains. The PEST domain predicted in *LD14951* is disrupted in *RE39037* due to the extra 20 amino acids inserted by the alternate splicing (Figure 3.2 C). Finally, a protein-protein interaction domain, the SH3 domain, makes up the C-terminal part of DCIP4. CIP4's SH3 domain has been shown to bind to proline-rich domains of proteins such as WASP and Huntingtin (Holbert et al., 2003; Tian et al., 2000).

As more genomes are being sequenced, the number of predicted DCIP4 homologues in other organisms is increasing. However, several DCIP4 homologues have already been at least partially characterised. Those that are most homologous to DCIP4 include mammalian CIP4s (Aspenstrom, 1997; Tian et al., 2000), vertebrate and mammalian TOCA-1 (Ho et al., 2004; Insall and Machesky, 2004), and the mammalian FBP17s/Rapostlins (Fujita et al., 2002; Kamioka et al., 2004) (Figure 3.3). Overall, the two possible DCIP4 splice forms (translations of *RE39037* and *LD14951*, named

Figure 3.3 Alignment of *LD14951* and *RE39037* translations with closest relatives and homologues from other species.

The alignment program Clustal X was used to produce alignments of DCIP4 isoforms and other homologous proteins. The sequence alignment was viewed with Genedoc. A four level shading system was used in Genedoc to visualise conservation of amino acid residues across the aligned proteins. The darkest to lightest shadings represents 100% (black), 80% or greater (dark grey), 60% or greater (light grey), and less than 60% (no shading) sequence conservation. The consensus line is displayed at the bottom of the alignment with upper and lower case letters representing residues that are 100% and 80% conserved, respectively. Numbers in the consensus line represent different amino acid similarity groups. Similarity groups represent amino acid residues that are considered similar with respect to the chemical properties and structure of their side chains.

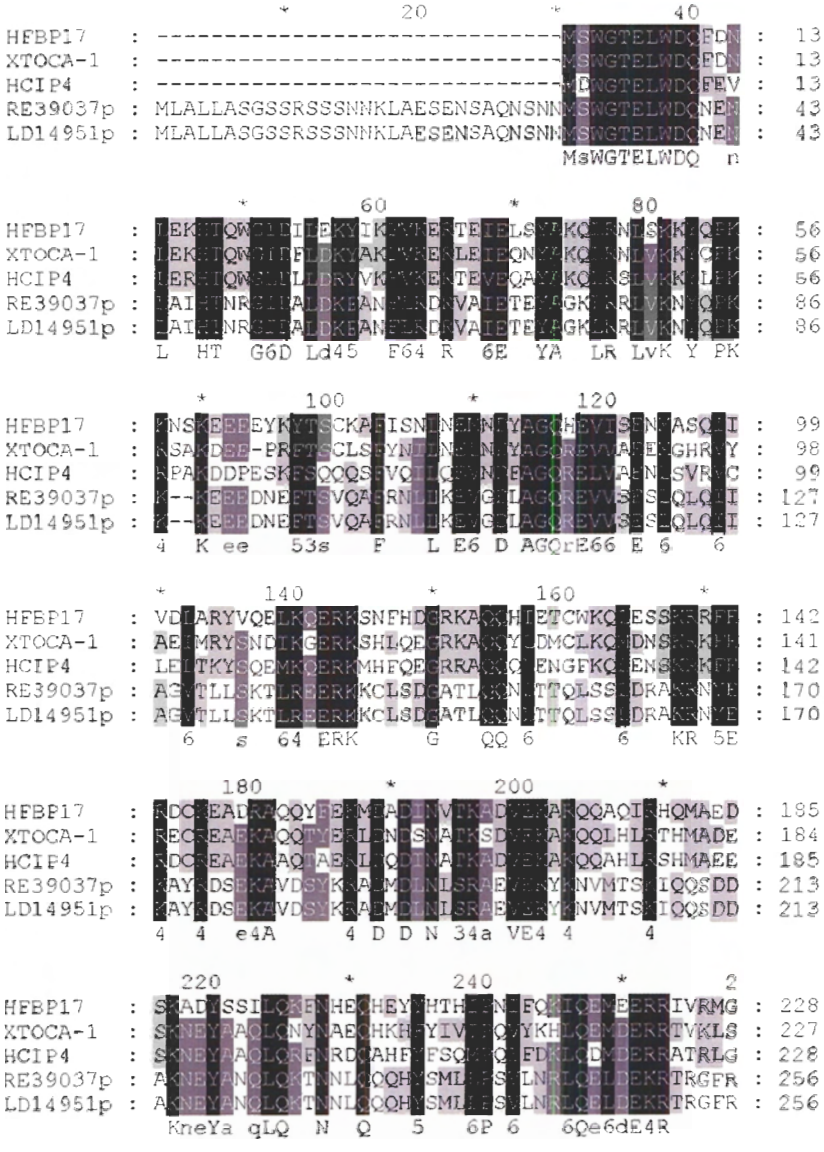

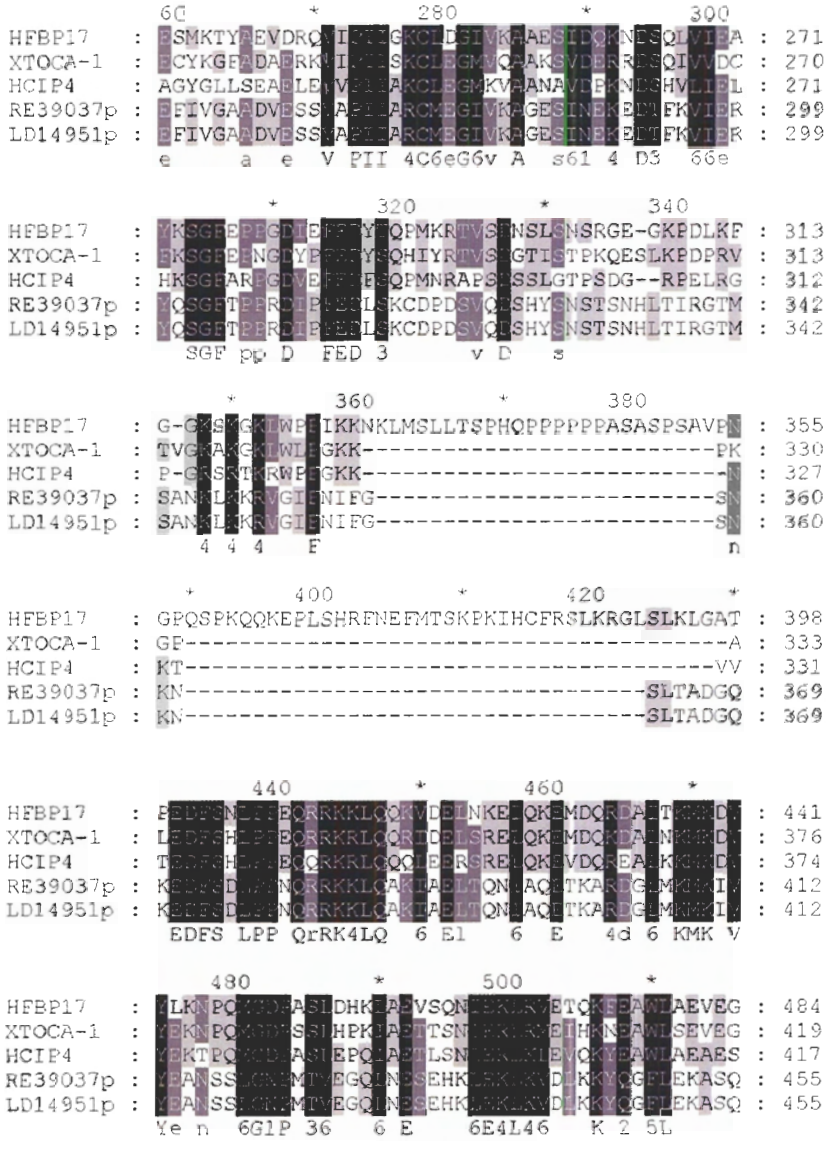

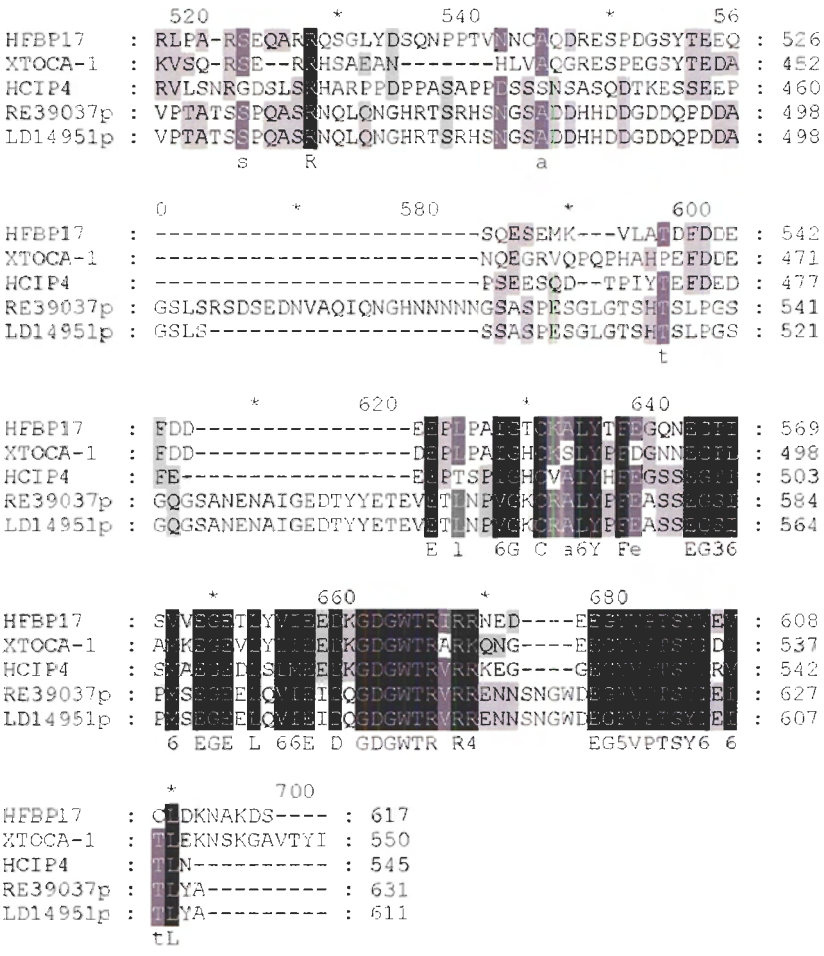

Table 3.1 Comparisons of identities and similarities between DCIP4 isoforms and their domains with homologues from other organisms.

Percentages were compiled from data returned from BLASTp searches with the conserved domains present in the RE39037p/LD14951p protein sequence or with translations of RE39037 and LD14951 against the nr (Non-redundant GenBank CDS translations + PDB + SwissProt + PIR + PRF, excluding those in env_nr.) protein databases.

Table 3.1 Comparisons of identities and similarities between DCIP4 isoforms and their domains with homologues from other organisms.

DCIP4	LD14951p		RE39037p		FCH		CC		HR1		SH3	
	%I	%S	%I	%S	%I	%S	%I	%S	%I	%S	%I	%S
Xenopus tropicalis TOCA-1	36	56	36	55	63	83	40	69	36	67	54	78
H. sapien FBP17	35	54	34	52	54	71	28	69	42	66	55	75
H. sapien CIP4	31	51	31	50	48	71	38	68	36	69	56	75

RE39037p and LD14951p, respectively) are most homologous to *Xenopus tropicalis* TOCA-1 (LD14951p and RE39037p: 36% amino acid identities and LD14951p: 56% and RE39037p: 55% amino acid similarities). However, *Homo sapiens* CIP4 and FBP17 bear similar levels of homology (31-35% and 50-54% identical and similar amino acid residues respectively) to DCIP4 (Table 3.1). The percentage of sequence identities increases in most cases (the exception being the % identities between the FBP17 and DCIP4 coiled-coil domains) when individual domains of the proteins are being compared to the corresponding domain in DCIP4. Thus, the percentage of similar residues increases to 68-83% demonstrating that these homologues bear greater resemblance in their individual domains than they do across the entire protein. It is important to note that the extra sequence present in the PEST domain of RE39037p due to alternate splicing does not align to the primary sequence of any of the homologues shown (Figure 3.3, region between numbers 560-620 shown above alignment).

3.3 *DCIP4* transcript and protein embryonic expression pattern

The wild-type embryonic expression pattern of the DCIP4 transcript and protein was determined using RNA *in situ* hybridization and antibody staining of either *Canton S* or w^{1118} embryos. Whole mount RNA *in situ* hybridization was performed using a DIG-labelled antisense probe generated from either *LD14951* or *RE39037* cDNAs, and the DCIP4 protein expression pattern was determined using the DCIP4 antibody described in Materials and Methods.

DCIP4 has a dynamic mRNA and protein expression pattern during embryonic development. The protein expression pattern not only confirmed stainings thought to be background in the RNA *in situs*, but also provided clues as to where and how DCIP4 may

Figure 3.4 *DCIP4* has a dynamic mRNA expression pattern throughout embryonic development.

(I) Northern blot of total RNA isolated from adult flies showing the *DCIP4* transcript in comparison with the loading control, *rp49*.

(II) Anterior is to the left. (A) Lateral view of a stage 8 embryo showing enrichment in the first few rows of epidermal cells of the maxilla (mx) and labium (lb). (B) Dorsal view of a stage 12 embryo showing enrichment in the brain (arrow) and hind gut (arrowhead). (C) Lateral view of a stage 12 embryo showing expression in the epidermis but absence from the amnioserosa (AS). (D) Dorsal view of a stage 14-15 embryo showing enrichment of *DCIP4* transcript along the dorsal midline (arrowheads) after completion of DC. (E) Ventral views of a stage 13, and a (F) stage 14 embryo, showing expression in the CNS. (G) Dorsal view of a stage 14 embryo showing expression in the visceral mesoderm (arrow). (H) Dorsal view of a stage 12 embryo showing expression in the developing visual system (arrows). (I) Dorsal view of a stage 15 embryos showing enrichment in the Bolwig's Organs (arrows) and in the dorsal longitudinal trunks of the trachea (arrowheads). (J) Dorsal view of a stage 17 embryo showing continuing expression in Bolwig's and in unidentified cells in the head arrows). (K, L, M, N) Lateral views of stage 12-13 embryos showing enrichment in the PNS. Arrows in K point to possible cells bodies of developing sensory neurons. (N) Higher power view of embryo in M showing enrichment of *DCIP4* mRNA in neuronal cluster comprising the lateral monocolopidial chordotonal organ, ventral campaniform sensillum, and ventral chordotonal organ. Arrows in (E) and (M) show enrichment of *DCIP4* in segmental stripes, possibly in the epidermis.

(I)

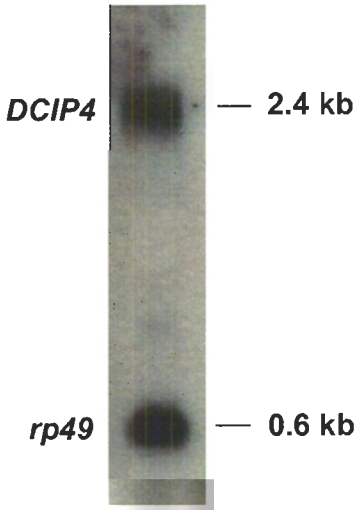

(II)

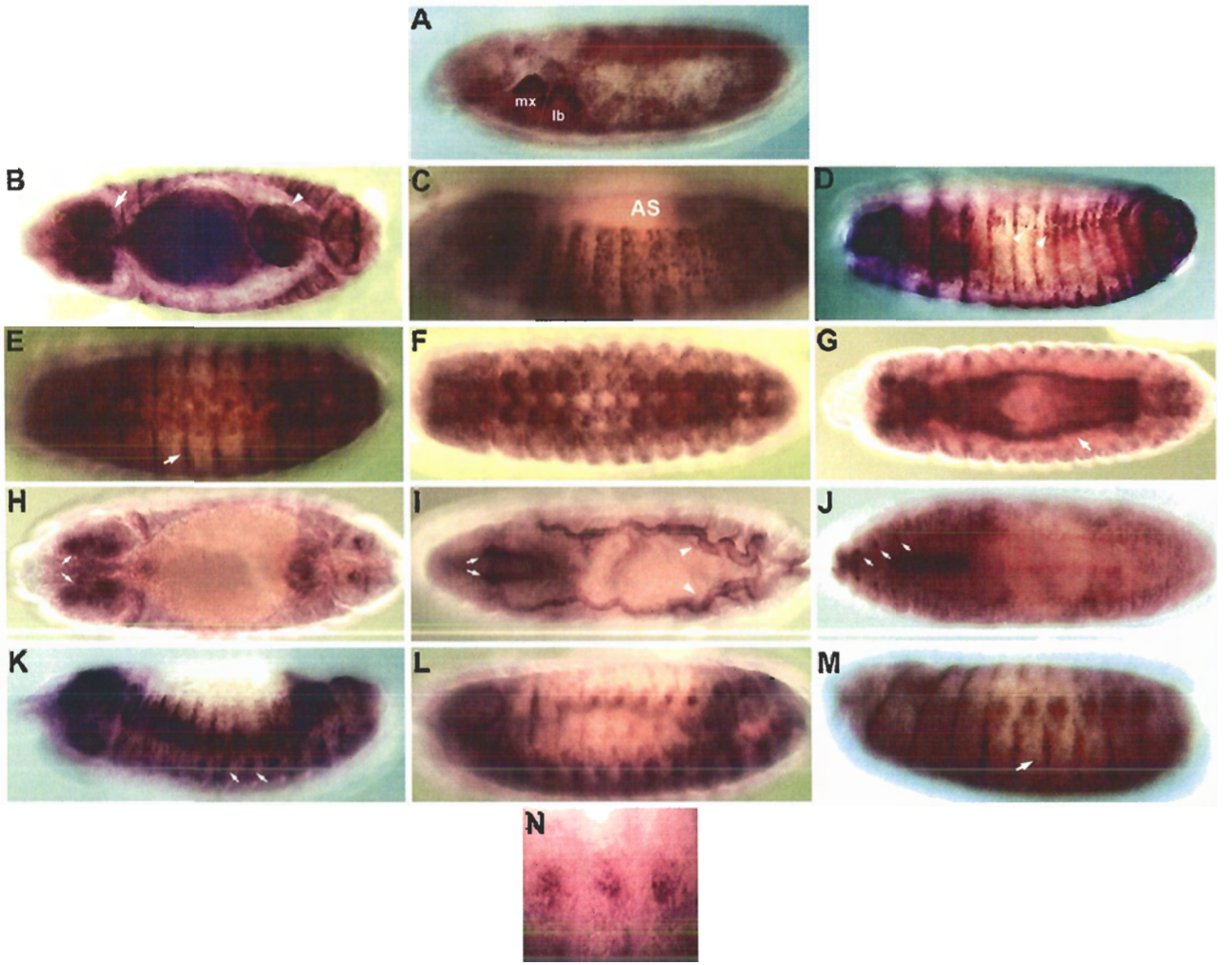

Figure 3.5 The DCIP4 protein is present throughout embryonic development.

(I) Western blot of protein prepared from w^{1118} adult flies showing a band recognized by an affinity-purified DCIP4 antibody used at a 1/10,000 dilution.

(II) Anterior is to the left. (A-C) Lateral views of early embryo showing DCIP4 protein throughout the progression of cellularization. Insets show high powered view. (A) DCIP4 is localized at the apical membrane prior to membrane invagination. (B) Apical DCIP4 localization is maintained in addition to its localization with the invaginating membrane. (C) DCIP4 localizes with apical, lateral and basal cell membranes when cellularization is complete. (D) Dorsal view of stage 12 embryo showing localization of DCIP4 in the hind gut (arrow). (D-F) Dorsal views of stage 13 (D), and early (E) and late (F) stage 14 embryos showing DCIP4 localization at the leading edge throughout DC (arrowhead). (G-I) Ventral views of embryos showing DCIP4 expression in the CNS at stage 12-13 (G) stage 14-15 (H) and stage 16 (I). Lateral view of a stage 13 embryo showing expression of DCIP4 in the ventral nerve chord (J). (K-L) Dorsal views of embryos showing DCIP4 expression in the developing embryonic visual system at stage14 (K) and stage 16 (L). (M) Ventral view of a late stage 13 embryo showing expression of DCIP4 in motor neuron axons of the segmental (arrows) and intersegmental (arrowhead) nerve roots. (N-O) Lateral views of embryos in (M) showing DCIP4 expression in neuronal cluster comprising the lateral monocolopidial chordotonal organ, ventral campaniform sensillum, and ventral chordotonal organ (N, arrow) and magnified in (O, arrow).

(I)

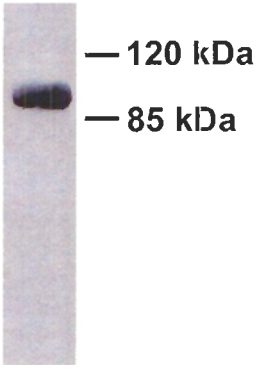

(II)

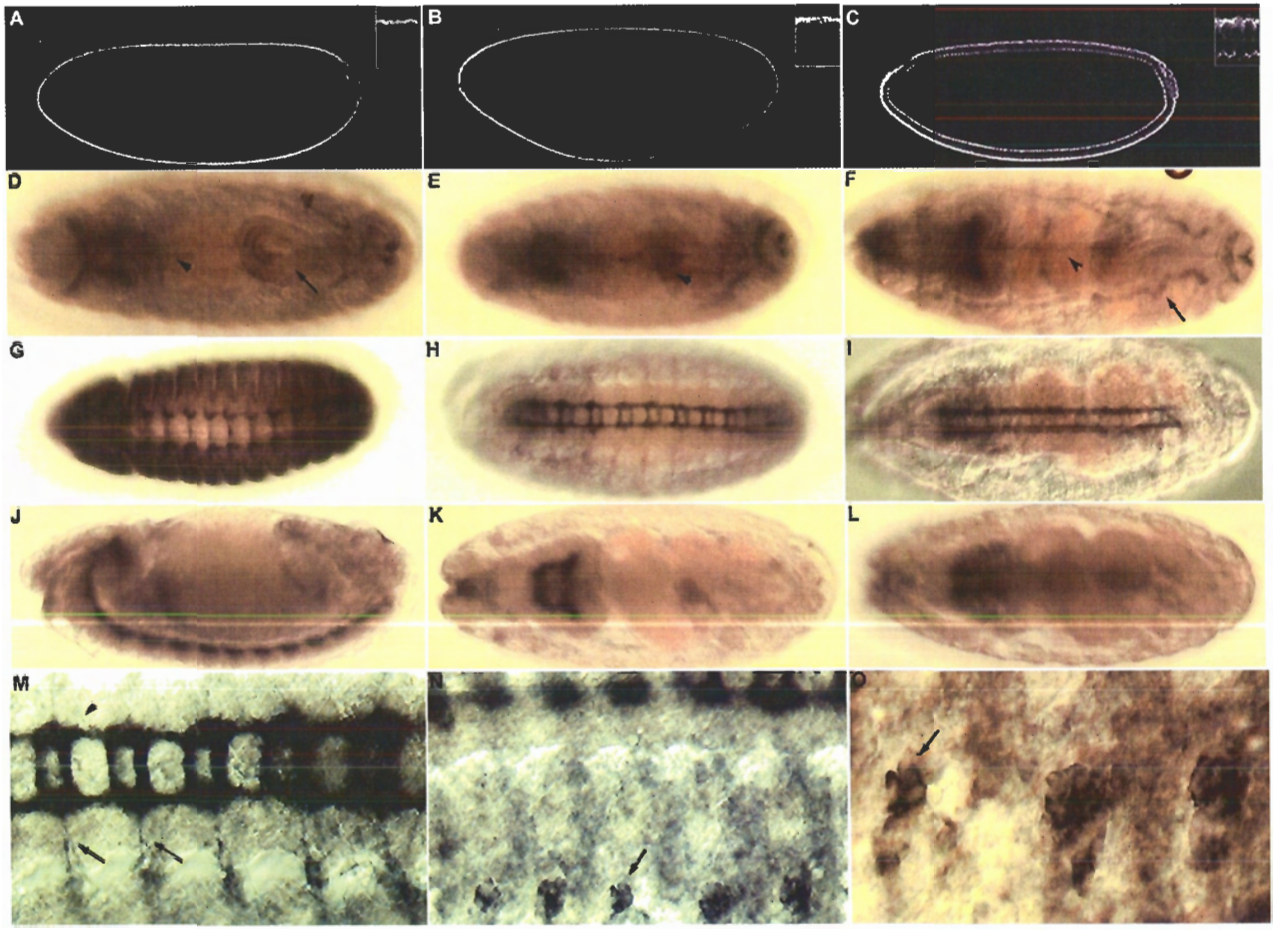

be functioning in particular embryonic processes. For example, the distribution of *DCIP4* transcript during cellularization and gastrulation was difficult to interpret as it was diffuse, making it seem like non-specific background. It is possible that this background is actually maternally contributed *DCIP4* mRNA. DCIP4 protein distribution during these stages was more specific. Beginning in early embryogenesis, the DCIP4 protein accumulates on the apical membrane prior to cellularization (Figure 3.5 II A). Once cellularization begins, the apical membrane invaginates to form peripheral cell membranes, and finally pinches to form the basal cell membrane, which seals each individual cell (Lecuit, 2004). In addition to remaining enriched apically, DCIP4 localizes with the membrane movement throughout cellularization (Figure 3.5 II A-C).

Later, during stage 8 of embryogenesis, the *DCIP4* transcript and protein are highly enriched in the first two developing segments of the embryo, the maxilla and the labium (Figure 3.4 II A and data not shown). DCIP4 continues to be present in these tissues during later stages of embryogenesis. A close up view of the cells that make up these two structures revealed DCIP4 expression in a fibrous and matted pattern, which was difficult to resolve using confocal microscopy (data not shown).

At stage 12, *DCIP4* transcript and protein are enriched in the developing hindgut and brain (Figure 3.4 II B and 3.5 II D). Though *DCIP4* is expressed throughout the epidermis during DC, which occurs between stages 12-14, it is not enriched in the amnioserosa (Figure 3.4 II C). A closer look at the DCIP4 protein distribution revealed weak enrichment of DCIP4 in the LE cells from stage 13 through until the end of hole closure (Figure 3.5 II D-F). Furthermore, *DCIP4* transcript and protein also seem to accumulate in cells along the dorsal midline after the completion of DC (Figure 3.4 II D

and 3.5 II F). *DCIP4* transcript is also found in the visceral mesoderm that forms a thin layer of muscle fibres that surround the digestive tract (Figure 3.4 II G). *DCIP4* transcript and protein may also be expressed in the dorsal longitudinal trunks of the embryonic trachea; however, these stainings could be artifacts due to probes and antibodies being trapped in these hollow structures (Figure 3.4 II I and 3.5 II F).

DCIP4 RNA and protein are also expressed in the embryonic central and peripheral nervous systems. Specifically, DCIP4 is enriched in the CNS from stage 12-14 (Figure 3.4 II E-F and 3.5 II G-I), and is also seen in the developing embryonic visual system (Figure 3.4 II H-J and 3.5 II J-L). DCIP4 protein distribution in the ventral nerve chord outlines the commisures and longitudinal connectives (Figure 3.5 II G-I). As well, DCIP4 is expressed in motor neuron axons that exit the CNS via the segmental (Figure 3.5 II M, arrows) and the intersegmental (Figure 3.5 II M, arrowhead) nerve roots. During PNS development at stage13, DCIP4 is enriched in the axons and cell bodies of a cluster of sensory neurons that are comprised of the lateral monoscolopidial chordotonal organ, ventral campaniform sensillum 5, and the ventral chordotonal organ (Figure 3.4 II K-N and Figure 3.5 II N-O). DCIP4 is also expressed in segmental stripes, which could be epidermal cells or neurons beneath the epidermis (Figure 3.5 II E and M). Finally, *DCIP4* is expressed in a subset of cells in the embryonic head region at stage 16 (Figure 3.4 II J).

3.4 DCIP4 expression during oogenesis

DCIP4 is predominantly expressed in the follicular epithelium throughout egg chamber development. However, it has a more dynamic expression pattern during earlier stages of oogenesis. Beginning in the germarium, DCIP4 is found weakly at all cell

surfaces and in cytoplasm, and localizes to unidentified actin-rich structures (Figure 3.6 D-F arrows). DCIP4 expression elevates during germ cell cyst encapsulation by follicle cells in region 2b of the germarium. In this region, DCIP4 is found in both the germ cells and follicle cells. DCIP4 is not restricted to the cell surface during this stage and can also be found in the cytoplasm. Interestingly, DCIP4 localises to sites of ring canal attachment to the cell membrane during cyst encapsulation and in stage 1-3 egg chambers (Figure 3.6 D-F, arrowheads). It is possible that DCIP4 may actually be part of the ring canal structure as some DCIP4 staining overlaps with the ring canals. DCIP4 staining becomes restricted to the follicular epithelium from stage 8. DCIP4 expression in the follicular epithelium is predominantly at the basal surface in a diffuse pattern. However, it outlines cell borders and accumulates at tricellular corners. Figure 3.6 P shows expression of DCIP4 at tricellular corners of squamous follicular epithelium in a stage 12 egg chamber, although this staining pattern is present in all follicle cells throughout egg chamber development.

3.5 Generation of mutations in the *DCIP4* gene by P element mobilization

A null mutation can be used to specifically characterize the functional role of a gene through phenotypic analysis and by interaction studies with other mutations and transgenic lines. To generate null mutations in the DCIP4 gene, EP elements inserted either upstream or downstream of DCIP4 were mobilized to generate random deletions in the flanking fly genomic DNA as described in Materials and Methods (Hawley and Waring, 1988). EP elements, as described previously, are immobile P-elements, which lack the active transposase enzyme they require for transposition. Inducing mobilization

Figure 3.6 DCIP4 expression during oogenesis.

Egg chambers were double stained with affinity-purified anti-DCIP4 (1/1000 dilution) (red) and FITC-phalloidin (green). (A-C) Ovariole showing different stages of egg chamber development. (A) DCIP4 is localized at the basal surface of follicle cells throughout egg chamber development, as well as at apical and lateral surfaces during early stages of egg chamber development. (D-F) Germarium. (D) DCIP4 staining is prominant at region 2b where follicle cells first surround the germ cells. DCIP4 staining in 2b is found within the cytoplasm and at the cell surface, and is enriched at sites of ring canal attachment to the cell membrane within the germ cells (arrowheads). In region 1-2a, DCIP4 localises to unidentified actin-rich areas (arrows). (G-H) Stage 1 egg chamber. (G) DCIP4 is enriched in follicle cells. (J-K) Stage 2-3 egg chamber. (J) DCIP4 is expressed at the cell surface of follicle cells (strong) and germ cells (weak). Punctate DCIP4 staining at the apical membrane co-localizes with F-actin rich areas (L, arrows). (M-O) Stage 7-8 egg chamber. (M) DCIP4 expression remains high at the basal surface of follicle cells but becomes weak at the apical and lateral surfaces. DCIP4 expression at this stage is absent from the nurse cells and oocyte. (P-R) Stage 12 egg chamber. DCIP4 localizes to cell boundaries and accumulates at tricellular junctions of the squamous follicular epithelium (P, arrow).

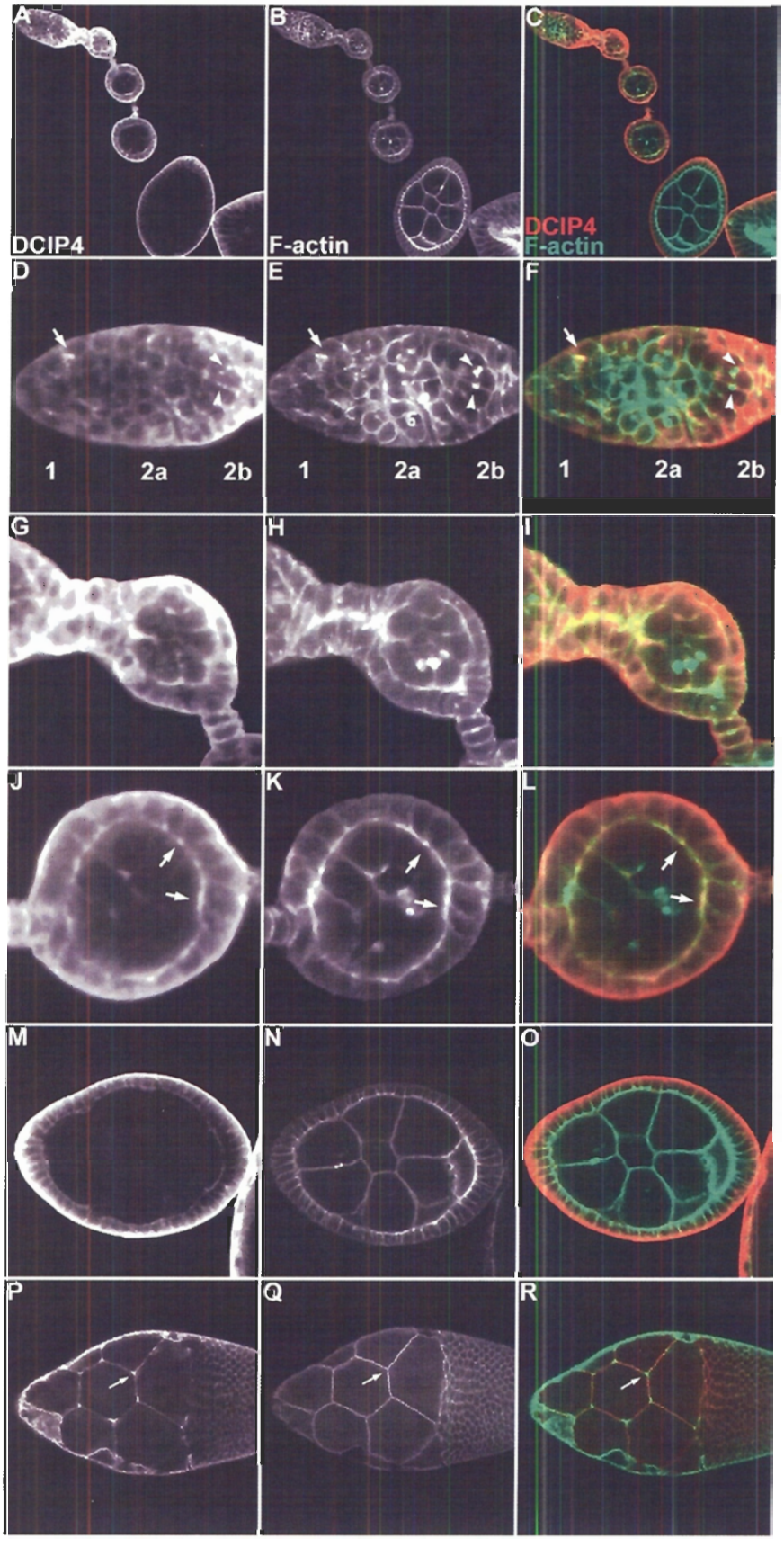
A
DCIP4
B
F-actin
C
DCIP4
F-actin
D
1
2a
2b
E
1
2a
2b
F
1
2a
2b
G
H
I
J
K
L
M
N
O
P
Q
R

of the EP construct by introducing a transposase source into the genetic background of the flies can result in random deletions of genomic sequences neighbouring the EP insertion site due to imprecise excision events.

About 70 excision events were generated from *EP(3)3507*, which is inserted 109 bases upstream of the predicted initiator methionine codon of the *DCIP4* gene. We later realised that there exists a second site mutation on the original *EP(3)3507* chromosome which results in larval lethality. This was confirmed by recombining this mutation away from the chromosome bearing the *EP* insertion. All of the chromosomes isolated from the excision of *EP(3)3507* contained this second site mutation. Excised lines generated from mobilization of *EP(3)3507* were phenotypically characterised and lines bearing a significant percentage of embryonic defects were kept. These lines were later characterized by Southern and Northern analysis and were shown to not carry deletions in the *DCIP4* gene (data not shown).

After completion of the *Drosophila* genome, and thus assembly of sequences flanking the *DCIP4* genomic region, another *EP* element, *EP(3)0671*, was positioned approximately 1.3 Kb away from the 3' end of the *DCIP4* gene (Figure 3.7 A). Incidentally, it is inserted after the first base of the neighbouring gene, *CG15014*. This *EP* element was mobilised to generate 200 excision events that were screened molecularly as described in Section 2.6 and below, to identify chromosomes containing lesions in *DCIP4*. Since the imprecise excision event results in deletions of random length and direction about the *EP* element insertion point (Adams and Sekelsky, 2002), many lines needed to be screened in order to only obtain a deletion in the *DCIP4* gene, and not in the neighbouring genomic regions.

Figure 3.7 Molecular characterization of *DCIP4* alleles.

(A) Schematic showing molecular breakpoints of *DCIP4* alleles, *34-1*, *32-1*, and *37-1*, as determined by genomic PCR. Red arrows indicate positions of forward and reverse primers used in PCR reactions. Numbers represent base positions along the left arm of the third chromosome. (B) Northern blots of total RNA prepared from adult flies showing loss of *DCIP4* transcript from flies homozygous for the *DCIP4* alleles *34-1*, *32-1*, and *37-1*. The transcript of *CG15014* is expressed at wild-type levels in these flies. (C) Northern blots of total RNA prepared form adult flies showing loss of *DCIP4* transcript in deficiencies *Df(3L) Exel8098*, *Df(3L)ED4342* and *Df(3L)GN40* but not *Df(3L)Exel9001* nor *Df(3L)GN19* when in combination with *34-1*. Flies homozygous for *Df(3L)Exel9001* also do not show loss of *DCIP4* transcript. The *DCIP4* allele, *49-1*, in combination with different deficiencies or *34-1* does not result in loss of *DCIP4* transcript, indicating this allele is not a null. RNA isolated from *Canton S* flies or w^{1118} was used as wild-type controls in (B) and (C) respectively. *rp49* was used as a loading control in (B) and (C).

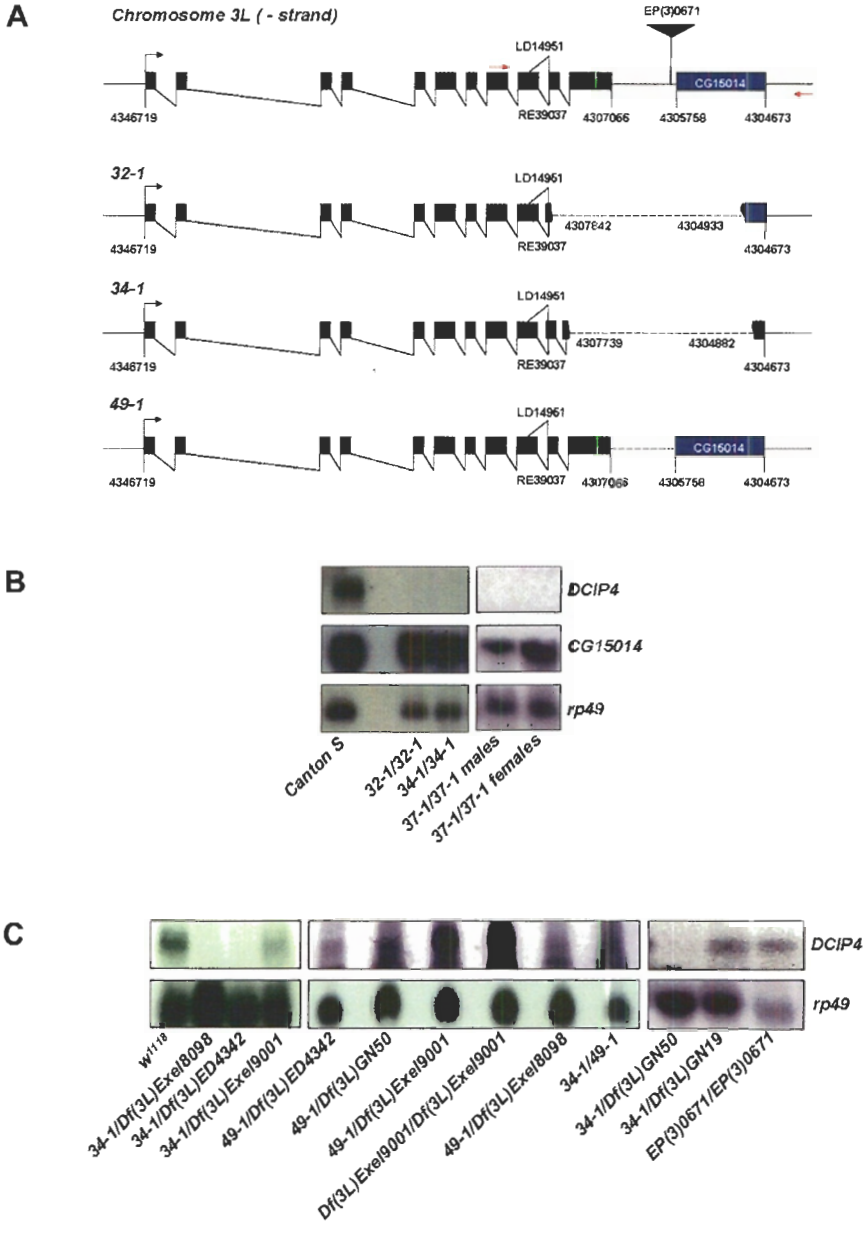
A
Chromosome 3L (- strand)
EP(3)0671
LD14951
CG15014
4346719
RE39037
4307066
4305758
4304673
32-1
4307642
4304933
34-1
4307739
4304882
49-1
B
DCIP4
CG15014
rp49
Canton S
32-1/32-1
34-1/34-1
37-1/37-1 males
37-1/37-1 females
C
DCIP4
rp49
w1118
34-1/Df(3L)Exel6098
34-1/Df(3L)ED4342
34-1/Df(3L)Exel9001
49-1/Df(3L)ED4342
49-1/Df(3L)GN50
49-1/Df(3L)Exel9001
Df(3L)Exel9001/Df(3L)Exel9001
49-1/Df(3L)Exel8098
34-1/49-1
34-1/Df(3L)GN50
34-1/Df(3L)GN19
EP(3)0671/EP(3)0671

EP(3)0671 excision lines were screened initially by Northern blot analysis for the lack of *DCIP4* transcript. Lines failing to produce *DCIP4* mRNA were examined by PCR with primers flanking genomic regions that encompassed the *EP* insertion site. PCR products of excision lines which gave shorter fragment sizes than the expected PCR product generated from wild-type genomic DNA, were sequenced to reveal the exact break points of the deletion. Lines with deletions too large to be characterized with PCR were analyzed by Southern hybridization, using the *DCIP4* cDNA and subsequently, the cDNA of the neighbouring gene, *CG15014*, as probes.

Three independent homozygous viable deletions, *32-1, 34-1* and *37-1,* each lacking the *DCIP4* transcript on Northern blots, were isolated (Figure 3.7 B). The chromosomal breakpoints of *32-1* and *34-1* were determined using PCR. It has been difficult to determine the exact breakpoints of the *37-1* allele. Another excision allele, *49-1,* removes the intergenic region between *DCIP4* and *CG15014.* This allele seems to express less *DCIP4* transcript compared to wild-type flies; however, the excised chromosome also contains a lethal mutation that was possibly generated during the excision of *EP(3)0671* (Figure 3.7 C). This second-site mutation complements GN50.

It is important to note that the sequence of the PCR fragments used to define the molecular breakpoints of the *32-1* and *34-1* alleles, suggest that most of *CG15014* is removed in *32-1,* and partially lost in *34-1.* However, Northern blot analysis of adult flies homozygous for these alleles show wild-type levels of *CG15014* transcript (Figure 3.7 C). We confirmed, by sequencing, that the cDNA (*GH15813*) we were using to probe for the *CG15014* transcript was correct. This transcript migrates to roughly 1.6 kilobases which is the same size as the predicted *CG15014* transcript. It is possible that

this gene was duplicated during the excision of *EP(3)0671* and now resides somewhere else within the DNA of *DCIP4* mutant flies. However, we have not been able to detect this in Southern blots (data not shown).

3.6 Identification of previously characterised chromosomal aberrations that lack *DCIP4*

The *DCIP4* mutations generated by mobilization of *EP(3)0671* show no *DCIP4* transcript in Northern blots, suggesting that they are null alleles. However, the 5' end of the *DCIP4* gene is still intact in these mutants since their molecularly determined breakpoints suggest that only the 3' end of *DCIP4* is truncated. It is therefore possible that transcript is still made but is undetectable on a Northern blot. We therefore set out to find stocks containing chromosomal deficiencies that had previously been mapped to the *DCIP4* region, 64B. Identification of such chromosomes would allow us to generate flies with the strongest *DCIP4* mutant background we could produce. With the aid of the Cytosearch tool on Flybase, we were able to identify several different stocks, including 5 which we tested for the loss of *DCIP4* (Figure 3.7 C). To check for loss of *DCIP4* in these deficiencies, *DCIP4* alleles were crossed to each deficiency and Northern blots were performed on flies heterozygous for the *DCIP4* allele and the particular deficiency. The deficiency stocks, *Df(3L)GN50* (GN50), *Df(3L)EXEL8089* (EXEL), and *Df(3L)ED4342* (ED) do not produce *DCIP4* transcript, but *Df(3L)GN19* and *Df(3L)EXEL9001* do (Drysdale, 2005). GN50 is a large deficiency predicted to remove regions 63E2-64B17 (Drysdale, 2005). EXEL and ED are smaller deficiencies estimated to remove 64A12-B and 64B1-13 respectively (Drysdale, 2005). These three deficiencies, in combination with the *DCIP4* excision alleles, were used to analyse the

phenotypic consequences of loss of *DCIP4* gene product throughout *Drosophila* development.

3.7 Characterization of *DCIP4* mutant phenotypes

3.7.1 *DCIP4* mutant adult phenotypes

The role of DCIP4 throughout development was analysed using the variety of alleles described above. Initially, heteroallelic combinations of different *DCIP4* alleles were generated to assess their affects on development. The heteroallelic combinations of *DCIP4* excision alleles are semi-lethal, as is homozygosity for each individual allele. The homozygous survivors that arise from the *34-1/TM3Sb* stocks represent only 11% (out of an expected 33.3%) of the total population within the stock. Though some *DCIP4* embryos are dying during embryogenesis (Table 3.2), the percentage is not large enough to account for the expected ratio of *DCIP4* mutants. Therefore, it is possible that the remainder of *DCIP4* mutants are dying throughout development and not at one particular stage.

Most DCIP4 homozygous mutant escapers are quiescent and unable to fly, with almost 50% bearing opaque, slightly held outward wings. However, combinations of either of the *DCIP4* alleles with chromosomes deficient in the *DCIP4* gene, such as GN50 or ED, produce different results. Flies heterozygous for either *DCIP4* alleles, *34-1* or *32-1*, with GN50 are behaviourally similarly to homozygous *34-1* and *32-1* flies. However, more than 50% of flies bearing the genotype *DCIP4* allele/GN50 have blistered wings (Figure 3.8 E and F). Wing blisters result from non-adherence of the two wing surfaces. In

Table 3.2 Cuticle phenotypes of *DCIP4* mutant embryos.

Embryos were obtained from various crosses to determine the cuticle phenotypes of *DCIP4* mutant embryos. To assess the embryonic phenotypes of loss of maternal *DCIP4*, embryos were collected from *Df(3L)GN50* females crossed to wild-type w^{1118} males. To control for phenotypes associated with heterozygosity for *Df(3L)GN50*, embryos were collected from *Df(3L)GN50/+* females and crossed to w^{1118} males. To assess the effects of loss of maternal and zygotic *DCIP4*, *Df(3L)GN50/34-1* females were crossed to either *Df(3L)GN50/34-1* or *34-1* homozygous males. Embryos were aged at 25°C for over 48 hours. A dash denotes that no embryos were found for the indicated category.

Table 3.2 Cuticle phenotypes of *DCIP4* mutant embryos

Cross	Larva	% Phenotype WT embryo	No cuticle	Dorsal defect	Head defect	Ventral defect	n
w1118	83.8	/	13.2	0.16	/	/	1277
34-1/TM3Sb ♀ *x 34-1/TM3Sb* ♂	53.8	27.1	14	1.9	1.9	/	236
Df(3L)GN50/+ ♀ *x w1118* ♂	65	4	26.7	0.7	3.25	0.4	277
Df(3L)GN50/34-1 ♀ *x w1118* ♂	75.8	3.8	13.7	3.8	2.2	0.6	182
Df(3L)GN50/34-1 ♀ *x Df(3L)GN50/34-1*♂	26.3	1.6	68.9	2.9	0.6	0.6	312
Df(3L)GN50/34-1 ♀ *x 34-1/34-1* ♂	22.8	2.9	66	3.6	2.8	3.5	140

Figure 3.8 *DCIP4* mutant wing phenotypes.

(A) Wild-type w^{1118} fly with wings folded towards the body. (B) *34-1/Df(3L)GN50* fly with wings held out, downwards and away from the body. (C) Wild-type w^{1118} wing. (D-F) *34-1/Df(3L)GN50* wings showing an extra anterior crossvein between veins L2 and L3 (D, arrow), and loss of adhesion between the wing surfaces (blistering) (E-F).

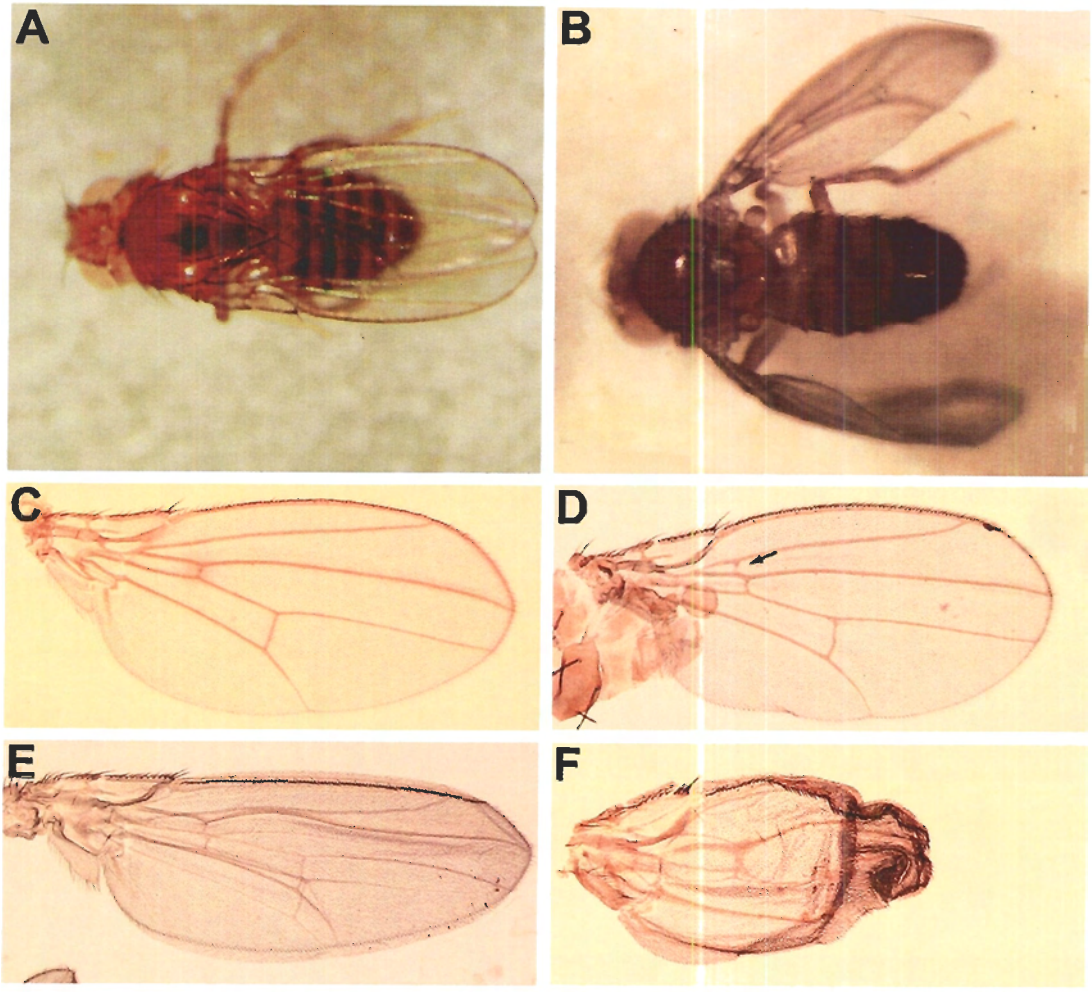
A
B
C
D
E
F

addition to the 50% of blistered wings, the rest of the wings have lost their integrity and are usually opaque, folded downwards, and pointing away from the body (Figure 3.8 B). A small percentage of wings (15%) also have extra anterior crossvein(s) between any two longitudinal veins (Figure 3.8 D, 34-1/GN50 wing showing extra ACV between L2-L3). Flies heterozygous for the *DCIP4* allele with ED behave similarly to flies that are homozygous for the individual *DCIP4* alleles. However, only a small subset of *DCIP4* allele/ED flies have blistered wings. As previously mentioned, GN50 is a much larger deficiency than ED, suggesting that the *DCIP4* mutant background is sensitive to the gene dosage of one or a combination of genes that are lost in the GN50 deficiency, resulting in a genetic interaction that generates wing blisters.

3.7.2 Loss of *DCIP4* results in semi-sterility in females

DCIP4 mutant males are fertile and produce wild-type progeny when crossed to w^{1118} virgin females. However, all different allelic combinations of *DCIP4* mutant females are semi-sterile and produce very few eggs. The eggs produced by these females are wild-type in structure, suggesting that the semi-sterility might be a result of developmental defects prior to egg formation. To address this question, *DCIP4* mutant ovaries were dissected to analyze egg chamber and ovariole development. It was observed that about 50% of *DCIP4* mutant egg chambers were degenerating (Figure 3. 9). The degeneration can be seen as early as stage 5-6 (Figure 3.9 H and K). Defects were also observed in F-actin distribution. First, cross-sectional views of many egg chambers showed discontinuities in F-actin staining (Figure 3.9 H and J). As well, the basal F-actin of follicle cells, which lies in parallel bundles perpendicular to the A/P axis, was randomly distributed and sometimes absent (Figure 3.9 F and I). There were gaps

Figure 3.9 Phenotypes of *DCIP4* mutant egg chambers.

Anterior is to the left. Assessment of developmental stages are based on the emergence and size of the oocyte. Wild-type (A-C). DCIP4 mutant egg chambers (D-O). F-actin staining (A-I). Wild-type ovariole (A) compared to *DCIP4* mutant ovarioles (D and G). The oldest egg chamber in the chain is degenerating in *DCIP4* mutant ovarioles. Cross-sectional view of wild-type stage 6 egg chamber (B) compared to cross-sectional view (H) of *DCIP4* mutant egg chambers. Wild-type egg chambers show large germ cells encapsulated by smaller follicle cells that are outlined by F-actin whereas *DCIP4* mutant egg chambers show loss of F-actin staining in some follicle cells (H, arrowhead). Sometimes ring canals of *DCIP4* mutant egg chambers are not attached to germ cell membranes and instead are found floating in the germ cell cytoplasm (arrow in H). Basal view of DCIP4 mutant egg chambers contain gaps in their follicular epithelium (E) leaving the germ cells unsurrounded (compare to basal view of wild type in C). Basal views of stage 5-6 egg chambers showing basal F-actin distribution in the follicular epithelium (C, F, and I). Wild-type follicle cell basal F-actin bundles lie parallel to each other perpendicular to the A/P axis (C). However, the follicular basal F-actin distribution in *DCIP4* mutant egg chambers is sometimes absent (F arrow) or random (I arrow) in certain cells. Cross-sectional view of stage 3 *DCIP4* mutant egg chamber (J-L) showing loss of F-actin from follicle cells. (J) F-actin, (K) DNA, (L) merge of F-actin and DNA staining. F-actin is lost in some regions where a nucleus is found and hence a cell is present (arrowhead in J-L). Gaps in the follicular epithelium are shown by the absence of nuclei (arrow in J-L). Stage 6 *DCIP4* mutant egg chamber (M-O) showing gaps in the follicular epithelium shown by loss of F-actin and by loss of cell surface markers such as Hts (M-O, arrow).

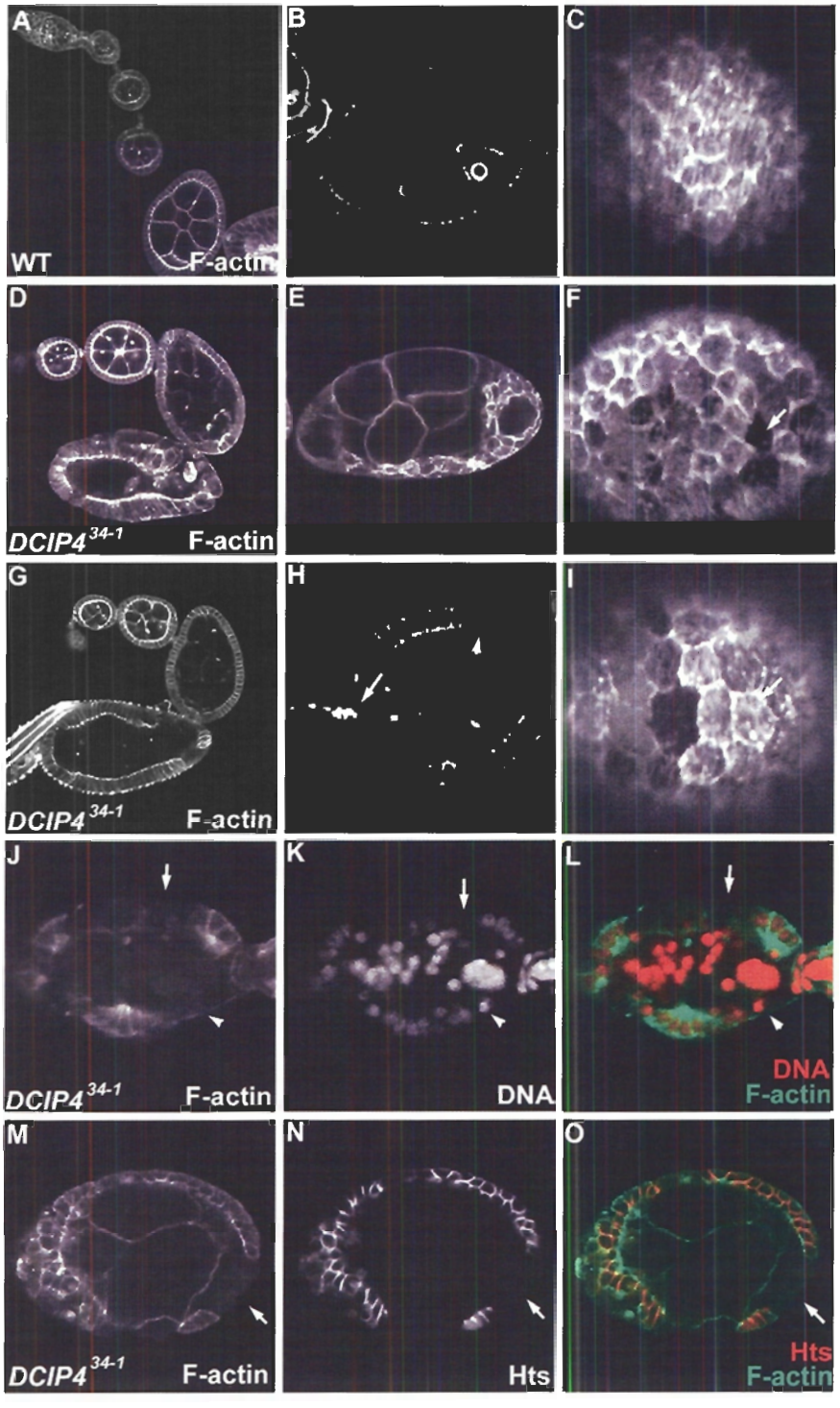
A
WT
F-actin
B
C
D
DCIP4 34-1
F-actin
E
F
G
DCIP4 34-1
F-actin
H
I
J
DCIP4 34-1
F-actin
K
DNA
L
DNA
F-actin
M
DCIP4 34-1
F-actin
N
Hts
O
Hts
F-actin

present in the follicular epithelium (Figure 3.9 E). Presence of gaps was confirmed by the absence of nuclei in these regions and absence of cell boundary markers such as Hu Li Tai Shao (Hts) (Figure 3.9 L and O). We also observed that older *DCIP4* mutant egg chambers contained multinucleated nurse cells (Figure 3.10).

3.7.3 *DCIP4* cuticle phenotypes

We assessed the effects of loss of *DCIP4* during embryogenesis by performing a series of crosses to generate embryos that lack either maternal or zygotic, or lack both maternal and zygotic (MZ) *DCIP4* (Table 3.2). As summarised in Table 3.2, a very low percentage of embryonic defects is seen in cuticle preparations of the crosses used to generate loss of maternal, zygotic, or MZ DCIP4 embryonic function. The percentage of the sum of all of these defects is quite low and may be due to genetic background. However, one thing that is striking is the number of embryos that did not secrete cuticle in cuticle preparations containing MZ mutant *DCIP4* embryos. A subset of embryos from any cuticle preparation will not secrete cuticle. Eggs that have not secreted cuticle (empty cuticles or ECs) are often unfertilised eggs. The amount of ECs in a given cuticle preparation is usually less than 30% (personal observations and Table 3.2). However, the percentage of ECs in cuticle preparations containing MZ *DCIP4* mutant embryos is greater than 60 %. This high percentage of ECs is not due to loss of maternal *DCIP4* as *DCIP4* mutant females lay normal levels of unfertilised eggs when mated to wild-type males (Table 3.2). As previously mentioned, *DCIP4* mutant males are fertile and produce wild-type progeny when mated to wild-type females. This suggests that the ECs are MZ *DCIP4* embryos that die due to a lack of epidermal development for cuticle secretion.

Figure 3.10 Loss *DCIP4* results in the formation of multinucleate nurse cells. Cross-sectional views of stage 8 *DCIP4* mutant egg chambers showing F-actin staining (A and D), DNA staining (B and E) and the merge of F-actin and DNA (C and F). Arrowheads point to multinucleated nurse cells. Arrow in (A and C) points to a ring canal that has detached from the germ cell membrane and is floating in the cytoplasm.

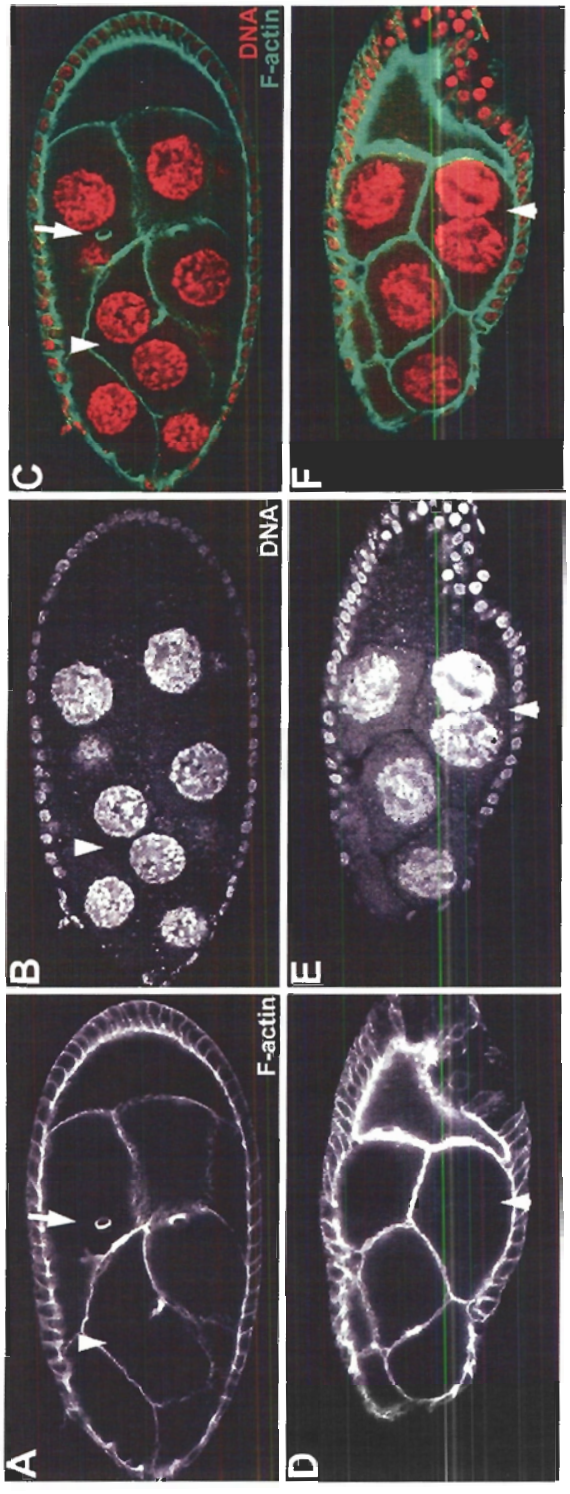
A
F-actin
B
DNA
C
DNA
F-actin
D
E
F

3.7.4 Loss of zygotic *DCIP4* does not affect the morphology of the larval photoreceptors, the embryonic nervous system or the embryonic hindgut

As previously mentioned, DCIP4 is expressed in the embryonic nervous system and hindgut. We assessed the morphology of these organs in *DCIP*4 zygotic mutant embryos. Hindgut development was visualised using the Crumbs specific monoclonal antibody, Cq4. No defects were observed in the overall morphology of the hindgut in *DCIP4* mutant embryos (data not shown). We also looked at the development of the embryonic nervous system using the following markers: anti-ELAV, anti-Futsch (mAb 22C10) (ELAV: marks neuronal nuclei, Futsch: marks all axons and cell bodies) to look at the number and morphology of PNS neurons; and anti-Fas II and anti-HRP to look at axons of motorneurons and the ventral nerve chord. No defects were observed in nervous system development in *DCIP4* mutant embryos using the above-mentioned markers (data not shown).

Another Cdc42 effector, DPAK, is required for photoreceptor cell axon guidance and targeting. To assess if DCIP4 was also required in this photoreceptor growth cone, we looked at the morphology of photoreceptor axons in the larval visual system of *DCIP4* zygotic mutants. Using the monoclonal antibody 24B10, which stains the axons of photoreceptor cells, we were able to conclude that loss of zygotic DCIP4, unlike the loss of zygotic DPAK, does not affect axon guidance and targeting of photoreceptor cells (data not shown).

3.8 Construction of transgenic *DCIP4* flies and DCIP4 overexpression phenotypes

We generated *UAS-DCIP4* transgenes to assess which developmental processes are affected by overexpression of DCIP4. Initially, the *DCIP4* cDNA, *LD14951* was cloned into the *Drosophila* nonautonomous P-element vector pUAST, thus placing its expression under the control of a UAS promoter, as described in Materials and Methods. Subsequently, the *RE39037* cDNA was cloned into 2 different UAS vectors, pUAST and pUASP, a vector that allows transgene expression in the germline, as well as other tissues (Joseph, 2002). Transgenic *Drosophila* lines bearing individual *UAS-DCIP4* insertions on the X, 2nd and 3rd chromosomes were established. The localization of the P-element insertions to each chromosome was determined by crossing the various lines to individual balancers for each chromosome and screening for the maintenance of heterozygosity of the balancer with the insertion in subsequent generations. Northern blot analysis of these lines crossed with *hs-GAL4*^{M4} and heat shocked for 1 hour at 37°C, were used to test that the *UAS-DCIP4* transgenes could in fact overexpress *DCIP4* (data not shown).

UAS-RE39037 (UAS-RE) and *UAS-LD14951 (UAS-LD)* were crossed to different tissue-specific GAL4 drivers to assess the effects of DCIP4 overexpression throughout development (Table 3.3). Overexpression of *UAS-LD* yielded interesting adult phenotypes. These phenotypes were seen when different *UAS-LD* lines were crossed to the same GAL4 driver and when the same *UAS-LD* line was crossed to GAL4 drivers with overlapping GAL4 expression domains. Expression of *UAS-LD* during bristle development using the drivers *elavGAL4, scaGAL4, apGAL4, pnrGAL4,* or *30AGAL4*, lead to abnormal bristle development (Table 3.3 and Figure 3.11 B-F). Particularly,

Table 3.3 Phenotypes of *UAS-LD14951* overexpression during *Drosophila* development.

GAL4 lines were crossed to *UAS-LD14951* lines *17-1* and *62*. Phenotypes generated with these *UAS-LD14951* transgenes were reconfirmed by repeating the GAL4-UAS crosses using the *UAS-LD14951* transgenic lines *5, 52-1, 30-1* and *39-1*. A slash indicates that no obvious phenotype was seen, L: lethal, PL: pupal lethal, L-PL: larval to pupal lethal. GAL4 drivers were also crossed to *UAS-RE39037* line *27-3* (generated with pUASP) and lines *18A* and *1A* (generated with pUAST), however, these produced no phenotypes.

Table 3.3 GAL4 drivers crossed to *UAS-LD14951* lines

GAL4 Driver	GAL4 Expression Pattern	Phenotype of *GAL4/UAS-LD14951*
ubiquitous	ubiquitous	/
198y	border cells and follicle cells over oocyte	L
185y	embryo: salivary gland;oocyte: stalk cells,germarium, follicle cells over nurse cells	L
repo	glial cells	/
scabrous (sca)	sensory organs	upwards bristles
c311	eye disc peripodial epithelia, wing disc peripodial & columnar epithelia, nervous system	PL
daughterless (da)	da[+] pattern>embryo, CNS	L-PL
decapentaplegic (dpp)	GAL4 in dpp(+) pattern>embryo,A/P boundary in imaginal tissue	multiple wing hairs, similar to *ptcGAL4,* except milder
eyeless (ey)	ey[+] pattern>embryo, CNS	/
elav	Nervous system	PL @25°C, thin scutellar bristles @ RT
epidermal	embryonic gate CNS/PNS	/
332.2	amnioserosa	/
Lp-I	amnioserosa, leading edge, other embryonic cells	PL
leading edge (LE)	Embryo>leading edge cells	/
c381	amnioserosa, PNS	singed, abnormal bristles at 25°C, wings don't unfold properly
24B	mesoderm>embryo, larva	L-PL
armadillo (arm)	arm[+] pattern> embryo, imaginal disc, CNS....	/
optomerblind(omb)	omb[+] pattern>imaginal discs,dorsal wing pouch	fertile, multiple wing hairs, enhanced *ombGAL4* wing phenotype
71B	imaginal dics	small wings @ RT
peripodial	peripodial membrane	/
bs	most intervein cells of wing	/
MS1096	wing imaginal disc	/
scalloped (sd)	Expresses GAL4 in the pattern of the scalloped (sd) gene	/
GMR	morphogenic furrow during eye development	/
T80	imaginal disc	/
T113	imaginal disc	/
T93	imaginal disc	/
A9	dorsal wing pouch	/
veinlet/rhomboid (ve)	ve[+] pattern in wing veins	/
vestigial (vg)	vg[+] pattern in wing disc	/
30A	antennal disc	ectopic scutellar bristles, enhancement of *30AGAL4* ectopic bristle
719a	wing pouch	small wings @ RT with multiple wing haris
pannier (pnr)	pnr[+] pattern> embryo, imaginal discs	bent, broken and fat scutellar bristles
32B	embryo, imaginal discs	very small flies with abnormal wings at RT
69B	embryo, imaginal discs	/
patched (ptc)	ptc(+) pattern> embryo, imaginal discs	multiple wing hairs, blistered wings, scutellar bristle defects,
apterous (ap)	ap[+] pattern>embryo, imaginal discs, nervous system...	Abnormal thick scutellar bristles
engrailed (en)	en[+] pattern>embryo imaginal discs	/

Figure 3.11 Phenotypes of *UAS-LD14951* overexpression during *Drosophila* development.

(A) Wild-type notum. (B) *pnrGAL4/UAS-LD14951* and (C) *apGAL4/ UAS-LD14951* notums showing abnormal bristle development. Machrochaetae look abnormal, however the positioning of the michrochaetae are also affected. (D) *30AGAL4* homozygous fly showing extra bristles (arrows) close to the anterior half of the scutellum. Note that regions with loss of bristles may have arisen due to the bristles falling off and may not necessarily be a cell fate change. (E) Overexpression of *UAS-LD14951* with *30AGAL4* leads to excess scutellar bristles. (F) Overexpression of *UAS-LD14951* with *719aGAL4* leads to a mild bristle phenotype where the posterior scutellar bristles cross upwards towards the anterior. Excess anterior bristles also cross laterally and are almost adhered to the scutellum along their length (arrow). (G) *ombGAL4/+* wings are mostly wild-type in appearance except for a mild margin defect caused by the presence of excess vein tissue (arrow). Wings of *UAS-LD14951* crossed to *ptc-GAL4* (H), *ombGAL4* (I), and *719aGAL4* (J) are smaller than wings of *ombGAL4/+* controls (G). Overexpression of *UAS-LD14951* with *ombGAL4* leads to an enhancement of the *ombGAL4/+* wing margin defect (arrow in I). Insets in (G-J) show a high power view of wing cell trichomes from positions marked with asterisks within each wing. Trichomes in *ombGAL4/+* are wild-type in appearance, distribution and polarity. However, overexpression of *UAS-LD14951* with all three drivers leads to development of multiple trichomes that are improperly oriented.

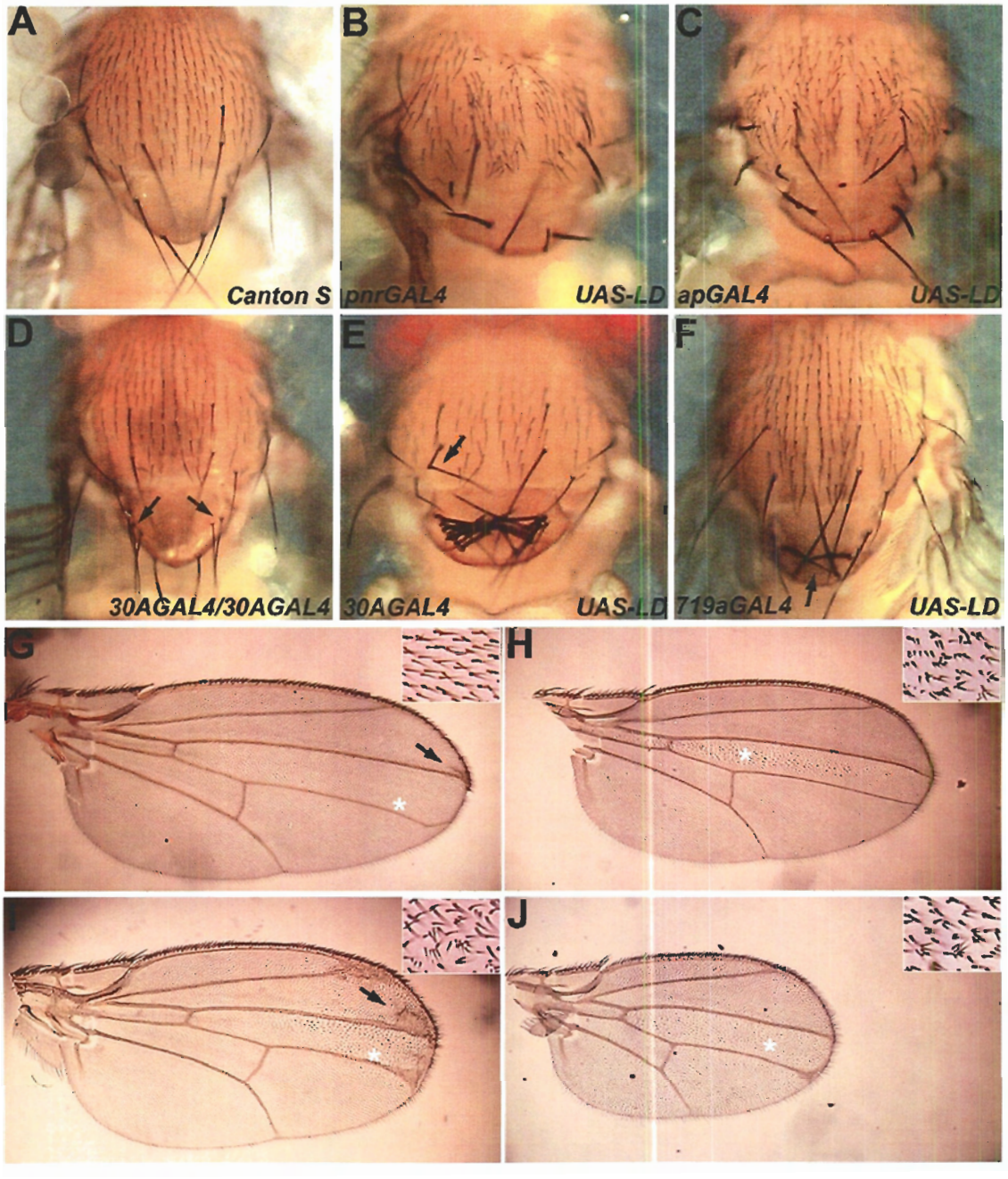
A
Canton S
B
pnrGAL4
UAS-LD
C
apGAL4
UAS-LD
D
30AGAL4/30AGAL4
E
30AGAL4
UAS-LD
F
719aGAL4
UAS-LD
G
H
I
J

UAS-LD expression with *pnrGAL4* or *apGAL4* in the notum resulted in fat, spikey, brittle, bristles (Figure 3.11 B and C). Overexpression of *UAS-LD* with *719aGAL4* or *30AGAL4* produced ectopic scutellar bristles that often cross and point towards the anterior (Figure 3.11 E and F).

Overexpression of *UAS-LD* with *719aGAL4* produced flies with small wings (Figure 3.11 J). Interestingly, *UAS-LD/32BGAL4* flies were generally half the size of wild-type flies. A second interesting phenotype was also seen in the wing. Overexpression of *UAS-LD* with *ptcGal4, dpp-GAL4, ombGAL4* and *719aGAL4* produced multiple wing hairs, or trichomes, on the surface of the wing epithelium. Normally, each epithelial cell in the wing reorganises its cytoskeleton to produce an actin spike at the distal vertex, which gives rise to the distally-oriented trichome, seen in adults (Mlodzik, 1999). However, the multiple trichomes associated with overexpression of *UAS-LD* are randomly oriented (Figure 3.11 H-J).

Suprisingly, expression of *RE39037* from transgenes made using the pUAST or pUASP vectors did not produce any of the *LD14951* phenotypes. In fact the *UAS-RE39037* transgene did not produce any phenotype when expressed by several different drivers (data not shown). This was not dependent on the strength of transgenes, as both weak and strong transgenes were tested.

3.9 Searching for genetic interactors of *DCIP4*

3.9.1 *DCIP4* may genetically interact with *Cdc42* during crossvein development

As DCIP4 is a potential effector protein for Cdc42, we searched for a link between *Cdc42* and *DCIP4* using several different approaches. First, we tested to see if

Cdc42 could affect *DCIP4* expression during embryogenesis. Ectopic expression of CA or DN Cdc42, Cdc42V12 and Cdc42N17 respectively, in the embryo did not affect *DCIP4* RNA expression. In addition, DCIP4 protein expression in *Cdc42* mutant embryos was not altered (data not shown).

We then began looking for genetic interaction between *DCIP4* and *Cdc42*. As *DCIP4* mutant females are semi-sterile, we tested the sterility of females heterozygous for weak or strong mutations in *Cdc42* and heterozygous for either of the *DCIP4* alleles, *32-1* or *34-1*. One copy of any of the *Cdc42* alleles alone or either of the *DCIP4* alleles alone does not result in female sterility. We found that *Cdc42/+;DCIP4/+*females were also fertile. Next, we assessed the defects associated with heterozygosity for *Cdc42* and loss of zygotic *DCIP4* in embryonic development. We crossed weak and strong *Cdc42* alleles to either *34-1* or *32-1* to establish females heterozygous for both a *DCIP4* and a *Cdc42* mutation and crossed these females to *34-1* homozygous males. Loss of 50% of functional MZ *Cdc42* had no effect on the low percentage of embryonic phenotypes associated with homozygosity for the *DCIP4* mutations.

Combinations of *Cdc42* mutants contain extra crossveins on their wings. Also wings of *34-1/GN50* show extra ACVs (Figure 3.7 D). We decided to see if we could sensitize the *DCIP4* mutant background by removing one functional copy of *Cdc42*. However, we were not successful in obtaining any interaction using this method. We then set out to look at crossvein development in a *Cdc42;DCIP4* double mutant. We chose two viable *Cdc42* alleles for our experiments, $Cdc42^{2}$ and $Cdc42^{6}$. We were unsuccessful in generating a double balanced *Cdc42;DCIP4* stock to generate a double mutant background due to difficulties in establishing an intermediate step that contained

the *Cdc42* allele and two balanced third chromosomes. However, we generated crosses that produced progeny that were 50% mutant for both *DCIP4* and *Cdc42*. Wings of progeny from this cross were mounted and the frequency of ectopic crossveins was analysed. Although the percentage of wings containing ectopic crossveins did not increase with respect to controls, we did see an increase in the frequency of ectopic crossveins in affected wings. $Cdc42^2$ hemizygous mutant males exhibit ectopic crossveins on roughly 50% of their wings (Table 3.4). To characterize the frequency of ectopic crossveins in this subset, we calculated the occurrence of incomplete, 1, or 2 or more crossveins. $Cdc42^2$ hemizygotes have 19.2%, 24.7% and 4.1% incomplete, 1, or 2 or more ectopic crossveins, respectively. However, in a *DCIP4* mutant background the number of wings with 2 or more ectopic crossveins in *Cdc42* hemizygotes increases to an estimated 25%. In *TM3* balancer-containing flies, half of which were heterozygous for *32-1*, a more modest increase in wings with 2 or more ectopic crossveins was seen (an estimated 9.6%).

3.9.2 Loss of zygotic *DCIP4* and *wsp* or *nwk* does not lead to defects in embryonic nervous system development

Both WASP and Nwk are expressed in the embryonic nervous system, and loss of maternal and zygotic *wsp* results in a duplication of embryonic sensory neurons. Similar to *DCIP4*, loss of zygotic *nwk* or *wsp* during embryogenesis does not cause defects in nervous system development of the embryo (data not shown). DCIP4 and Nwk are both PCH family proteins and may have overlapping functions. As previously mentioned, DCIP4 has been shown to bind to WASP in the *Drosophila* comprehensive yeast 2 hybrid study. Our collaborators have been successful in demonstrating that DCIP4 can activate

Wsp in *in vitro* actin polymerization assays: the DCIP4-mediated Wsp activation does not require Cdc42 but is potentiated by the presence of Cdc42 (Avi Rodal, personal communications). We tested to see if *wsp,DCIP4* or *nwk,DCIP4* double zygotic mutants would have an effect on the development of the embryonic nervous system. Using the previously described markers (anti-elav, anti-Futsch, anti-HRP, and anti-FasII), we were able to determine that these double mutants did not have an effect on nervous system development during *Drosophila* embryogenesis (data not shown).

Table 3.4 Loss of DCIP4 enhances Cdc42 mutant wing phenotypes.

To generate progeny that were homozygous mutant for *DCIP4* and *Cdc42*, we crossed *$Cdc42^2$/+; 32-1/+* females to *+/Y;32-1/TM3Sb* males. We separated males that contained the *TM3* balancer from those that did not by scoring for the presence of the dominant visible marker, *Sb*, on the balancer chromosome. Wings of *Sb* vs. Non-*Sb* males were mounted and analysed. Non-*Sb* males were the following genotypes: *$Cdc42^2$/Y;32-1/32-1*, *$Cdc42^2$/Y;32-1/+*, *+/Y;32-1/32-1*, *+/Y;32-1/+*. *Sb* males were used as an internal control for genetic background and were of the following genotypes: *Cdc422/Y; 32-1/TM3Sb, Cdc422/Y; +/TM3Sb, +/Y; 32-1/TM3Sb, +/Y; +/TM3Sb.*

Table 3.3 GAL4 drivers crossed to *UAS-LD14951* lines

GAL4 Driver	GAL4 Expression Pattern	Phenotype of *GAL4/UAS-LD14951*
ubiquitous	ubiquitous	/
198y	border cells and follicle cells over oocyte	L
185y	embryo: salivary gland;oocyte: stalk cells,germarium, follicle cells over nurse cells	L
repo	glial cells	/
scabrous (sca)	sensory organs	upwards bristles
c311	eye disc peripodial epithelia, wing disc peripodial & columnar epithelia, nervous system	PL
daughterless (da)	da[+] pattern>embryo, CNS	L-PL
decapentaplegic (dpp)	GAL4 in dpp(+) pattern>embryo,A/P boundary in imaginal tissue	multiple wing hairs, similar to *ptcGAL4*, except milder
eyeless (ey)	ey[+] pattern>embryo, CNS	/
elav	Nervous system	PL @25°C, thin scutellar bristles @ RT
epidermal	embryonic gate CNS/PNS	/
332.2	amnioserosa	/
Lp-I	amnioserosa, leading edge, other embryonic cells	PL
leading edge (LE)	Embryo>leading edge cells	/
c381	amnioserosa, PNS	singed, abnormal bristles at 25°C, wings don't unfold properly
24B	mesoderm>embryo, larva	L-PL
armadillo (arm)	arm[+] pattern> embryo, imaginal disc, CNS....	/
optomerblind(omb)	omb[+] pattern>imaginal discs,dorsal wing pouch	fertile, multiple wing hairs, enhanced *ombGAL4* wing phenotype
71B	imaginal dics	small wings @ RT
peripodial	peripodial membrane	/
bs	most intervein cells of wing	/
MS1096	wing imaginal disc	/
scalloped (sd)	Expresses GAL4 in the pattern of the scalloped (sd) gene	/
GMR	morphogenic furrow during eye development	/
T80	imaginal disc	/
T113	imaginal disc	/
T93	imaginal disc	/
A9	dorsal wing pouch	/
veinlet/rhomboid (ve)	ve[+] pattern in wing veins	/
vestigial (vg)	vg[+] pattern in wing disc	/
30A	antennal disc	ectopic scutellar bristles, enhancement of *30AGAL4* ectopic bristle
719a	wing pouch	small wings @ RT with multiple wing haris
pannier (pnr)	pnr[+] pattern> embryo, imaginal discs	bent, broken and fat scutellar bristles
32B	embryo, imaginal discs	very small flies with abnormal wings at RT
69B	embryo, imaginal discs	/
patched (ptc)	ptc(+) pattern> embryo, imaginal discs	multiple wing hairs, blistered wings, scutellar bristle defects,
apterous (ap)	ap[+] pattern>embryo, imaginal discs, nervous system...	Abnormal thick scutellar bristles
engrailed (en)	en[+] pattern>embryo imaginal discs	/

4 DISCUSSION: DCIP4

4.1 The *DCIP4* gene and cDNAs

Collections of full-length, sequenced cDNAs allow the accurate determination of protein sequence and can identify inaccuracies in protein sequences predicted from genomic sequence data (Misra et al., 2002). An example of an error that often occurs in the prediction of large genes or genes with large introns, is that the gene is split into two separate annotations. These errors can be rectified by comparing the translated annotations to translations of full-length cDNAs and/or by alignment with available homologous protein sequences from other species. As most of the initial genome annotation of *Drosophila melanogaster* (Release 1 and 2) was done using computational gene-prediction algorithms, some predictions were synthetic and required subsequent manual annotations by human curators, as well as, supporting data from cDNA sequences (Misra et al., 2002).

Initially, *DCIP4* was annotated as two separated predicted genes, *CG15015* and *CG11341*. These two predictions were separated by a large 24 Kb intron and were corrected in Release 3 of the genome sequence. With the aid of the euchromatic genome sequence, completed to high quality, several different sources of full-length cDNA sequences, and the expertise of human curators, Release 3 was a more correct annotation of the *Drosophila* euchromatic genome (Misra et al., 2002) and thus could correct for errors such as those described for the *DCIP4* gene.

Collections of cDNA sequence can also offer the prediction of alternately spliced transcripts. In the case of *DCIP4*, sequences of two different cDNAs, which were used and described in this study, indicate that *DCIP4* is alternately spliced. Alignment of these cDNA sequences with the *DCIP4* genomic sequence revealed that these two cDNAs differ by a 60 bp region that could have resulted from alternate splicing of the 9th *DCIP4* intron. It is quite possible that *DCIP4* transcripts corresponding to both *RE39037* and *LD14951* exist, as the band corresponding to the *DCIP4* mRNA on Northern blots is fairly broad suggesting that it is a possible doublet (Figure 3.4 I and Figure 3.6 B-C). However, it has been very difficult to confirm the presence of two transcripts corresponding to *DCIP4* with Northern hybridization. Using techniques such as Reverse Transcriptase (RT)-PCR may help in identifying alternate splicing of *DCIP4*. The extra sequence in RE39037p does not align to sequence in any of its closest homologues nor other members of the PCH family (Figure 3.3 and data not shown), providing evidence that this cDNA may be an artifact. It was surprising that transgenes generated from these two different cDNAs, produced a variety of phenotypes when expressed under the control of different tissue-specific GAL4 drivers (Table 3.3). Although *LD14951* transgenes produced different phenotypes when ectopically expressed throughout development, expression of weak or strong *RE39037* transgenes did not show any observable phenotypes.

4.2 *LD14951* overexpression leads to actin-linked phenotypes

Overexpression of *LD14951* under the control of different GAL4 drivers produced phenotypes possibly associated with changes in the actin cytoskeleton. First, ectopic expression of *LD14951* led to formation of multiple trichomes, or hairs, on the

surface of wing epithelial cells. Normally, each epithelial cell in the wing reorganises its cytoskeleton to produce an actin spike at the distal vertex, which gives rise to the distally-oriented trichome, seen in adults (Mlodzik, 1999). Formation of multiple trichomes has been associated with a failure in cytokinesis in the developing wing epithelium, with the formation of multiple prehair initiation centres on the apical surface of a single wing epithelial cell, and with the formation of multiple prehairs from what seems to be one initiation centre (Adler et al., 2000). Extra trichomes resulting from polyploidy are typically separated from hairs of neighbouring cells by a larger than normal cell-to-cell distance (Adler et al., 2000). This phenotype is seen with both the reduction of the Rho GEF, *pebble* and the expression of a DN version of a GAP for Rac and Cdc42, RhoGAP50C, in the wing (Shandala et al., 2004); (Sotillos and Campuzano, 2000). Both of these proteins have been shown to be required for cytokinesis in *Drosophila* S2 cells (Echard et al., 2004). Cell-cell distance is normal when multiple hairs arise from a single initiation centre. *UAS-LD*-associated trichomes resemble those of DN RhoGAP50C and *pebble* reduction, and thus may result from a failure in cytokinesis. The involvement of yeast PCH family proteins in maintenance of the actin bridge during cytokinesis supports a role for this DCIP4 splice variant in cell division. Also, as DCIP4's *in vitro* function is to activate Wsp to promote actin nucleation, it can be assumed that a role for DCIP4 in cytokinesis may be actin-related.

UAS-LD-associated multiple trichomes were also shorter than wild-type trichomes. This phenotype has been seen with mutations in cytoskeletal components such as a Type VI myosin, *crinkled*, and suggests that disruption of the cytoskeleton leads to defects in prehair elongation (Adler et al., 2000). This phenotype has also been seen

when wing epithelium is treated with cytochalasin D, a known inhibitor of the actin cytoskeleton (Adler et al., 2000). Therefore it is possible that DCIP4 is also required for prehair elongation. Interestingly, endogenous Cdc42 localizes to the tips of elongating trichomes, while overexpression of a DN Cdc42 construct, Cdc42S89, in the wing epithelium resulted in loss of trichomes (Eaton et al., 1996).

An actin-based function for DCIP4 in wing hair development is further supported by overexpression phenotypes of *UAS-LD* during bristle development. *UAS-LD* expressing scutellar machrochaetae were often short, bent, or brittle. This phenotype has been seen with mutations in several actin associated proteins, such as the *Drosophila* actin capping protein and *Drosophila* profilin, Chickadee (Hopmann and Miller, 2003) (Hopmann et al., 1996; Verheyen and Cooley, 1994b). This phenotype is also associated with loss or gain of function of Wsp family regulators, such as Abi and Kette (Bogdan et al., 2004; Bogdan et al., 2005).

Interpretation of overexpression phenotypes can often be misleading when trying to establish a role for an endogenous protein, such as DCIP4, in a given process. Phenotypes caused by ectopic placement of DCIP4 in a given process do not necessarily suggest that the endogenous protein function is actually required for that developmental event. We can however find clues about the endogenous function of DCIP4 by looking for similar effects or patterns generated by ectopically expressed protein in different developmental processes, and then make educated guesses about the mechanism by which it is causing this disruption. These educated guesses would be based on what is known about DCIP4 through mutant analysis, expression patterns or literature review. By looking at the overexpression phenotypes generated with overexpression of *UAS-LD*,

we can conclude that too much of this *DCIP4* splice variant is causing a disruption in cytoskeletal regulation. This maybe achieved through blocking/promoting the functions of Cdc42 and/or Wsp, or the function of unknown components.

4.3 The role of DCIP4 during embryonic development

DCIP4 is expressed during several stages of embryonic development (Figure 3.4 II and Figure 3.5 II). However, the majority of *DCIP4* zygotic mutants embryos complete embryogenesis (Table 3.2) suggesting at least three different possibilities. The first possibility is that *DCIP4* is not essential for embryonic development. The second possibility is that embryos are relying on maternal *DCIP4* RNA and protein to complete embryogenesis. Finally, it is possible that the *DCIP4* deletions generated are not nulls and thus a small zygotic (and possible maternal) DCIP4 contribution is sufficient for *DCIP4* mutant embryos to complete development. As demonstrated by sequencing of the molecular breakpoints of the *DCIP4* alleles, the 3' end of the *DCIP4* gene was removed during the excision of *EP*(3)0671 (Figure 3.6). Although the 5' of *DCIP4* is still intact in these mutants, no truncated transcript is seen in Northern blots, suggesting that either *DCIP4* is not transcribed in these mutants or that the truncated transcript is unstable, due to loss of a polyA tail, and is degraded. It is therefore more likely that either *DCIP4* is not essential during embryogenesis or that maternal *DCIP4* is contributing to the survival of zygotically mutant embryos. The maternal *DCIP4* contribution may be in the form of mRNA as we do not see accumulation of DCIP4 protein in the nurse cells or oocytes of late stage egg chambers (Figure 3.8). In order to address the possibility that maternal *DCIP4* is contributing to the survival of zygotic mutant embryos, germline clone embryos must be generated that lack both maternal and zygotic *DCIP4*.

As shown in Table 3.1, *DCIP4* mutant males crossed to *DCIP4* mutant females produced a high percentage of embryos that failed to secrete cuticle. These maternal and zygotic mutant embryos may have died prior to cuticle secretion which begins at stage 12 (Martinez-Arias, 1993). It is possible that these embryos died as a result of failure to complete cellularization and/or gastrulation. This would be consistent with the DCIP4 expression pattern. Beginning in early embryogenesis, DCIP4 is found at the apical membrane and remains localised apically during membrane cleavage. Post-cellularization and throughout gastrulation, DCIP4 protein remains localised to the cell membrane, and can be found surrounding all epithelial cells (Figure 3.5 A-C).

As previously mentioned, cellularization requires the actin cytoskeleton as well as microtubule networks (Foe et al., 2000). Microinjection of activated Cdc42 into pre-cellularization or cellularization-stage embryos blocked further development. However, no effect was seen with microinjection of mammalian PAKs, suggesting that Cdc42 was acting through other downstream components, possibly DCIP4. Unfortunately, examining the role of Cdc42 in early embryogenesis through mutation analysis has not been possible as strong Cdc42 alleles are lethal and germline clones cannot be produced due to the requirement of Cdc42 during oogenesis (Genova et al., 2000).

Cellularization also requires the donation of internal membrane from endocytic compartments such as endosomes, and from cellular compartment such as the endoplamic reticulum and the Goli apparatus (Mazumdar and Mazumdar, 2002). This membrane movement requires many proteins involved in endocytosis, including Rab GTPases and Dynamin (Mazumdar and Mazumdar, 2002; Strickland and Burgess, 2004). As previously mentioned, PCH family proteins such as Syndapin and FBP17 can bind to the

Dynamin proline-rich regions via their SH3 domains. Given the strong similarities between the FBP17 SH3 domain primary sequence and that of DCIP4, it is possible that DCIP4 may also bind to Dynamin in an SH3-proline-rich-dependent manner. This speculation can be further supported by the punctate staining of DCIP4 seen within the nervous system. It is possible that these punctate structures are vesicles or sites of vesicle budding. If DCIP4 can bind *Drosophila* Dynamin, it would be interesting to see if DCIP4 is required for actin-mediated vesicle trafficking during cellularization.

Although DCIP4 is highly expressed in the embryonic nervous system, we were unable to detect any defects in nervous system development in *DCIP4* zygotic mutant embryos. It is possible that both maternal and zygotic DCIP4 must be removed to see a assess phenotypes within embryonic development. The same reason could explain why no defects were observed in DC or hindgut development in *DCIP4* zygotic mutant embryos.

4.4 The role of *DCIP4* during oogenesis

DCIP4 mutants are semisterile and dissection of *DCIP4* mutant ovaries reveals that many egg chambers degenerate. These egg chambers may be degenerating due to a loss of F-actin, which is seen in *DCIP4* mutant egg chambers. Specifically, cortical and basal F-actin distribution is disrupted and sometimes lost in the FE. This correlates well with the DCIP4 protein distribution as it is mostly present in the follicle cells and becomes mainly basal beyond stage 6 (Figure 3.6). Some *DCIP4* mutant egg chambers display multinucleated nurse cells which can result from detachment of the ring canals from the nurse cell membrane (Figure 3.10). This is also consistent with the expression pattern of DCIP4 as it seem that DCIP4 protein accumulates at sites of ring canal

attachment to the germ cell membrane in early stage 1-3 egg chambers. Similar effects have been observed in Cdc42 mutants (Genova et al., 2000), when CA or DN Cdc42 is expressed during oogenesis, and in egg chambers mutant for *chickadee* (Murphy and Montell, 1996; Verheyen and Cooley, 1994b). Interestingly, a study conducted to find regions in the genome that interacted with the gene *cut* identified two deficiencies that removed *DCIP4* (Jackson and Berg, 1999). Cut is a homeodomain protein that regulates soma-to-germline signalling during *Drosophila* oogenesis. Loss of *cut* leads to multinucleated nurse cells, and this phenotype was enhanced in the presence of one copy of the two different deficiencies that remove *DCIP4*. The gene responsible for this interaction was not identified. As loss of *DCIP4* also produces multinucleated nurse cells, it may be possible that *DCIP4* is the gene responsible for this interaction.

Another phenotype observed in *DCIP4* mutant ovaries was the presence of gaps in the follicular epithelium. This phenotype could be due to a reduced number of follicle cells covering the cyst, or due to detachment of follicle cells from their neighbours (Tanentzapf et al., 2000). A reduced number of follicle cells could result if follicle cell proliferation was defective (Dobens and Raftery, 2000).

It has been documented that degeneration correlates with breakdown of the actin cytoskeleton (Nezis et al., 2000). When looking at degeneration as a phenotype, it is difficult to decipher if cell death is occurring as a secondary effect to loss of cell structure and specificity provided by the cytoskeleton, or if degeneration is leading to the breakdown of the cytoskeleton. Given that DCIP4 is implicated in Cdc42-mediated actin nucleation, it is plausible to speculate that degeneration of egg chambers in *DCIP4* mutants occurs as a cause of disruption of the cytoskeleton. Degeneration and disruption

of the actin cytoskeleton has also been linked to malnourishment (Mazumdar and Mazumdar, 2002). That is, weak flies that are kept in overpopulated stocks, with less fresh food available often do not produce many mature eggs. As previously mentioned, *DCIP4* flies are dormant, and thus may not be feeding properly. Therefore, it is also possible that the defects seen in egg chambers of *DCIP4* mutant females are as a result of malnutrition.

4.5 *DCIP4* is required with *Cdc42* in crossvein development

Homozygosity for weak *Cdc42* alleles or heteroallelic combinations of weak and strong *Cdc42* mutations produces flies with ectopic crossveins. This phenotype was shown to be enhanced in a *DCIP4* mutant background. It is not known why loss of Cdc42 function results in ectopic cross vein formation. Also, the role of the cytoskeleton in crossvein development has not been well-defined. Therefore, it is difficult to interpret the reason for why loss of *DCIP4* enhances this *Cdc42* phenotype. Nonetheless, this result does demonstrate that DCIP4 and Cdc42 function in a common process *in vivo*.

5 RESULTS PART 2: THE *DROSOPHILA* ACK FAMILY

5.1 Characterization of the *Drosophila* ACK family

As part of our efforts to understand Cdc42 signalling in *Drosophila*, we set out to generate loss-of-function mutations in *DACK* and *DPR2*. The results presented here are not in chronological order. Only in the past year have we obtained a mutation in *DPR2,* thus most of our analysis has been with *DACK*. As we were able to generate wild-type and kinase inactive *DACK* transgenes two years prior to successfully obtaining mutations in the *DACK* gene, we have accumulated a large body of data using *DACK* transgenes. Here, I will present the characterization of *DACK* and *DPR2* alleles first and follow with transgenic and mutant analysis of DACK function. We cannot eliminate the possibility that DACK transgene expression may also affect DPR2 function, therefore we will assume that expression of wild-type or kinase inactive (KD) DACK transgenes is affecting the function of both members of the ACK family.

5.1.1 Characterization of *DACK* null alleles

DACK is located on the left arm of the third chromosome at the cytological region *64A10*. Initially, we set out to generate *DACK* loss-of-function alleles using an EMS mutagenesis screen. We screened for alleles that failed to complement the deficiency *Df(3L)C175* (Drysdale, 2005); (Sem et al., 2002), which removes *DACK*. We generated 500 EMS-mutated chromosomes, only one of which failed to complement *Df(3)C175*. This chromosome did not contain a mutation in *DACK*. Concurrently, a P element, *KG00869* (Bellen, 2004), was identified that was inserted 4bp prior to the start

point of the longer of the two *DACK* splice forms. This P element was excised by a Master's student in our lab, Xing (Barton) Xu, to generate *DACK* null alleles. Three independent excisions were isolated that showed loss of *DACK* transcript but retention of transcripts of *DACK*'s two neighbouring genes, *GC14991* and *CG14996*, on Northern blots (Figure 5.1 B). Through Southern blotting, Barton was able to show that the allele, $DACK^{10b}$, still contains part of the P element sequence. However, he was unable to determine if the DACK initiator methionine was deleted in this allele. Using genomic PCR, he determined the molecular breakpoints of the $DACK^{86}$ allele. This allele removes roughly 2.8 Kb of the *DACK* gene, including the first exon, but does not affect the *DACK* coding sequence. The molecular breakpoints of the $DACK^{29b}$ allele have not been determined (Figure 5.1 A). All three *DACK* alleles are homozygous viable and are fertile when in combination with *Df(3L)C175*. However, all three *DACK* alleles carry a second site mutation that results in male sterility either alone or in conjunction with homozygosity for *DACK*.

5.1.2 *DPR2* hypomorphic allele

DPR2 is located on the right arm of the second chromosome at the cytological region *49F3-4*. *DPR2* and another gene, *TppII*, reside in an intron of *CapG* (Figure 5.2 A). A piggy-Bac element, *PBc02472* (*PB*), was identified that inserts into the first intron of *DPR2* (Thibault et al., 2004). Piggy-Bac elements have been shown to silence the region where they are inserted (Thibault et al., 2004). This *PB* element causes a decrease in *DPR2* transcription (Figure 5.2 B). Although *PB* is also in close proximity to *CapG* and *TppII*, its presence does not affect the transcription of these two genes (Figure 5.2 B).

Figure 5.1 *DACK* null alleles.

(A) Schematic representing the *DACK* gene region. Numbers represent base positions on scaffold *AE003480* of chromosome 3L. Southern analysis of $DACK^{10b}$ indicates retention of partial P element sequence within the allele. $DACK^{86}$ contains a deletion of 2,769 nucleotides (positions 9726-12495 of *AE003480*) and the deletion does not remove the *DACK* coding sequence. It has not been determined if the DACK coding sequence is disrupted in the $DACK^{10b}$ or $DACK^{29b}$ alleles. (B) Northern blots showing loss of *DACK* transcript in flies homozygous for the $DACK^{10b}$, $DACK^{29b}$ and $DACK^{86}$ alleles. *rp49* was used as a loading control. The work shown in this figure was completed by Xing (Barton) Xu.

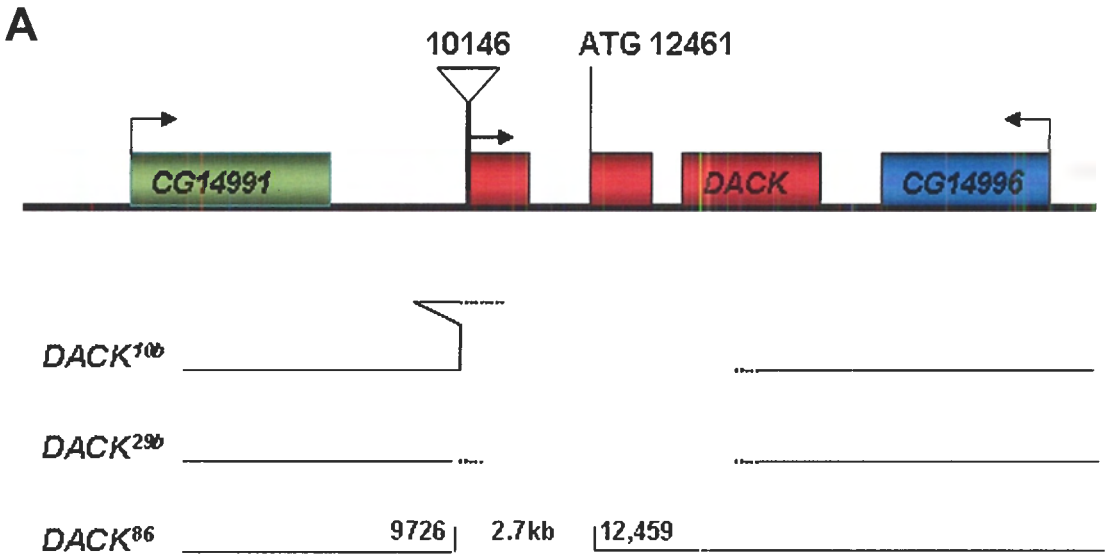
A
10146
ATG 12461
CG14991
DACK
CG14996
DACK10b
DACK29b
DACK86
9726
2.7kb
12,459

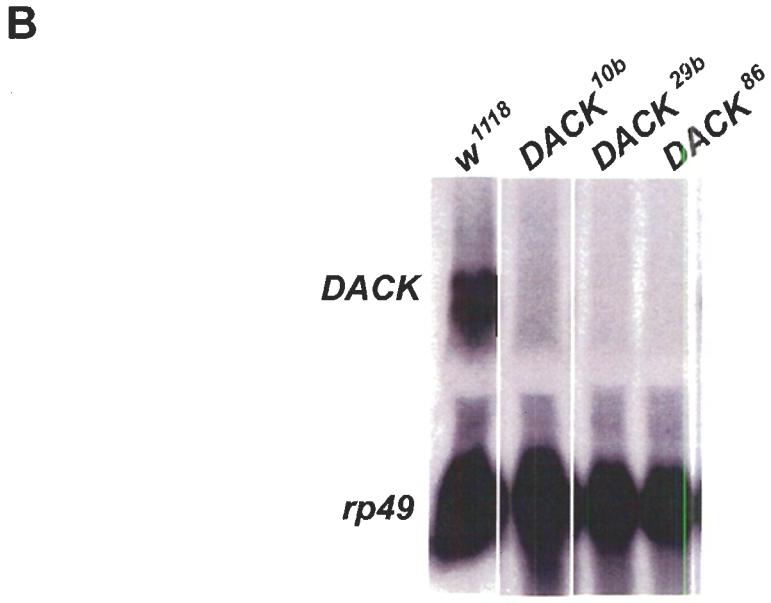
B
w1118
DACK10b
DACK29b
DACK86
DACK
rp49

Figure 5.2 Characterization of a *DPR2* hypomorphic allele, *PBc02472*.

(A) Schematic of the *DPR2* gene region showing cut sites for the restriction enzymes *Xho*I and *Xba*I. Genomic fragments that would result from a *Xho*I or *Xba*I digest and would hybridize to a probe generated from a *DPR2* cDNA template are represented in the box. The schematic is not drawn to scale. (B) Northern blots showing the two *DPR2* transcripts are decreased in *PBc02472* homoygotes. However, *CapG* and *TppII* transcript levels in *PBc02427* homozygotes are similar to w^{1118} wild-type controls. (C) Southern blot of genomic DNA from w^{1118}, *PBc02472/CyO* and homozygotes from *PBc02472* reversion lines, *4Bii*, *5Ai*, *10Bii*, and *14Bii*, digested with *Xho*I or *Xba*I. A *DPR2* cDNA was used as a template to generate a probe. Expected genomic fragments from the two different digests are presented in (A). The bands corresponding to the asterisks in the *Xho*I w^{1118} and *PBc02472/CyO* lanes are most likely undigested DNA as they are not present in the other w^{1118} and *PBc02472/CyO* lanes shown. A band that is smaller than 2kb is present in the *Xho* I *PBc02472/CyO* lanes. This band may be due to the *CyO* balancer as it is not present in the lane showing *PBc02472* homozygotes digested with *Xho* I. (D) Northern blot showing *DPR2* reversion lines from (C) express wild-type levels of *DPR2* transcript. *rp49* was used as a loading control.

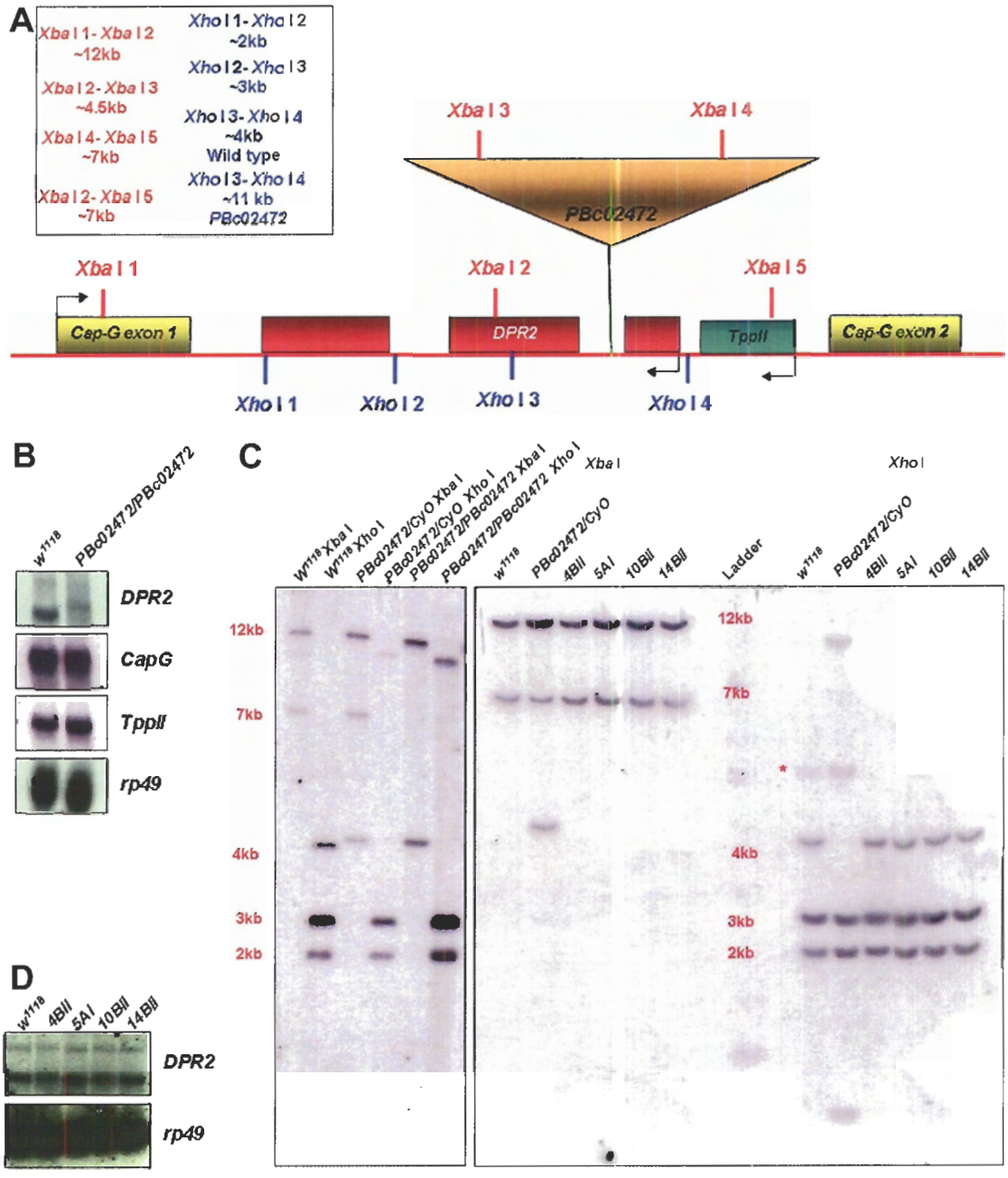
A
Xba I 1- Xba I 2
~12kb
Xba I 2- Xba I 3
~4.5kb
Xba I 4- Xba I 5
~7kb
Xba I 2- Xba I 5
~7kb
Xho I 1- Xho I 2
~2kb
Xho I 2- Xho I 3
~3kb
Xho I 3- Xho I 4
~4kb
Wild type
Xho I 3- Xho I 4
~11 kb
PBc02472
Xba I 3
Xba I 4
PBc02472
Xba I 1
Xba I 2
Xba I 5
Cap-G exon 1
DPR2
TppII
Cap-G exon 2
Xho I 1
Xho I 2
Xho I 3
Xho I 4
B
w1118
PBc02472/PBc02472
DPR2
CapG
TppII
rp49
C
Xba I
Xho I
w1118 Xba I
w1118 Xho I
PBc02472/CyO Xba I
PBc02472/CyO Xho I
PBc02472/PBc02472 Xba I
PBc02472/PBc02472 Xho I
w1118
PBc02472/CyO
4BII
5AI
10BII
14BII
Ladder
w1118
PBc02472/CyO
4BII
5AI
10BII
14BII
12kb
7kb
4kb
3kb
2kb
12kb
7kb
4kb
3kb
2kb
D
w1118
4BII
5AI
10BII
14BII
DPR2
rp49

The *PB* insertion is semi-lethal and completely lethal when in trans to deficiencies that remove *DPR2*, *Df(2R)VgB* and *Df(2R)CX1* (Drysdale, 2005). Homozygous PB males are fertile; however, homozygous females are sterile, as they do not lay eggs.

In order to ensure that the decrease in *DPR2* transcription was due to the *PB* insertion, we remobilized this element in order to isolate a precise excision, thus reverting the *DPR2* gene to wild-type. Flies that no longer contained the *PB* element were identified by the loss of the *mini-white* gene associated with *PB* (Thibault et al., 2004). We generated 50 lines that no longer contained the *PB* element. All of these lines were homozygous viable suggesting that all had reverted back to wild-type. We performed Southern and Northern analysis on five of these putative revertants to assess the condition of the *DPR2* gene and transcript, respectively. All five lines showed that the *DPR2* genomic region and *DPR2* transcript levels had reverted to wild-type (Figure 5.2 C-D). It has been observed that PB elements excise precisely in comparison to EP elements (Thibault et al., 2004). We in fact noticed that all 50 of our excisions were viable, suggesting that they had all reverted to wild-type, thus supporting the prior observations of (Thibault et al., 2004) .

5.2 *DACK* and *DPR2* transcripts and DACK protein are enriched at the leading edge of the epidermis during dorsal closure

We looked at *DACK* and *DPR2* transcript distribution during embryogenesis using whole-mount *in situ* hybridization with a *DACK* or *DPR2* RNA probe. *DACK* transcript was widely distributed during embryogenesis. In the early stages of DC,

Figure 5.3 ACK family expression during embryonic development.

(A) Dorsal view of a late stage 13 embryo showing DACK protein expression at the leading edge of the epidermis late in dorsal closure (arrowhead). (B) Lateral view of stage 13 wild-type embryo at the beginning of dorsal closure showing enrichment of *DACK* transcript at the leading edge of the epidermis (arrowhead). (C) Lateral view of stage 13 wild-type embryo during dorsal closure showing enrichment of *DPR2* transcript at the leading edge of the epidermis (arrowhead). *DPR2* transcript is also found in the developing tracheal system (arrow).

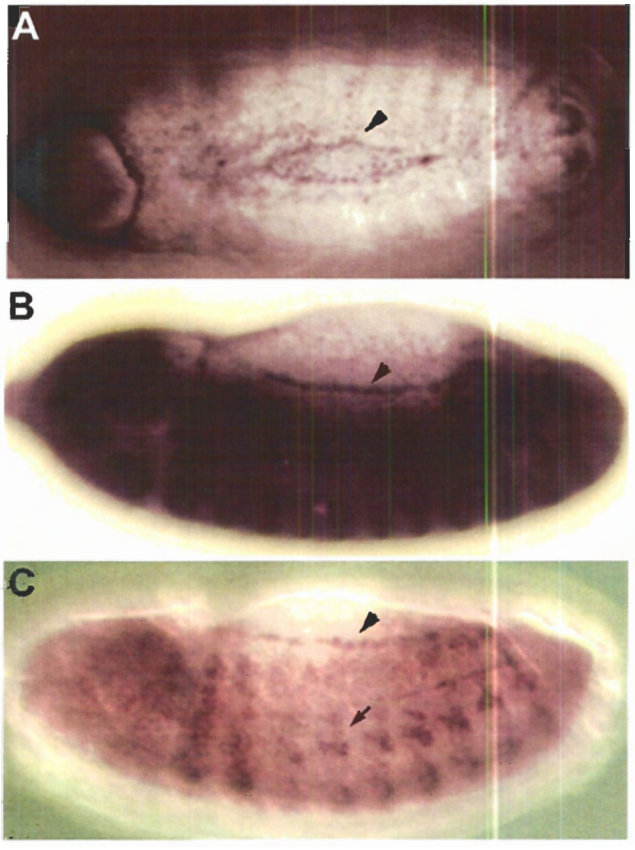
A
B
C

DACK transcript was elevated at the leading edge of the advancing epidermis (Figure 5.3 A). Affinity purified polyclonal antibodies against a GST-fusion protein containing amino acids 873 to 979 from the C-terminal, non-conserved region of *DACK* (Sem et al., 2002) or an antiserum raised against the full-length *DACK* (Clemens et al., 2000) showed elevated *DACK* staining along the LE similar to what was seen with *DACK* RNA *in situ* hybridizations. However, DACK protein persisted at the LE until a later stage of DC than the transcript (Figure 5.3 B). *DPR2* transcript is also found at the leading edge epidermis during DC at similar times as *DACK* transcript (Figure 5.3 C arrowhead). Unlike *DACK*, which has a more ubiquitous staining throughout the embryo, *DPR2* transcript is also highly enriched in the developing embryonic tracheal system (Figure 5.3 C arrow). We unfortunately do not have an antibody against DPR2 to assess its protein distribution during embryogenesis.

5.3 Embryos zygotically mutant for *DACK* and *DPR2* do not display dorsal closure defects

Cuticle preparations revealed that *DACK* mutant embryos had a low frequency of holes in the dorsal and anterior surfaces, indicative of defects in DC and possibly head involution (Table 5.1). We wondered if this low penetrance of defects was due to the presence of DPR2. As both ACKs are enriched in the LE cells (Figure 5.3 and (Sem et al., 2002), it is likely that they have overlapping functions during DC. First, we tested to see if reduction of *DPR2* alone had any affect on DC. Although we do not have a null allele in *DPR2*, we generated *DPR2* mutant embryos that were heterozygous for *PB* and *Df(2R)VgB*, a deficiency that removes *DPR2*. Cuticle preparations of these embryos also revealed no DC defects (data not shown). A higher frequency of DC defects was seen in

Table 5.1 ***DACK*** **and** ***DPR2*** **embryonic phenotypes.**

PB represents the *DPR2* piggy-Bac allele, *PBc02472*. N/A is used when cuticle preparations were not scored for a particular phenotype. As described in the text, scars refer to possible wounds that may be present in the dorsal surface leading to defects in cuticle secretion. Some embryos in the dorsal hole category also contained head defects. All crosses were completed at 25°C. Each cross produced similar levels of embryos that did not secrete cuticle. Therefore, these embryos were assumed to be unfertilized eggs and not included in the total number of embryos counted.

Table 5.1 *DACK* and *DPR2* embryonic mutant phenotypes

Cross	% Phenotype					n
	Wild-type	Dorsal hole	Scar	Head defect	Ventral hole	
w^{1118}♀ x w^{1118}♂	99.41	0.16	N/A	0.27	0.16	1277
$DACK^{86}/DACK^{86}$♀ x $DACK^{86}/TM3Sb$♂	92.65	5.47	N/A	0.72	1.16	1116
$DACK^{86}/DACK^{86}$♀ x $DACK^{10b}/TM3Sb$♂	93.02	2.13	N/A	2.39	1.46	753
$DACK^{86}/DACK^{86}$♀ x $DACK^{29b}/TM3Sb$♂	94.38	1.63	N/A	2.51	1.48	676
$DACK^{86}/DACK^{86}$♀ x *Df(3L) C175/TM3Sb*♂	98.93	1.07	N/A	/	/	561
PB/CyO ♀ x *PB/PB*♂	98.9	1.01	N/A	/	/	360
PB/CyO;$DACK^{10b}/DACK^{10b}$♀ x *PB/PB;*$DACK^{10b}/TM3Sb$♂	98.87	1.13	N/A	/	/	617
PB/CyO;$DACK^{10b}/DACK^{10b}$♀ x *Df(2R)VgB/+;*$DACK^{86}$/+♂	97.5	/	2.5	/	/	196

embryos expressing *KD-DACK*, which could be acting in a dominant negative manner to impede signalling from both kinases (Sem et al., 2002). We therefore set out to generate embryos that were zygotically mutant for both *DACK* and *DPR2* using the alleles described. As females homozygous for *DACK* alleles are fertile, we crossed females that were maternal and zygotic mutant for *DACK* and heterozygous for *DPR2* to males that were homozygous mutant for *DPR2* and heterozygous mutant for $DACK^{10b}$ (we could not use males homozygous for *DACK* due to the male sterility present in the $DACK^{10b}$ homozygous mutant background). Twenty-five percent of the F1 from this cross were homozygous mutant for both *DACK* and *DPR2*. Progeny of this cross did not fail to complete DC. As *PB* is a hypomorphic *DPR2* allele, we introduced into the crossing scheme a copy of *Df(2R)VgB* to decrease the amount of *DPR2* transcript, and hopefully DPR2 protein, present in F1 embryos. We mated females that were heterozygous for the *PB* allele and homozygous for $DACK^{10b}$ to males that were heterozygous for *Df(2R)VgB* and $DACK^{86}$ and performed cuticle preparations of the resulting progeny. Twelve percent of the F1 from this cross were zygotically mutant for both *DPR2* and *DACK*. Out of 191 embryos counted, 97.5% were wild-type, 1.5% percent showed possible scars that may be due to certain cells on the dorsal surface failing to secrete cuticle properly, and 1% displayed head defects. We conclude that a dramatic reduction in zygotic ACK family function is not sufficient to produce DC defects. One possibility is that we need to remove not just zygotic ACK function, but also maternal function to see defects in DC.

5.4 Overexpression of DACK can rescue the dorsal closure defects caused by expression of dominant negative Cdc42

Although *DACK* mutants successfully complete embryogenesis, induction of wild-type or KD *DACK* transgenes in the embryo cause a range of defects in embryonic epithelial morphogenesis, including dorsal holes (Sem et al., 2002). The DC failures caused by *DACK* transgene expression and the presence of endogenous *DACK* and *DPR2* at the LE are indicative of a role for ACK family kinases in DC. We therefore wondered if ACK family tyrosine kinase activity was operating downstream of Cdc42 during DC. We tested to see if overexpression of DACK could rescue the DC defects caused by ectopic expression of *UAS-Cdc42N17*. Flies heterozygous for a chromosome bearing both *UAS-Cdc42N17* and the heat shock-inducible GAL4 driver *Hs-GAL4*^{2207} were mated to either a control line or flies homozygous for a *UAS-DACK* transgene. The F1 progeny were heat shocked as embryos 6 to 12 h AEL, allowed to age to the appropriate stage for cuticle secretion, and examined with cuticle preparations. Heat shock times were kept to 30 minutes to avoid embryonic phenotypes result from overexpressing DACK. For each experiment in which the *UAS-DACK* transgene was co-expressed with *UAS-Cdc42N17*, a control cross was performed in parallel. Co-expression of *UAS-Cdc42N17* with *UAS-DACK* produced significantly lower dorsal hole frequencies with respect to expression of *UAS-Cdc42N17* alone (Table 5.2). Half of the progeny in each cross will have transgene expression, thus the actual frequencies of phenotypic effects in transgene-expressing embryos are estimated to be twice the values shown. In the two experiments shown in Table 5.2, the control cross was designed to account for possible genetic background effects of *UAS-DACK* flies. For this, the *Hs-GAL4*^{2207},*UAS-Cdc42N17* line was crossed to the *yw* strain that had been used to establish the *UAS-DACK* line. Following induction

of *UAS-Cdc42N17*, 8.9% and 22.4% of the progeny from this cross had dorsal holes. In the parallel cross, in which *UAS-DACK* was co-expressed with *UAS-Cdc42N17*, the frequency of dorsal holes decreased to 1.1% and 3.2%, respectively.

Table 5.2 Overexpression of DACK can suppress the dorsal closure defects caused by expression of dominant negative Cdc42.

Percentage of embryonic phenotypes are shown for two independent experiments, each of which consisted of one control expression of *UAS-Cdc42N17* and one co-expression of *UAS-Cdc42N17* with *UAS-DACK*. The rescue experiment was conducted on two independent occasions, with results shown as Experiment 1 and Experiment 2. The F1 progeny from each cross were heat shocked for 30 minutes at 37°C as embryos 6 to 12 hours AEL, allowed to age to the appropriate stage for cuticle secretion, and examined with cuticle preparations. Control and experimental crosses were performed in parallel and heat shocked simultaneously. Heat shock was kept to 30 minutes to avoid generation of DACK-specific phenotypes. Each cross produced similar levels of embryos that did not secrete cuticle. Therefore, these embryos were assumed to be unfertilized eggs and not included in the total number of embryos counted.

Table 5.2 Overexpression of DACK can suppress dorsal closure defects associated with expression of Cdc42N17

Cross	%Phenotype Wild-type	%Phenotype Dorsal hole	n
Experiment 1			
Hs-GAL42207, UAS-Cdc42N17/CyO♀ x yw♂	91.11	8.89	531
Hs-GAL42207, UAS-Cdc42N17/CyO♀ x UAS-DACK/UAS-DACK♂	98.88	1.12	624
Experiment 2			
Hs-GAL42207, UAS-Cdc42N17/CyO♀ x yw♂	77.59	22.41	290
Hs-GAL42207, UAS-Cdc42N17/CyO♀ x UAS-DACK/UAS-DACK♂	96.76	3.24	741

5.5 *DACK* transcript levels in tissues participating in dorsal closure are affected by the level of Cdc42 function

To determine if alterations in Cdc42 signalling had any effect on *DACK* expression in embryos, we looked at *DACK* transcript levels in embryos expressing *UAS-Cdc42V12* and *UAS-Cdc42N17* transgenes under the control of a ubiquitous heat shock GAL4 driver, *Hs-GAL4*$^{M-4}$. RNA *in situ* hybridizations were subsequently performed using a *DACK* RNA probe. As controls, we hybridized *DACK* probe to wild-type embryos, transgenic embryos not exposed to heat shock, as well as heat shocked *Hs-GAL4*$^{M-4}$ embryos. A strong staining for *DACK* transcripts was observed in the amnioserosa late in DC in *UAS-Cdc42V12/Hs-GAL4*$^{M-4}$ embryos that had been exposed to a 1 h heat shock (Figure 5.4 A). None of the control embryos showed enrichment of *DACK* transcript in the amnioserosa (Figure 5.4 C and data not shown). Accumulation of *DACK* transcripts at the leading edge of the epidermis persisted until late in DC following *Cdc42N17* expression with a 1 h heat shock (Figure 5.4 B). Control wild-type embryos, heat shocked *Hs-GAL4*$^{M-4}$ embryos, and *UAS-Cdc42N17;Hs-GAL4*$^{M-4}$ embryos that were not exposed to heat shock, only showed *DACK* transcript accumulation at the LE at the beginning of DC and not later (Figure 5.3 B, Figure 5.4 D and data not shown).

Figure 5.4 *DACK* transcript levels in tissues participating in dorsal closure are affected by the level of Cdc42 function.

(A) Dorsal views of stage 15 *UAS-Cdc42V12/Hs-GAL4*$^{M-4}$ embryos that had been heat shocked for 1 h at 37°C, showing *DACK* transcript accumulation in the amnioserosa (arrowheads). (B) Dorsal views of stage 15 *UAS-Cdc42N17;Hs-GAL4*$^{M-4}$ embryos that had been heat shocked for 1 h at 37°C, showing *DACK* transcript accumulation at the leading edge at later stages than seen in wild-type embryos (arrowheads). (C) Dorsal view of stage 15 *UAS-Cdc42V12/Hs-GAL4*$^{M-4}$ embryo that had been maintained at 21°C, showing no areas of elevated *DACK* transcription on the dorsal surface. (D) Dorsal view of stage 15 *UAS-Cdc42N17;Hs-GAL4*$^{M-4}$ embryo that had been maintained at 21°C, showing no areas of elevated *DACK* transcription on the dorsal surface.

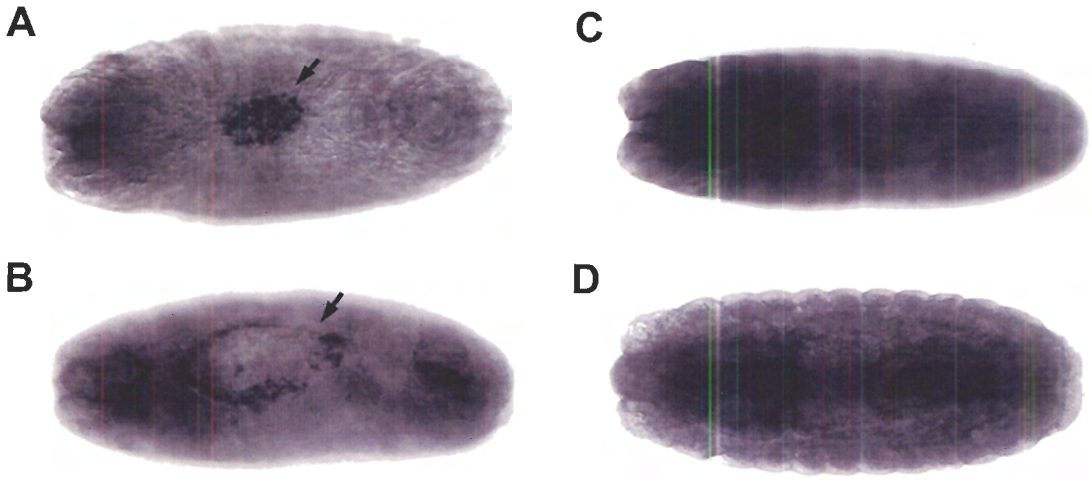
A
B
C
D

5.6 DACK does not participate in activation of gene expression downstream of the JNK cascade, and the JNK cascade is not required for the leading edge expression of DACK

A key regulator of DC in the LE cells is the JNK cascade. Since both ACKs are expressed at the LE, and expression of wild-type and KD-DACK induce dorsal holes, we wondered if ACK family kinases are required for JNK signalling. Previously, a Master's student from our lab, Kaiping Sem, showed that overexpression of DACK did not lead to ectopic expression of *puc*, a target gene downstream of the JNK cascade (Sem et al., 2002). We tested the effects of DACK overexpression on the JNK-dependent transcription of *dpp* at the LE. Embryos in which DACK had been overexpressed in the amnioserosa, using the $GAL4^{332.2}$ driver (Sem et al., 2002), or in the epidermis in segmental *ptc* stripes, using the $GAL4^{559.1}$ driver (Hinz et al., 1994) were hybridized with a *dpp* riboprobe. Ectopic expression of *dpp* expression was not observed and the distribution of *dpp* transcripts in these embryos was identical to wild-type (data not shown and (Sem et al., 2002). We looked at the effects of impairment of DACK function on the JNK cascade by examining the LE transcription of *dpp* in embryos homozygous for *Df(3L)C175,* which removes the *DACK* gene, and in embryos expressing KD-DACK. We also looked at *dpp* expression in embryos that were maternally and zygotically devoid of *DACK*. In both cases, *dpp* transcription was maintained at the LE (data not shown and (Sem et al., 2002).

Given that DACK is expressed at the LE during DC, it is possible that DACK itself could be a target gene of the JNK cascade. We looked at *DACK* transcript levels in *basket* mutant embryos, which bear a loss-of-function mutation in the gene encoding

Drosophila JNK (Riesgo-Escovar et al., 1996; Sluss et al., 1996). The LE expression of *DACK* was intact in these mutant embryos (data not shown). We also ectopically activated the JNK cascade in *engrailed* (*en*) segmental stripes by expressing *UAS-Drac1V12* with *en-GAL4* (Sem et al., 2002) and looked at *DACK* transcript levels in these embryos. We did not observe ectopic *DACK* transcript levels in *en* stripes (data not shown and (Sem et al., 2002).

5.7 DACK can suppress the dorsal closure defects associated with mutations in the TGF-β/BMP-2 Type I and Type II receptors, Tkv and Put

DACK does not seem to signal through the JNK cascade during DC. We next asked if DACK functions downstream of the JNK target gene, *dpp*. Dpp, as previously mentioned, is a fly homologue of the mammalian BMP-2 ligand. It relays its signals to two fly TGF-β/BMP-2 receptors, Thickveins (Tkv) and Punt (Put) in the epidermis during DC. Mutations in *tkv* or *put* result in holes in the dorsal cuticle due to the requirement for these genes in DC. Ricos et al. previously showed that expression of constitutively active Cdc42, Cdc42V12, could suppress the DC defects associated with a *tkv* loss-of-function allele, tkv^7 (Ricos et al., 1999).

Roughly thirty-five percent of embryos laid by tkv^7/CyO parents die with dorsal defects in the form of head holes, germband retraction failures, and/or dorsal holes (Table 5.3; also see Figure 1.2 for a review of morphogenetic events during embryogenesis). Embryos homozygous for the *CyO* balancer die without dorsal defects; it can therefore be assumed that these defects are due to homozygosity for the tkv^7 mutation. We attempted to rescue the DC defects associated with tkv^7 by overexpression of DACK. Flies

heterozygous for a chromosome bearing both *Hs-GAL4*^{2207} and the *tkv*^{7} mutation were mated to either flies heterozygous for the *tkv*^{7} allele, or flies heterozygous for a chromosome bearing *tkv*^{7} and a *UAS-DACK* transgene. Therefore, 25% of the progeny from either cross will be homozygous for *tkv*^{7}, and either expressing or not expressing DACK. We found that *tkv*^{7} mutant embryos developed slower than wild-type, therefore, we aged embryos to 7-14 hours AEL, instead of 6-12 hours AEL, for our DACK heat shock inductions. Similar to activated Cdc42, overexpression of DACK could suppress the DC defects of *tkv*^{7} from 27.1% to 4.3%. However, the head defects or germband retraction failures were not suppressed. As explained in the legend of Table 5.3, any given embryo was counted only once. Many of the embryos counted in the "dorsal hole" category for the *tkv*^{7} control and experimental crosses also contained head defects and germband retraction failures. The increase in the frequency of head hole and/or germband retraction failures seen in the progeny of the experimental cross (*tkv*^{7}, *hs-Gal4/CyO*♀ *x tkv*^{7}, *UAS-DACK/CyO*♂) most likely represent the percentage of *tkv*^{7} mutant embryos whose DC defects, but not their head defects or germband retraction failures, were rescued by overexpression of DACK (Table 5.3). This suggests that DACK only contributes to Tkv function in DC, and not in germband retraction or head development. We also noticed that 5.1% of embryos from the experimental cross had small specks, scars, or puckers on their dorsal surfaces, indicating that DC may not have completed properly, and/or that cuticle was not secreted properly by a subset of cells on the dorsal surface. These scars may represent the dorsal holes of *tkv*^{7} mutant embryos that were suppressed, but not rescued to completion, by overexpression of DACK.

Table 5.3 Suppression of the dorsal hole defects of *tkv*^{7} and *put*^{135} by expression of *UAS-DACK.*

The F1 progeny from each cross were heat shocked for 30 minutes at 37°C as embryos 7 to 14 hours AEL, allowed to age to the appropriate stage for cuticle secretion, and examined with cuticle preparations. Control and experimental crosses were performed in parallel and heat shocked simultaneously. Any given embryo was only counted once. Any embryo containing a dorsal hole was assigned to the "dorsal hole" category. However, many of the embryos counted for the "dorsal hole" category for both of the crosses *tkv*^{7}, *hs-Gal4/CyO*♀ x *tkv*^{7}*/CyO*♂ and *tkv*^{7}, *hs-Gal4/CyO*♀ x *tkv*^{7}, *UAS-DACK/CyO*♂ also contained head holes and/or germband retraction failures.

Table 5.3 Suppression of the dorsal hole phenotype of *tkv*^{7} and *put*^{135} by expression of *UAS-DACK*

	% Phenotype					
Genotype	**Wild-type**	**Dorsal hole**	**Scar or puckered**	**Germband retraction failure with head defect**	**Head defect**	**n**
tkv^{7}, *hs-Gal4/CyO*♀ x *tkv*^{7}*/CyO*♂	64.8	27.1	/	6.9	1.2	509
tkv^{7}, *hs-Gal4/CyO*♀ x *tkv*^{7}, *UAS-DACK/CyO*♂	61.4	4.3	5.1	19.4	7.1	490
put^{135}, *Hs-Gal4M-4/TM3Sb*♀ x *put*^{135}*/TM3Sb*♂	75.6	24.4	/	/	/	396
put^{135}, *Hs-Gal4M-4/TM3Sb*♀ x *put*^{135}, *UAS-DACK/TM3Sb*♂	93.4	3.3	1.3	/	2.0	396

Similar rescue experiments were conducted with a mutation for *put*, put^{135} (Table 5.3). All embryos homozygous for the put^{135} mutation die with holes on their dorsal surfaces. However, unlike tkv^{7}, put^{135} mutant embryos do not display defects in head development or germband retraction. To attempt our rescue of the $punt^{135}$ embryonic phenotype, we crossed flies heterozygous for a chromosome bearing the $punt^{135}$ mutation and *Hs-GAL4-*^{M4} to either flies heterozygous for the $punt^{135}$ mutation, or flies heterozygous for a chromosome bearing the $punt^{135}$ mutation and *UAS-DACK*. Twenty-five percent of the F1 from these crosses will contain embryos homozygous for $punt^{135}$, and will either be expressing or not expressing DACK. For each cross, embryos 8-12 hours AEL (another common time point used for heat shock driven transgene expression during DC) were subjected to a half hour heat shock and allowed to age to the appropriate stage for cuticle secretion, then analysed by cuticle preparations. Overexpression of DACK reduced the percentage of dorsal holes associated with $punt^{135}$ from 24.4% to 3.3%.

5.8 DACK can induce ectopic expression of Dpp target genes

To investigate the role of DACK in Dpp signalling, we asked if DACK could ectopically induce transcription of genes previously shown to be targets of Dpp receptor signalling. We chose to look at two Dpp target genes which are themselves required for proper DC to occur: *kayak* (*kay*) (also known as *Dfos*) and *zipper* (*zip*). *Dfos* and *zip* encode the *Drosophila* orthologues of the transcription factor Fos and non-muscle myosin-II heavy chain, respectively (Arquier et al., 2001; Riesgo-Escovar and Hafen, 1997; Zeitlinger et al., 1997). *Dfos* transcription in the lateral epidermis is severely reduced in *tkv* and *put* mutant embryos, while expression of an activated Tkv receptor can

induce ectopic *Dfos* expression (Riesgo-Escovar and Hafen, 1997). In embryos zygotically mutant for *tkv*, transcription of *zip* in the LE cells is greatly reduced (Arquier et al., 2001).

The *Dfos* and *zip* transcripts are not normally expressed in the amnioserosa (Figure 5.5 A and C). However, when *UAS-DACK* was expressed in the amnioserosa using the driver $GAL4^{332.2}$ (Wodarz et al., 1995), ectopic expression of both target genes was induced (Figure 5.5 B and D). This induction was dependent on the kinase function of DACK, as expression of a *KD-DACK* transgene did not lead to ectopic expression of *Dfos* or *zip* (data not shown). The induction of gene expression was specific, as the *dpp* transcript was not upregulated as a consequence of DACK misexpression (Figure 5.5 F). This result also confirms that DACK is not driving Dpp signalling by upstream activation of the JNK cascade. This is consistent with our earlier studies showing that *dpp* expression is normal in embryos homozygous for a deficiency in DACK and in embryos expressing KD-DACK (Sem et al., 2002). Expression of *DCIP4* was also not upregulated in response to DACK expression in the amnioserosa (data not shown).

5.9 DACK-induced gene expression of Dpp target genes is not due to ectopic phosphorylation of Mad

The Dpp/BMP2 signal is transduced to the nucleus by a complex of transcription factors and cofactors which includes the Smad proteins (reviewed in (Shi and Massague, 2003). Upon activation of the receptor complex, initiated by ligand binding, the Type I receptor phosphorylates Smad1/5 which then binds to its cofactor, Smad 4, and translocates into the nucleus to regulate gene expression. We asked whether changes in ACK function could affect receptor-mediated phosphorylation of the *Drosophila*

Figure 5.5 DACK can induce expression of Dpp target genes.

Lateral views of stage 14 w^{1118} embryos showing (A, C, E) wild-type RNA expression pattern of *Dfos* (A), *zip* (C), and *dpp* (E) or *UAS-DACK / GAL4*$^{332.2}$ embryos (B, D, E) showing ectopic expression of *Dfos* (B), *zip* (D) in the amnioserosa but no ectopic expression of *dpp* (F).

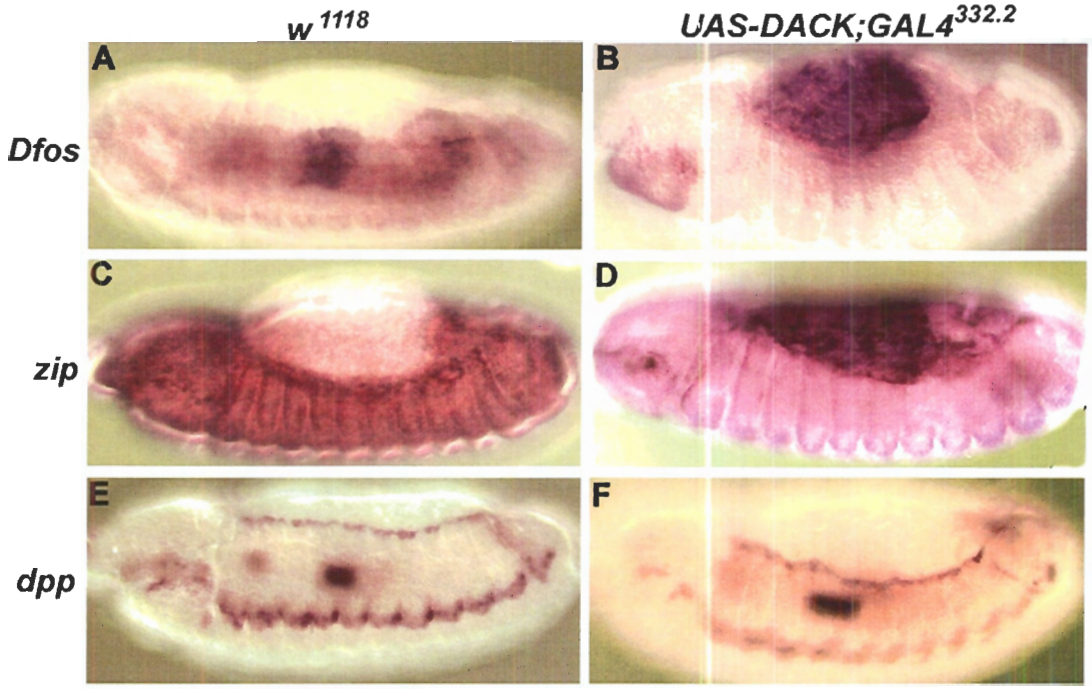
w 1118
UAS-DACK;GAL4 332.2
A
B
Dfos
C
D
zip
E
F
dpp

Smad 1/5 homologue, Mad. Activation of the Dpp pathway at the level of the receptor complex can be visualized by staining embryos with an antibody that recognizes the receptor-phosphorylated Mad, p-Mad (Persson et al., 1998). Ectopic activation of the Dpp pathway can be triggered by overexpression of Dpp or by a CA version of the Tkv receptor, Tkv^{Q199D} (Hoodless et al., 1996). For example, expression of *UAS-Dpp* or *UAS-*Tkv^{Q199D} with a *prd-GAL4* driver leads to p-Mad accumulation in prd stripes (Figure 5.6 C, D, G and (Dorfman and Shilo, 2001). However, expression of *UAS-DACK* with the *prd* driver, or with $GAL4^{332.2}$, does not produce ectopic p-Mad (Figure 5.6 F and data not shown). Furthermore, *UAS-*Tkv^{Q199D} or *UAS-Dpp* expression can still induce ectopic p-Mad, either when co-expressed with *UAS-KD-DACK* (Figure 5.6 E and data not shown) or in a maternal and zygotic DACK mutant background (data not shown and Figure 5.6 H).

5.10 Loss-of-function *DACK* alleles genetically interact with components of Dpp signalling

In *DACK* mutant embryos, Dpp signalling may be impaired, but not sufficiently to cause a strong phenotype. We reasoned that if we further impaired Dpp signalling in *DACK* mutant embryos we might see a DC phenotype. We were successful in achieving this goal when we impaired Dpp signalling in *DACK* mutant embryos at three different levels — ligand, pathway member, and target gene — by reducing the amount of *dpp*, *medea* (*med*), and *Dfos*, respectively (Table 5.4). We used three *dpp* alleles in this analysis: a pharate adult lethal, dpp^{s11}, and two embryonic lethals, dpp^{hr27} and dpp^{hr92} (St Johnston et al., 1990; Wharton et al., 1993). Embryos heterozygous for these *dpp* alleles

Figure 5.6 DACK-induced expression of Dpp target genes is not due to ectopic phosphorylation of Mad.

Lateral views of stage 10 (A, C, F) and stage 13 (B, D, F, G, H) embryos stained with an antibody against p-Mad. (A, B) w^{1118} embryos showing wild-type p-Mad staining during DC. (C, D) *UAS-Tkv*^{Q199D}*/prd-GAL4* embryos showing ectopic p-Mad in *prd* stripes. (E) *UAS-Tkv*^{Q199D}*, UAS-KD-DACK/prdGAL4* embryo showing ectopic p-Mad is not affected by expression of KD-DACK. (F) *UAS-DACK / prd-GAL4* embryo showing that ectopic expression of DACK in *prd* stripes does not lead to elevated p-Mad levels. (G) *UAS-Dpp/prd-GAL4* embryo showing a broader domain of ectopic p-Mad than seen in *UAS-Tkv*^{Q199D}*/prd-GAL4* embryos. (H) *UAS-Dpp, DACK*^{10b}*/prdGAL4, DACK*^{10b} embryo generated from *UAS-Dpp, DACK*^{10b}*/UAS-Dpp, DACK*^{10b} females, showing the broader ectopic p-Mad domains are not affected by loss of maternal and zygotic (MZ) *DACK*.

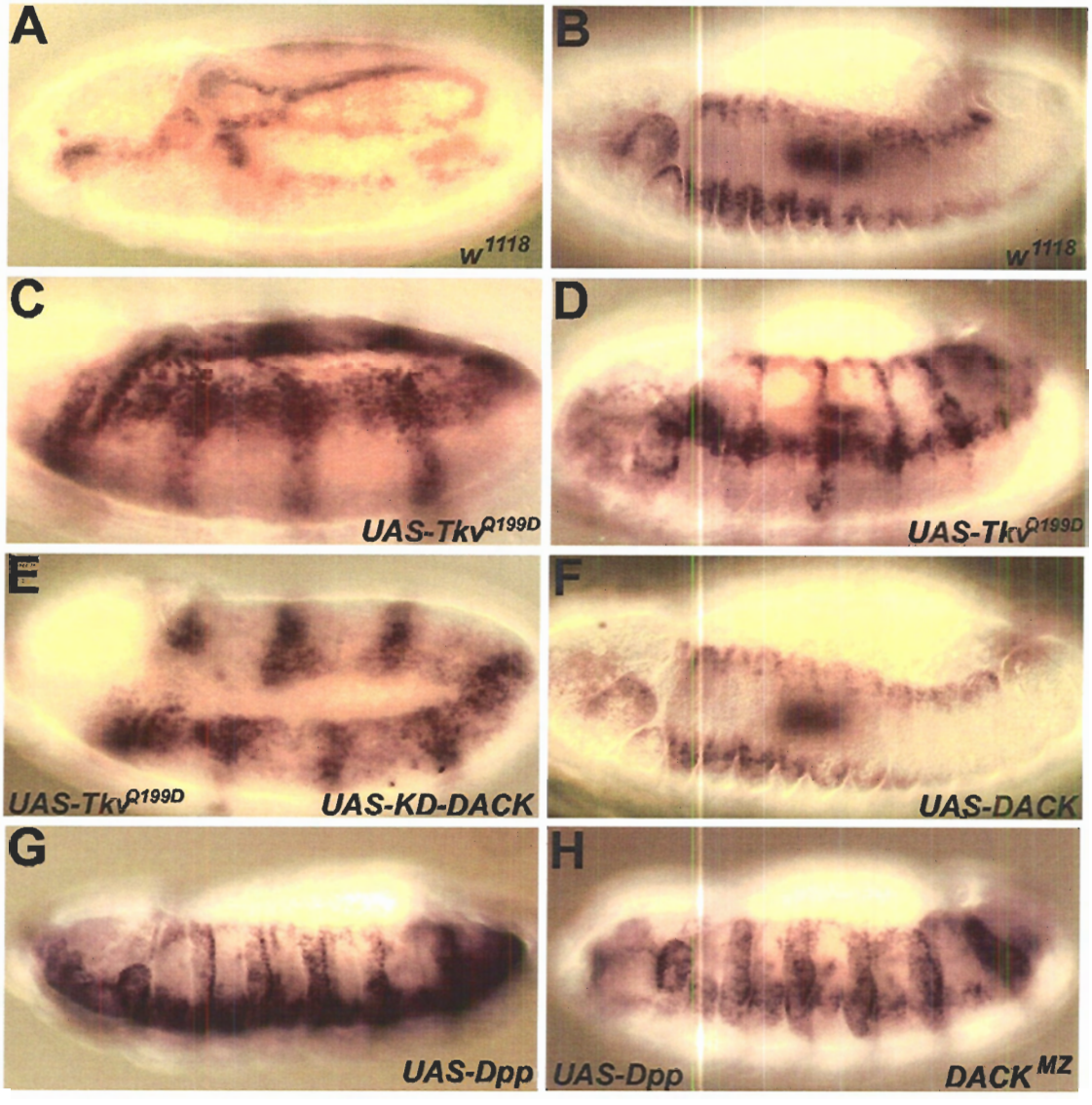
A
w1118
B
w1118
C
UAS-TkvQ199D
D
UAS-TkvQ199D
E
UAS-TkvQ199D
UAS-KD-DACK
F
UAS-DACK
G
UAS-Dpp
H
UAS-Dpp
DACKMZ

alone showed a low frequency of DC defects. We made *DACK* mutant embryos heterozygous mutant for *dpp* and looked for effects on DC. Heterozygosity for any of the *dpp* alleles resulted in an increased frequency of DC defects in $DACK^{86}$ embryos, with the weakest allele, dpp^{s11}, having the mildest effect. Embryos homozygous for med^{23} (Das et al., 1998) showed a low frequency of anterior cuticle defects which was significantly increased when they were made homozygous for $DACK^{29b}$. kay^{2} (Riesgo-Escovar and Hafen, 1997; Zeitlinger et al., 1997) is a weak hypomorphic allele of *Dfos*, homozygotes for which showed a low penetrance of dorsal and anterior holes in the cuticle. Embryos doubly mutant for kay^{2} and $DACK^{29b}$ showed an increased frequency of dorsal and anterior holes compared to homozygosity for either alone. We also tested if heterozygosity for mutations in *tkv* (tkv^{7}), *mad* (mad^{12}), *zip* (zip^{1}), the *Drosophila* TGF-β ligand, *screw* (scw^{5}) and a transcription factor that positively contributes to Dpp signalling during DC, *schnurri* (shn^{1}), could enhance the frequency of dorsal defects of a *DACK* mutant background. Heterozygosity for alleles of these genes did not result in an increase in the dorsal defects in a maternal and zygotic *DACK* mutant background (data not shown).

5.11 Effects of constitutively active Tkv can be suppressed by loss of DACK function

Thus far we have only tested the ability of DACK to suppress or enhance the loss-of-function phenotypes of Dpp pathway components. We therefore asked if loss of DACK function could suppress the effect of ectopically expressed CA Tkv, Tkv^{Q199D}. Previously, it had been shown that ectopic expression of either Dpp or activated Tkv in

Table 5.4 DACK mutants genetically interact with components of Dpp signalling. To generate control and experimental crosses for Dpp/DACK interactions, *dpp/CyO;+/+* flies were mated to *+/+;DACK^{86}/TM3Sb*. F1 males of genotype *dpp/+; DACK^{86}/+* were then crossed to *+/+;DACK^{86}/DACK^{86}* females. For control crosses, F1 males from the initial cross, bearing the genotype *dpp/+;TM3Sb/+* were crossed to *w^{1118}* females. The percentage of defects is assumed to be associated with the presence of the various alleles in the F1 of each cross. Therefore, (**) represent the estimated frequencies of dorsal and anterior holes present in individuals that are *DACK/DACK* (A-B), *dpp/+;DACK/DACK* (C,F, and H), *dpp/+;+/+* (D, G, and I), *kay^{2}, DACK^{29b}/ kay^{2}, DACK^{29b}* (J), *kay^{2}/kay^{2}* (K), *med^{23}, DACK^{29b}/ med^{23}, DACK^{29b}* (L), or *med^{23}/med^{23}*(M).

Table 5.4 *DACK* mutants genetically interact with components of Dpp signalling

Cross	% Phenotype			n
	Wild-type	Dorsal defect (**)	Anterior defect (**)	
A) +/+;$DACK^{86}$/ $DACK^{86}$ ♀ x +/+;$DACK^{86}$/TM3Sb♂	93.86	5.42 (10.84)	0.72 (1.44)	1116
B) +/+;$DACK^{29b}$/ $DACK^{29b}$ ♀ x +/+;$DACK^{29b}$/TM3Sb♂	99.18	0.39 (0.78)	0.78 (1.56)	258
C) +/+;$DACK^{86}$/$DACK^{86}$ ♀ x dpp^{s11}/+;$DACK^{86}$/+ ♂	92.19	7.81 (31.24)	/	116
D) +/+;+/+ ♀ x dpp^{s11}/+;TM3Sb/+ ♂	99.01	0.66 (2.64)	0.33 (1.32)	303
F) +/+;$DACK^{86}$/$DACK^{86}$ ♀ x dpp^{hr27}/+;$DACK^{86}$/+♂	89.12	10.2 (40.8)	0.68 (1.85)	147
G) +/+;+/+ ♀ x dpp^{hr27}/+;TM3Sb/+♂	98.21	1.49 (5.96)	0.3 (1.20)	336
H) +/+;$DACK^{86}$/$DACK^{86}$ ♀ x dpp^{hr92}/+;$DACK^{86}$/+♂	67.25	14.5 (58.0)	18.25 (73.0)	400
I) +/+;+/+ ♀ x dpp^{hr92}/+;TM3Sb/+♂	89.66	2.64 (10.56)	7.7 (30.8)	1480
J) kay^2, $DACK^{29b}$/TM3Sb ♀ x kay^2, $DACK^{29b}$/TM3Sb♂	84.7	2.1 (8.4)	13.2 (52.8)	523
K) kay^2/TM3Sb ♀ x kay^2/TM3Sb♂	96.55	0.66 (2.64)	2.79 (11.16)	609
L) med^{23}, $DACK^{29b}$/TM3Sb ♀ x med^{23}, $DACK^{29b}$/TM3Sb♂	87.29	1.75 (7.02)	10.96 (43.86)	228
M) med^{23}/TM3Sb ♀ x med^{23}/TM3Sb♂	98.08	1.10 (4.38)	0.82 (3.29)	365

the *prd* expression domain during embryogenesis results in a variety of defects in denticle development on the ventral cuticle, including regions with loss of denticles and loss of naked cuticle, which can lead to fusion of the denticle belts (Figure 5.7 B, C, and (Arquier et al., 2001). Denticles are membrane protrusions that form on the surface of the most anterior cells of each segment on the ventral surface of the embryo. The *prdGAL4* driver expresses GAL4 in cells that become competent to form denticles. We wondered if disruption of endogenous DACK function by co-expression of KD-DACK, or by loss of maternal and zygotic DACK, could suppress the denticle phenotypes resulting from an excess of Dpp signalling. First, we crossed virgin females homozygous for *UAS-Tkv*^{Q199D}, or a chromosome bearing *UAS-TkvQ199D* and *UAS-KD-DACK*, to males heterozygous for the *prdGAL4* driver. 50% of embryos from either of these crosses will be expressing the transgenes. An estimated 60% of embryos that express Tkv^{Q199D} die with denticle defects on their ventral surface. Simultaneous expression of KD-DACK can suppress these phenotypes, but not the lethality of the embryos (Figure 5.7 E and F, embryonic frequencies of this suppression are not shown). We next tested to see if loss of maternal and zygotic DACK could affect the ability of the activated Tkv transgene to induce defects in the ventral cuticle. We crossed virgin females homozygous for *DACK*^{10b} and *UAS-Tkv*^{Q199D} with males heterozygous for a chromosome bearing both the *prdGAL4* driver and *DACK*^{10b}. Loss of maternal and zygotic DACK not only rescued the denticle ventral cuticle phenotypes but also the embryonic lethality associated with expression of activated Tkv in the *prd* pattern (Figure 5.7 D and Table 5.5).

We next asked if DACK could also suppress activated Tkv phenotypes in wing development. In our experiment we used *TAJ3*, an enhancer piracy line that expresses Tkv^{Q199D} in the wing pouch under the control of an unknown promoter (Hoodless et al., 1996). Homozygosity for *TAJ3* results in 100% of wings containing ectopic vein tissue between L3-L4 (Figure 5.8 B). However, in a $DACK^{10b}$ mutant background, this phenotype is suppressed in 100% of the wings to a milder ectopic vein phenotype (Figure 5.8 C).

Figure 5.7 Loss of DACK function can suppress the phenotypes associated with ectopic expression of activated Tkv.

Ventral views of larval embryonic cuticle of (A) w^{1118}, (B, C) *UAS-Tkv*^{Q199D}*/prdGAL4*. Arrowheads in (B) point to regions where denticles of adjacent segments have fused, possibly due to loss of naked cuticle. Arrow in (C) points to a region where there is a loss of denticles. (D) Ventral view of larval cuticle of *UAS-Tkv*^{Q199D}*, DACK*^{10b}*/prdGAL4, DACK*^{10b}. (E, F) Ventral view of embryonic cuticle of *UAS-Tkv*^{Q199D}*, UAS-KD-DACK/prdGAL4*.

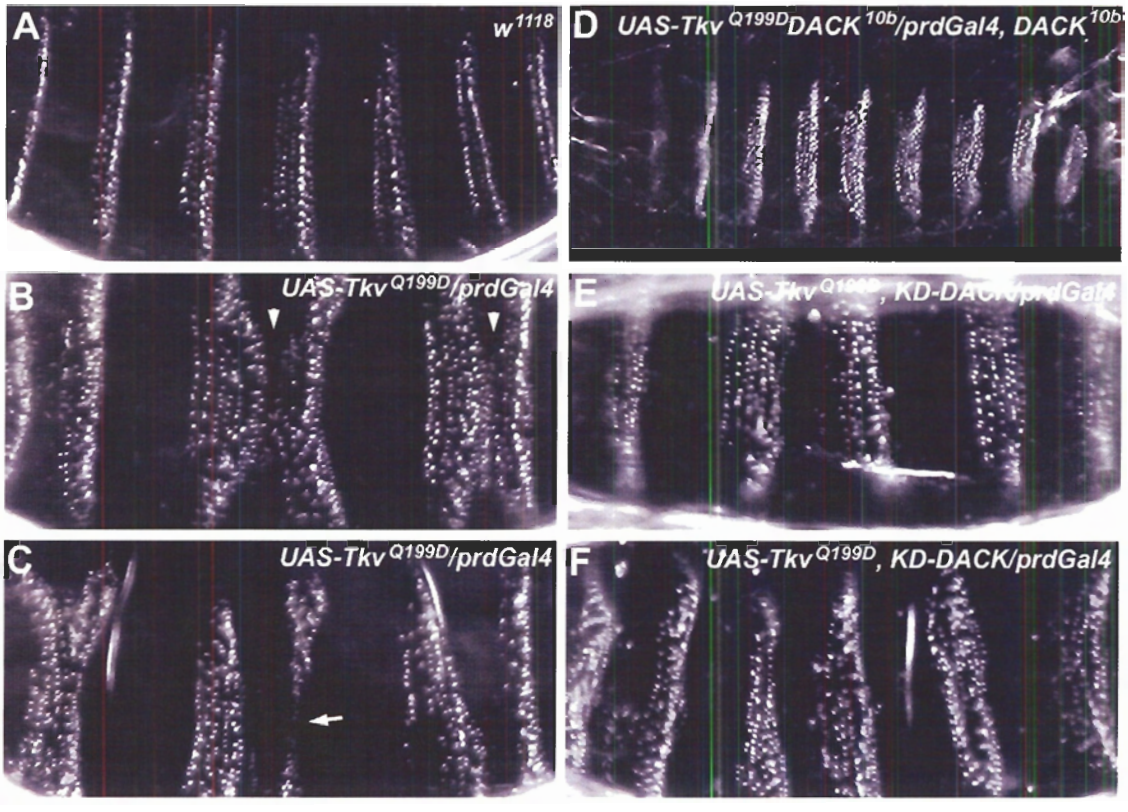
A
w1118
D
UAS-Tkv Q199D DACK 10b/prdGal4, DACK 10b
B
UAS-Tkv Q199D/prdGal4
E
C
UAS-Tkv Q199D/prdGal4
F
UAS-Tkv Q199D, KD-DACK/prdGal4

Table 5.5 Loss of DACK function can suppress the phenotypes associated with ectopic expression of activated Tkv.

Crosses were maintained at 25° C.

Table 5.5 Denticle defects associated with ectopic expression of activated Tkv are suppressed by loss of *DACK*

Cross	Wild-type	% Phenotype Denticle defects	n
Tkv^{Q199D}/Tkv^{Q199D}♀ x *prdGAL4/TM3Sb*♂	70.37	29.62	216
Tkv^{Q199D},$DACK^{10b}/Tkv^{Q199D}$, $DACK^{10b}$♀ x *prdGAL4,*$DACK^{10b}$*/TM3Sb*♂	99.01	0.99	606

Figure 5.8 Loss of *DACK* can suppress wing phenotypes of ectopically activated Tkv.

(A) Wild-type wing. (B) TAJ3/TAJ3 wing showing ectopic vein tissue between L3 and L4 (arrowhead). (C) TAJ3, $DACK^{10b}$/ TAJ3, $DACK^{10b}$ wings produce a milder ectopic vein phenotype (arrowhead).

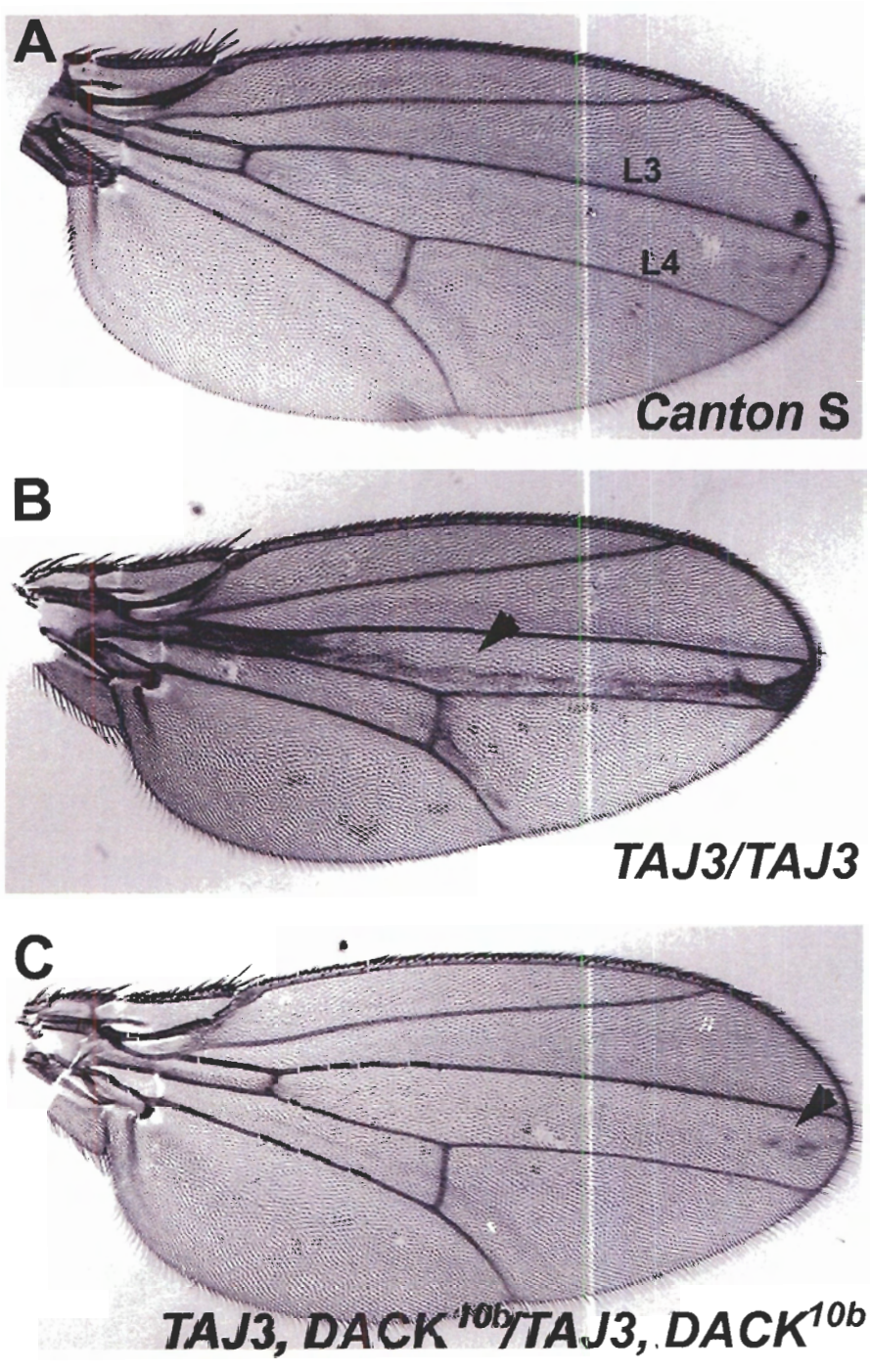
A
L3
L4
Canton S
B
TAJ3/TAJ3
C
TAJ3, DACK10b/TAJ3, DACK10b

6 DISCUSSION: THE *DROSOPHILA* ACK FAMILY

6.1 DACK is required for Cdc42 signalling during dorsal closure

Several studies have demonstrated that Cdc42 is a key signalling component for DC. DACK, unlike DPR2 and the mammalian ACKs, does not contain a CRIB domain and Kaiping Sem was not able to show that DACK binds to *Drosophila* Cdc42. However, ectopic expression of wild-type and KD-DACK transgenes throughout development produce similar phenotypes to expression of CA and DN Cdc42, respectively (Sem et al., 2002), suggesting that these proteins function in a similar pathway. We therefore asked if DACK is a component of Cdc42 signalling during DC. Overexpression of wild-type DACK was able to suppress DC defects caused by Cdc42N17 expression. Also, the LE enrichment of DACK, and the alterations in *DACK* transcription in the LE and amnioserosa in response to Cdc42 transgene expression, are indications that DACK has a role in Cdc42 signalling during DC.

The transcriptional regulation of *DACK* does not appear to be a simple homeostatic response as it is tissue-specific, and works in opposite directions in two tissues: DN Cdc42 causes upregulation of *DACK* transcripts at the LE, whereas CA Cdc42 causes upregulation of transcription in the amnioserosa. The relevance of this transcriptional regulation of *DACK* remains unknown, but it may provide a route for Cdc42 to regulate DACK function during DC. The serine/threonine kinase DPAK, a downstream effector for Rac1 and Cdc42, also responds transcriptionally to a change in Cdc42 signalling in the amnioserosa, but interestingly in the opposite direction from

DACK in that DN Cdc42 induces upregulation of *DPAK* transcription in this tissue (Sem et al., 2002). Cdc42 might also regulate DACK through its GTPase activity. Although Cdc42 does not appear to bind DACK directly, it could possibly influence DACK function indirectly in a signalling complex. An indirect mode of activation of ACK proteins by Cdc42 proteins is consistent with the finding in mammalian cells that CA Cdc42 fails to activate ACK2 *in vitro*, but can promote activation when cotransfected with ACK2 *in vivo* (Yang and Cerione, 1997).

6.2 DACK is not a component of the JNK pathway during dorsal closure

During our analysis of the role of DACK in Cdc42 signalling, we simultaneously tested if DACK functions downstream of the JNK pathway, another key signal required for DC. We tested to see if overexpression of DACK could trigger ectopic activation of JNK. It had previously been shown that ectopic expression of CA Cdc42 could induce ectopic JNK activation (Glise and Noselli, 1997). However, overexpression of DACK was not able to trigger ectopic activation of the JNK cascade, in contrast to the results obtained with CA Cdc42. We know that our DACK transgene is functional *in vivo* because DACK overexpression is capable of elevating phosphotyrosine levels in the embryo, in the absence of a corresponding increase in Cdc42 function (Sem et al., 2002). Furthermore, the JNK cascade is not disrupted by either impairment of ACK family tyrosine kinase function through expression of KD-DACK, or by loss of zygotic DACK through a deficiency removing the *DACK* gene. These results suggest that the JNK cascade does not lie downstream of ACK family tyrosine kinase activity in Cdc42 signalling. The LE expression of DACK was also not under the control of the JNK

cascade. These results are consistent with analysis of loss-of-function alleles of Cdc42 which indicates that the JNK cascade is not a major component of Cdc42 signalling (Genova et al., 2000). Cdc42 may normally make a minor contribution to the activation of the JNK cascade that could be greatly amplified by expression of Cdc42V12.

6.3 DACK function is required for Dpp signalling

As DACK does not signal through the JNK pathway during DC, we asked if perhaps it functions downstream of Dpp in this process. Our reasoning was based on the fact that expression of CA Cdc42 could suppress the DC defects associated with the *tkv* loss-of-function allele, tkv^{7} (Ricos et al., 1999). Similar to CA Cdc42, DACK overexpression was able to suppress the DC defects associated with loss-of-function mutations in *tkv*. In addition, DACK could also suppress DC defects of *put*. Although *DACK* mutants do not display DC defects we were able to show that we could sensitize the *DACK* mutant genetic background to generate DC defects by decreasing the dose of Dpp pathway components. DACK was able to ectopically activate the expression of two Dpp target genes, *zip* and *Dfos,* which themselves are required for DC. These results demonstrated that DACK functions in Dpp signalling during DC. To determine a possible route by which DACK functions in Dpp signalling, we tested to see if loss of DACK could block receptor phosphorylation of Mad. We were unable to inhibit phosphorylation of Mad by Tkv *in vivo*, suggesting that this is not the route by which DACK functions in Dpp signalling. These results indicated that DACK either functions downstream of Mad, possibly in the nucleus, or is part of a pathway parallel to the canonical Dpp cascade. With regard to a possible nuclear role for DACK, it is interesting

to note that a recent study found that mammalian ACK-1 can translocate into the nucleus in a Cdc42-dependent manner (Ahmed et al., 2004).

We have yet to establish if DACK is a downstream effector for Dpp *per se*; that is, if the kinase activity of DACK is activated by the Dpp receptor complex. In support of this possibility is the dramatic suppression of *tkv* and *put* mutant phenotypes by DACK overexpression, and the finding that TGF-β can induce activation of Cdc42 in mammalian cells (Barrios-Rodiles et al., 2005; Edlund et al., 2002; Ozdamar et al., 2005). If DACK were found to be activated by Dpp, it would suggest the existence of a Dpp pathway parallel to the canonical Dpp/Smad pathway, as DACK function does not affect Mad phosphorylation. Alternatively, DACK might not be a direct component of a Dpp-induced cascade but rather could be activated in a parallel pathway to positively contribute to Dpp signalling during DC. Based on what is known in the literature about mammalian ACKs, it is possible that DACK's contribution to Dpp signalling is through an association of DACK with EGFR and/or integrin signalling during DC. One possibility is that DACK, similar to ACK2, is activated by EGFR, and this activation leads to positive regulation of Dpp signalling. A role for EGFR in DC has not been established; however, recent data obtained by a Ph.D. student in our lab, Weiping Shen, suggests that loss of EGFR signalling leads to failure in DC (unpublished data). Similarly, DACK could be contributing to Dpp signalling through an association with integrins. Integrin signalling is known to be required for DC and interestingly, integrins are required for Dpp signalling during wing development (Araujo et al., 2003; Hutson et al., 2003; Stark et al., 1997). Whatever the mechanism through which it acts, we have established DACK as an important contributor to Dpp function in DC.

6.4 Loss of DACK function can suppress ectopic activation of the Dpp pathway

We wished to address if loss of DACK could suppress ectopic activation of Dpp signalling during DC. However, we found that induction of CA Tkv during DC did not lead to DC defects. We therefore searched the literature for other processes that are affected by ectopic activation of the Dpp pathway. We found that expression of CA Tkv during ventral patterning of the embryo lead to defects in denticle development (Arquier et al., 2001). Loss of DACK function greatly reduced this phenotype, again demonstrating that DACK functions with Dpp signalling components. A similar result was obtained with an activated Tkv phenotype generated in wing development. Loss of DACK also greatly reduced the ability of CA Tkv to generate ectopic vein tissue. Together these results demonstrate that DACK function is utilised by Dpp signalling, whether in a parallel pathway, or either in a canonical or a non-canonical manner.

6.5 Loss of zygotic ACK family function during embryogenesis does not produce dorsal closure defects

As previously stated, zygotic *DACK;DPR2* double mutants can complete DC and hatch into larva, despite the fact that both kinases are expressed during DC. One reason for this may be that our *DPR2* allele is not a null, and that the low amount of DPR2 transcript is sufficient to produce enough protein to compensate for ACK function during DC. As well, since the DPR2 maternal contribution was not removed in our experiments, it is possible that the pool of DPR2 transcript/protein from this source is aiding in the survival of the *ACK* double mutant embryos. It is also possible that the ACK contribution to DC is not essential for hole closure. However, the results discussed above would argue against this point. Another possibility is that the function of ACKs during

DC overlaps with other kinases or signalling factors. The generation of *ACK* null double mutants may aid in determining which of these possibilities is true.

7 CONCLUSIONS

The objective of this thesis was to gain a better understanding of the function of *Drosophila* Cdc42 through gain- and loss-of-function studies on the putative Cdc42 effectors, DCIP4 and the ACK family of non-receptor tyrosine kinases. The model system that we set out to study the function of these effectors in was DC of the *Drosophila* embryo. DC has proven to be an excellent model for characterizing signalling proteins that regulate the actin cytoskeleton. Here we have shown that one of these regulators, DACK, affects Dpp signalling and can induce expression of two Dpp target genes, *zip* and *Dfos*, that themselves impinge on actin cytoskeletal function during DC, directly and indirectly, respectively. These findings suggest a possible route of action for the Cdc42-dependent reorganization of the actin cytoskeleton induced by TGF-β seen in mammalian cell culture (Edlund et al., 2002; Edlund et al., 2004). Though both Cdc42 signalling and gene expression were shown to be required for TGF-β-induced reorganization of the cytoskeleton in these earlier studies, the authors did not address whether the gene expression was dependent on Cdc42 signalling. As we have already established DACK as an effector for Cdc42 during DC, the results shown here are the first to link Cdc42 signalling to regulation of TGF-β/BMP target gene expression.

We were unable to establish a role for DCIP4 during DC, although we identified the possibility of a role for DCIP4 in several other tissues/processes that have been shown to be affected by Cdc42 signalling, such as cellularization, nervous system development, wing development, and oogenesis. However, it cannot be concluded that DCIP4 does not

function in DC, as DCIP4 protein is weakly present in the LE cells. Further analysis is required to determine the role of this protein during DC. This thesis provides the ground work for future study of these three *Drosophila* Cdc42 effector proteins.

APPENDICES

APPENDIX A: DACK MISEXPRESSION PHENOTYPES

Table A.1 Phenotypes of DACK overexpression.

Gal4 Driver	Results of crosses to *UAS-WTACK ZF*		
	18°C	RT	25°C
Ap-gal4	1-2° L	1-2° L	1-2° L
332.2-gal4 (AS)	EL	EL	EL
As-gal4 c381	abnormal wings, pigmented intervein region	abnormal wings, pigmented intervein region	abnormal wings, pigmented intervein region
A9-gal4	small wing, loss of margin bristles, expansion of L3, blister @ tip	PL	3° L
bs-gal4	upward, ectopic scutellar machrochaetae	L-P L	L-P L
c768-gal4	1-2° L	1-2° L	1-2° L
y[1] C311-gal4	1-2° L	1-2° L	1-2° L
da-gal4	1-2° L	1-2° L	1-2° L
dpp-gal4	most P L, notum less scutellar machrochatae, eyes abnormal	dies as larva and undeveloped pupae	L-P L, 3° L wing discs long in length, extremely abnomal morphology
Lp-1 gal4(AS)	/	/	wings pigmented intervein region
omb-gal4	P L, dissected pupae have undeveloped wings	die as dies as extremely large 3° larva	die as dies as extremely large 3° larva
ms 1096-gal4	die as early pupae	die as large pupae	die as dies as extremely large 3° larva
pnr-gal4	P L	P L	L-P L
ptc-gal4	most P L, escapers: wings blistered, small, expansion ofACV, loss of scutellar machrochaetae	PL: pupae undeveloped	PL: pupae undeveloped, 3° larval wing discs similar to UAS-DACK/dppG4 discs
repo-gal4	abnormal wings	L-P L	E-1° L
sca-gal4	abnormal wings, loss of body hairs	P L	P L
309-gal4	abnormal wings, loss of body hairs	abnormal wings, loss of body hairs	P L
sd-gal4	die as large 3° L	die as large 3° L	die as large 3° L
T113-gal4	abnormal positioning of sensory neurons of vein L3, small wing, loss of CVs, ectopic CVs	P L	P L
T93-gal4	abnormal positioning of sensory neurons of vein L3	P L	P L
vg-gal4	loss of tip of L5, blister, expansion of posterior end of wing,	wing blister, abnormal vein positioning, loss of wing margin bristles, loss of ACV, extra scutellar bristles	L L
w;32B-gal4	EL	EL	EL
24B-gal4	EL	EL	EL
185y-gal4	/	/	L
198y-gal4	2° L	2° L	2° L
719a-gal4	1°-2° L	1°-2° L	1°-2° L

Table A.2 Phenotypes of kinase inactive DACK misexpression.			
Gal4	**Results of crosses to *UAS-KDACK 31***		
Driver	**18°C**	**RT**	**25°C**
Ap-gal4	E-L L	E-L L	1°-2° L
332.2-gal4 (AS)	E L	E L	E L
As-gal4 c381	/	/	/
A9-gal4	small wing, expanded L3, blister at tip, loss of marginal bristles	small wings, completely blistered	P L
bs-gal4	extra scutellar bristles, smudged veins	extra scutellar bristles, smudged veins	extra scutellar bristles, smudged veins
c768-gal4	E L, puckers denticle defect	E L, puckers denticle defect	E L, puckers denticle defect
C311-gal4	1°-2°L	1°-2°L	1°-2°L
da-gal4	1°-2°L	1°-2°L	1°-2°L
dpp-gal4	smal square shaped wings, blistered, L3 expansion leading to loss of ACV,extra upward machrochatae	smal square shaped wings, blistered, bifurcated, L3 expansion leading to loss of ACV,extra upward machrochatae	P L, 3° wing pouch bifurcated
Lp-1 gal4	/	/	die as small pupae, sometimes tubby like
omb-gal4	die as somewhat differentiated pupae to pharate adults except wings not developed	die as somewhat differentiated pupae to pharate adults except wings not developed	L-P L
ms 1096-gal4	P L	P L	P L
pnr-gal4	P L	P L	P L
ptc-gal4	P L	L-P L	1°L-P L
repo-gal4	/	P L	P L
sca-gal4	P L, extra hairs all over body	P L, extra hairs all over body	P L, extra hairs all over body
309-gal4	extra hairs all over body	extra hairs all over body	PL, extra hairs all over body
sd-gal4	PL	PL	PL
T113-gal4	abnormal positioning of sensory organs in L3	small abnormal wings, blistered, loss of ACV, abnormal positioning of sensory organs on L3, abnormal legs	PL
T93-gal4	ok	small abnormal wings, extra sensory organs in L3,abnormally positioned	L-P L
vg-gal4	PL, survivor: underdevelop.wings, long extra machrochatae	PL, survivor: underdevelop.wings, long extra machrochatae	L-P L
w;32B-gal4	PL	PL	E L
24B-gal4	E-1°L	E-1°L	E-1°L
185y-gal4	held up scutellar britles	held up scutellar britles	held up scutellar britles
198y-gal4	L	L	L
719a-gal4	1°-2° L	1°-2° L	1°-2° L

Figure A.1 Misexpression of DACK and KD-DACK during SOP development

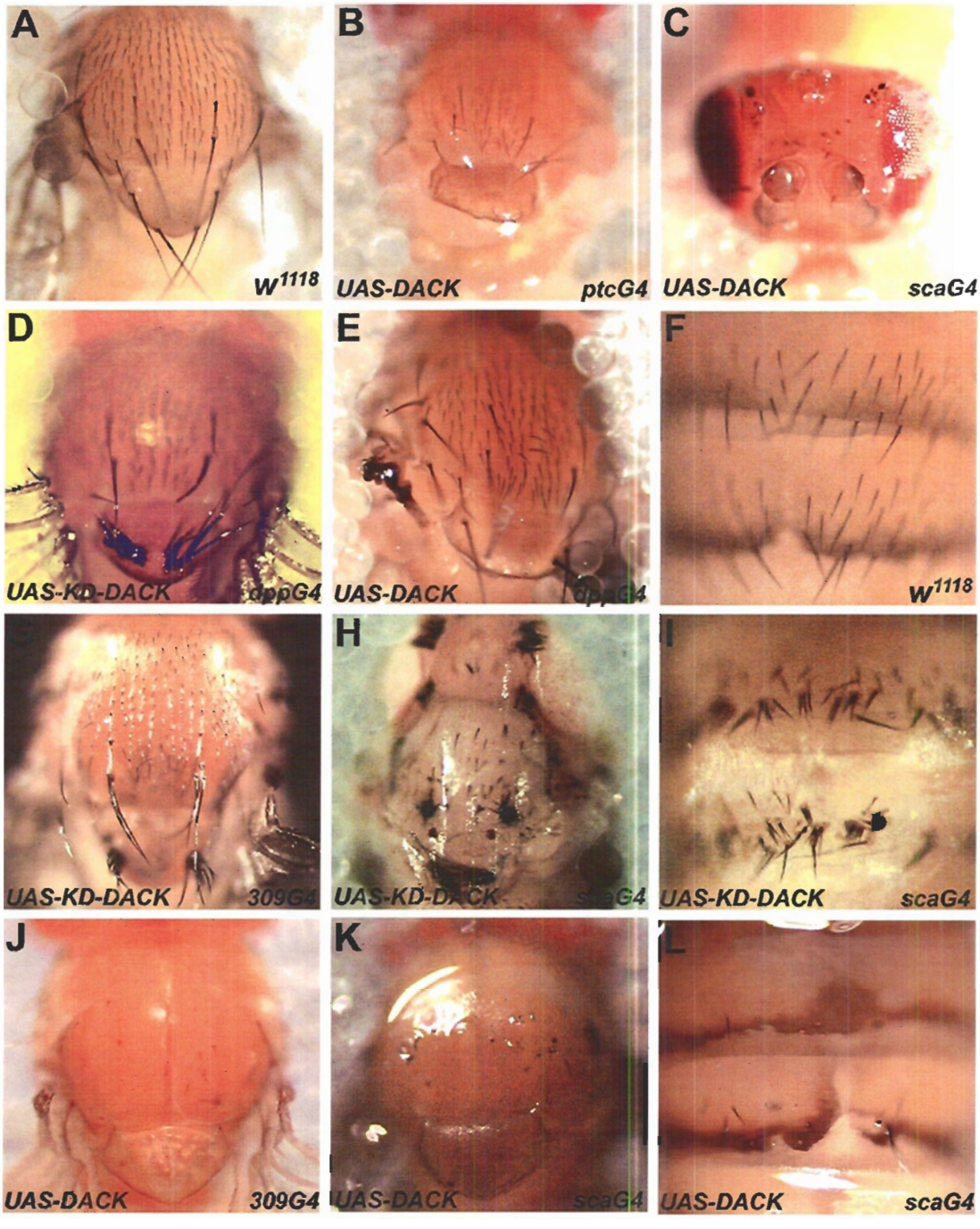

Figure A.2 Phenotypes of DACK misexpression during wing development.

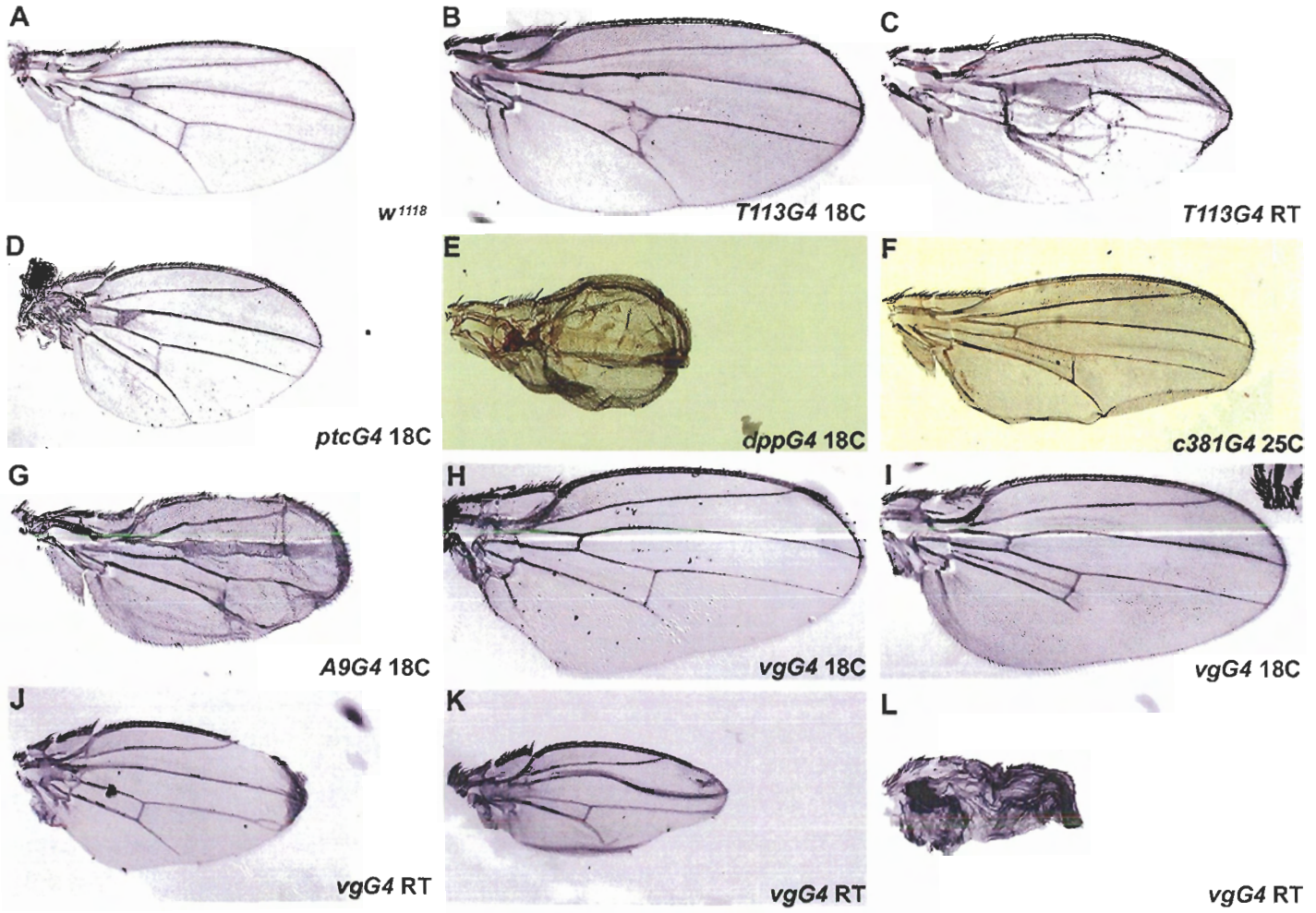

Figure A.3 Phenotypes of KD-DACK misexpression during wing development.

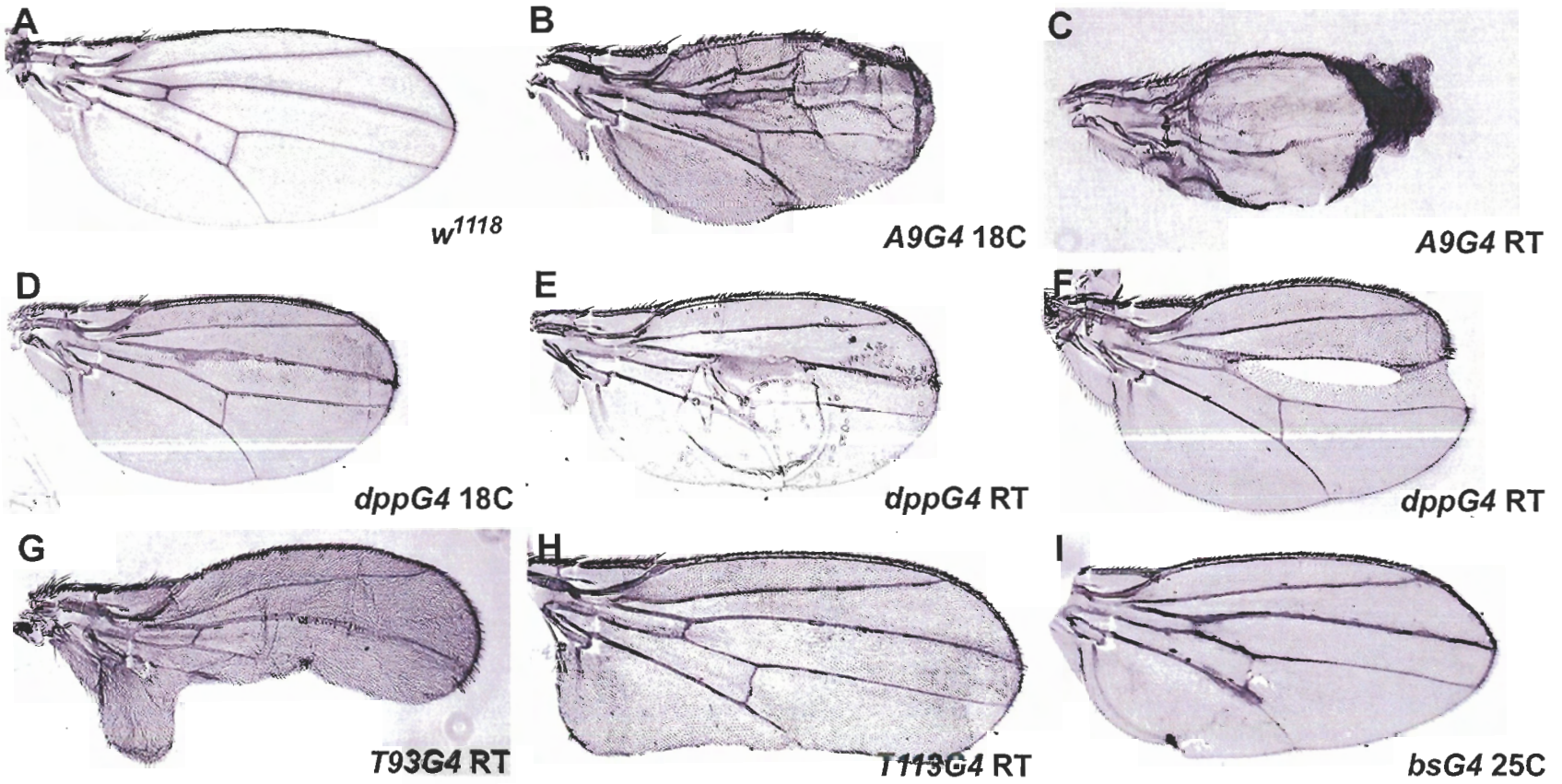

APPENDIX B: DEFICIENCY SCREEN TO IDENTIFY MODIFIERS OF PHENOTYPES ASSOCIATED WITH MISEXPRESSION OF DACK DURING EYE DEVELOPMENT

Table B.1 Chromosome 2 Deficiencies

Deficiency	Locus	Effect on *GMR;UAS-DACK RE*	Deficiency	Locus	Effect on *GMR;UAS-DACK RE*
Df(2L)net-PMF	21A1;21B7-8	S	*Df(2R)M41A4*	41A;41A	L
Df(2L)BSC4	21B7-C1;21C2-3	L	*In(2R)bw[VDe2L] Cy[R]*	41A-B;42A2-3	/
Df(2L)al	21B8-C1;21C8-D1, 22D1-2;33F5-34A1	/	*Df(2R)ST1*	42B3-5;43E15-18	/
Df(2L)ast2	21D1-2;22B2-3	S	Df(2R)Drl[rv18]	42E3-7;44A3	E
In(2LR)bw[V1]	21C8-D1;60D1-2 + 40F;59D4-E1	/	*Df(2R)H3C1*	43F;44D3-8	/
Df(2L)JS32	23C3-5;23D1-2	E	*Df(2R)H3E1*	44D1-4;44F12	/
Df(2L)JS17	23C1-2;23E1-2	L	*Df(2R)Np5*	44F10;45D9-E1	/
Df(2L)S2590	23D2;23E3	/	*Df(2R)w45-30n*	45A6-7;45E2-3	/
Df(2L)ed1	24A2;24D4	E	*Df(2R)B5*	46A;46C	L
Df(2L)sc19-8	24C2-8;25C8-9	E	*Df(2R)X1*	46C;47A1	S
Df(2L)sc19-4	25A5;25E5	S	*Df(2R)stan1*	46D7-9;47F15-16	E
Df(2L)cl-h3	25D2-4;26B2-5	/	*Df(2R)en-A*	47D3;48B2	S
Df(2L)E110	25F3-26A1;26D3-11	<S	*Df(2R)en30*	48A3-4;48C6-8	V
Df(2L)BSC5	26B1-2;26D1-2	/	*Df(2R)CB21*	48E;49A	/
Df(2L)BSC6	26D3-E1;26F4-7	E	*Df(2R)BSC3*	48E12-F4;49A11-B6	E
Df(2L)BSC7	26D10-E1;27C1	E	*Df(2R)vg-C*	49A4-13;49E7-F1	E
Df(2L)Dwee-delta5	27A;28A	S	*Df(2R)CX1*	49C1-4;50C23-D2	/
Df(2L)J-H	27C2-9;28B3-4	MS	*Df(2R)BSC11*	50E6-F1;51E2-4	S
Df(2L)Dwee1-W05	27C2-3;27C4-5	S	*Df(2R)Jp1*	51D3-8;52F5-9	/
Df(2L)spd,	26A6-B1;27E1-3;28B1-3	S	*Df(2R)Jp8*	52F5-9;52F10-53A1	/
Df(2L)XE-2750	28A5-B1;28C1-9	E	*Df(2R)P803-Delta15*	53E;53F11	/
Df(2L)Trf-C6R31	28DE;28DE	/	*Df(2R)robl-c*	54B17-C4;54C1-4	/
Df(2L)TE29Aa-11	28E4-7;29B2-C1	/	*Df(2R)k10408*	54C1-4;54C1-4	/
Df(2L)N22-14	29C1-2;30C8-9	L	Df(2R)Pcl7B	54E8-F1;55B9-C1	S
Df(2L)BSC17	30C3-5;30F1	E	*Df(2R)PC4*	55A;55F	/
Df(2L)J39	31C;32D1-E5	S	*Df(2R)P34*	55E2-4;56C1-11	E
Df(2L)FCK-20	32D1;32F1-3	/	*Df(2R)017*	56F5;56F15	S
Df(2L)Prl	32F1-3;33F1-2	/	*Df(2R)AA21*	56F9-17;57D11-12	S
Df(2L)prd1.7	33B2-3;34A1-2	L	Df(2R)X58-3	58C3-7;58D6-8	/
Df(2L)b87e25	34B12-C1;35B10-C1	L	*Df(2R)X58-12*	58D1-2;59A	/
Df(2L)TE35BC-24	35B4-6;35F1-7	S	*Df(2R)59AD*	59A1-3;59D1-4	S
Df(2L)r10	35D1;36A6-7	/	Df(2R)bw-S46	59D8-11;60A7	S
Df(2L)cact-255rv64	35F-36A;36D	/	Df(2R)Chi[g230]	60A3-7;60B4-7	/
Df(2L)H20	36A8-9;36E1-2	L	Df(2R)106	60A3;60A7	S
Df(2L)TW137	36C2-4;37B9-C1	S	*Df(2R)Px2*	60C5-6;60D9-10	<S
Df(2L)TW50	36E4-F1;38A6-7	/	Df(2R)Dll-MP	60E3-4;60E5-6	/
Df(2L)TW161	38A6-B1;40A4-B1	E	*Df(2R)ES1*	60E6-8;60F1-2	L
Df(2L)C'	h35;h38L	/	*Df(2R)Kr10*	60F1;60F5	/

Table B.2 Chromosome 3 Deficiencies

Deficiency	Locus	Effect on *GMR;UAS-DACK RE*	*Deficiency*	Locus	Effect on *GMR;UAS-DACK RE*
Df(3L)emc-E12	61A;61D3	/	*Df(3L)Pc-101*	78C3-4;78C8-9	L
Df(3L)Ar12-1	61C;61F	S	*Df(3L)Pc-2q*	78C5-6;78E3-79A1	L
Df(3L)Aprt-32	62B1;62E3	V	*Df(3L)Ten-m-AL29*	79C1-3;79E3-8	/
Df(3L)1227	63C01-02;63F01-02	<S	*Df(3L)HD1*	79D3-E1;79F3-6	S
Df(3L)HR119	63C2;63F7	E	*Df(3L)Delta1AK*	79E05-F01;79F02-06	/
Df(3L)GN34	63E6-9;64A8-9	E	*Df(3R)ME15*	81F3-6;82F5-7	/
Df(3L)GN24	63F6-7;64C13-15	/	*Df(3R)3-4*	82F3-4;82F10-11	/
Df(3L)v65c	64F2-5;65D1-3	/	*Df(3R)e1025-14*	82F8-10;83A1-3	/
Df(3L)XDI98	65A2;65E1	/	*Df(3R)Tpl10*	83C1-2;84B1-2	/
Df(3L)pbl-X1	65F3;66B10	/	*Df(3R)WIN11*	83E1-2;84A4-5	S
Df(3L)ZP1	66A17-20;66C1-5	S	*Df(3R)Scr*	84A1-2;84B1-2	/
Df(3L)66C-G28	66B8-9;66C9-10	S	*Df(3R)Antp17*	84B1-2;84D11-12 or 84A6;84D14	/
Df(3L)h-i22	66D10-11;66E1-2	/	*Df(3R)p712*	84D4-6;85B6	E
Df(3L)Scf-R6	66E1-6;66F1-6	/	*Df(3R)p-XT103*	85A2;85C1-2	<S
Df(3L)Rdl-2	66F05;66F05	S	*Df(3R)by10*	85D8-12;85E7-F1	L
Df(3L)29A6	66F05;67B01	/	*Df(3R)M-Kx1*	86C1;87B1-5	L
Df(3L)AC1	67A2;67D11-13	/	*Df(3R)T-32*	86E2-4;87C6-7	/
Df(3L)lxd6	67E05-07;68C02-04	/	*Df(3R)ry615*	87B11-13;87E8-11	L
Df(3L)BSC14	67E3-7;68A2-6	/	*Tp(3;Y)ry506-85C*	87D1-2;88E5-6	/
Df(3L)vin5	68A2-3;69A1-3	/	*Df(3R)ea*	88E7-13;89A1	FS
Df(3L)vin7	68C8-11;69B4-5	S	*Df(3R)Spf*	89B20-22;89D09-E01	S
Df(3L)eyg[C1]	69A4-5;69D4-6	/	*Df(3R)C4*	89E03-04;90A01-07	/
Df(3L)BSC10	69D4-5;69F5-7	S	*Df(3R)Cha7*	90F1-F4;91F5	S
Df(3L)BSC12	69F6-70A1;70A1-2	/	*Df(3R)DI-KX23*	91C07-D03;92A05-08	E
Df(3L)Ly	70A02-03;70A05-06	E	*Df(3R)e-R1*	93B6-7;93D2	/
Df(3L)fz-GF3b	70C01-02;70D04-05	E	*Df(3R)e-H4*	93D01;93F06-08	E
Df(3L)fz-M21	70D2-3;71E4-5	/	*Df(3R)93F[x2]/*	93F05;94A08	/
Df(3L)Ly, Df(3L)BK10	70A02-03;70A05-06, 71C;71F	S	*Df(3R)hh*	93F11-14;94D10-13	E
Df(3L)brm11	71F1-4;72D1-10	/	*Df(3R)23D1*	94A3-4;94D1-4	<S
Df(3L)st-f13	72C1-D1;73A3-4	S	*Df(3R)mbc-30*	95A5-7;95C10-11	/
Df(3L)81k19	73A3;74F	S	*Df(3R)mbc-R1*	95A5-7;95D6-11	S
Df(3L)BSC8	74D3-75A1;75B2-5	V	*Df(3R)crb-F89-4*	95D7-D11;95F15	/
Df(3L)W10	75A6-7;75C1-2	S	*Df(3R)crb87-4*	95E08-F01;95F15	V
Df(3L)VW3	76A3-76B2	/	*Df(3R)96B*	096A21;096B08-10	V
Df(3L)kto2	76B1-2;76D5	S	*Df(3R)Espl3*	96F1;97B1	E
Df(3L)XS533	76B4;77B	S	*Df(3R)TI-P*	97A;98A1-2	E
Df(3L)rdgC-co2	77A1;77D1	/	*Df(3R)D605*	97E3;98A5	/
Df(3L)ri-79c	77B-C;77F-78A	/	*Df(3R)3450*	98E3;99A6-8	V
Df(3L)ri-XT1	77E2-4;78A2-4	/	*Df(3R)Dr-rv1*	99A1-2;99B6-11	L
Df(3L)ME107	77F3;78C8-9	S	*Df(3R)L127*	99B5-6;99E4-F1	V
Df(3L)Pc-MK	78A02;78C09	S	*Df(3R)B81*	99C8;100F5	L

Table B.3 Break down of suppressive regions within Chromosome 2

Deficiency	Smaller deficiencies within suppressive region	Locus	Effect on *GMR;UA SDACK RE*	Gene (Allele) within suppressive regions	Locus	Effect on *GMR;UA SDACK RE*
Df(2L)net-PMF	*Df(2L)net18*	21A4;21B3-4	E			
21A1;21B7-8	*Df(2L)net62*	21A1;21B4-5	E			
	Df(2L)TE21A	21A1;21B4-6	E			
	Df(2L)net-PMC	21A1;21B6-7	E			
Df(2L)ast2	*Df(2L)S3*	21D2-3;21F2-22A1	S	*dbe[k05428]*	21D4-E1	/
21D1-2;22B2-3	*Df(2L)ast4/*	21D1-2;21E1-2	S	*S[1]*	21E2-3	<E
	Df(2L)ast6	21E1-2;21E2-3	/	*capt[E593]*	21F2	/
				capt[E636]	21F2	/
Df(2L)E110				*ee[1]*	25A3-27F2	E
25F3-26A1;26D3-11				*wee[DS1]*	27C4	S
				nop5, xl6xl6[k00230]	27C4-5	S
Df(2L)Dwee-delta5	*Df(2L)J-H*	27C2-9;28B3-4				
27A;28A	*Df(2L)Dwee1-W05*	27C2-3;27C4-5				
	Df(2L)spd[j2]	27C1-2;28A	S			
	Df(2L)spd	26A6-B1;27E1-3;28B1-3				
	Df(2L)wg-CX3	27F1-3;28A	L	*Wingless*	27F1	E
	Df(2L)DE	27E1-2;28A1-2	/	*wg[cx4]*		
	Df(2L)RF	27E3-F;28B3-4				
Df(2L)J39	*Df(2L)J77*	31C;31E	E			
31C;32D1-E5				*daughterless-like*	31F1-32D4	E
				dal[1]		
Df(2L)TE35BC-24	*Df(2L)A48*	35B2-3;35D5-7	S>			
35B4-6;35F1-7	*Df(2L)TE35BC-7*	35B3;35B9-10				
	Df(2L)A220	35B1-2;35B9	/			

Table B.3 Break down of suppressive regions within Chromosome 2

Deficiency	Smaller deficiencies within suppressive region	Locus	Effect on *GMR;UA SDACK RE*	Gene (Allele) within suppressive regions	Locus	Effect on *GMR;UA SDACK RE*
	Df(2L)nNxF1	35B3;35B10	E			
	Df(2L)osp29	35B1-3;35E6	S			
	Df(2L)rd9	35C2;35C5	S	*esg[35Ce-1]*		
	Df(2L)osp18	35B2;35C4-5	/	*Reduced*	35C3+	S>
				rd[1]		
				Reduced	35C3+	S>
				Rd[s]		
				Alcohol dehydrogenase Adh[n10]; guftagu gft[2]	35B3; 35C3-D1	/
				ms(2)35Ci	35D1	S>
				Escargot	35D2	/
Df(2L)TW137	*Df(2L)T317*	36C;36E-F	/			
36C2-4;37B9-C1	*Df(2L)M36F-S5*	36D1-E1;36F1-37A1, 36F + ?	E			
	Df(2L)OD15	36F7-9;37B9-C1	/			
Df(2R)X1	*Df(2R)X3*	46C;46E1-2	/			
46C;47A1	*Df(2R)12*	46E1-F11;47A13-B14	/			
Df(2R)en-A	*Df(2R)en-B*	47E3;48A4	/			
47D3;48B2	*Df(2R)en-SFX31*	048A-B	/			
	Df(2R)stan2	46F1-2;47D1-2	E>			
	Df(2R)E3363	47A;47F	E>			
Df(2R)vg135	*No further breakdown*		S			
49A;49E1-2;47F4-18						
Df(2R)BSC11	*Df(2R)trix*	51A1-2;51B6	S	*Lobe L[2]*	51A2	S
50E6-F1;51E2-4				*Auk auk[2R-4]*	51A2-B6	/
				Additional sex combs Asx[XF23]	51A4	vary

Table B.3 Break down of suppressive regions within Chromosome 2

Deficiency	Smaller deficiencies within suppressive region	Locus	Effect on *GMR;UA SDACK RE*	Gene (Allele) within suppressive regions	Locus	Effect on *GMR;UA SDACK RE*
				Asc[1]	51A4	E
				Xenicid xen[72-3]	51A5-C1	S
				Transformer2 tra2[ts1]	51B6	E
Df(2R)Pcl7B 54E8-F1;55B9-C1	*Df(2R)Pcl11B*	54F6-55A1;55C1-3	/			
	Df(2R)RM2-1	54F2;56A1	S			
Df(2R)017 56F5;56F15	*Df(2R)173*	56F	S>			
	Df(2R)min	56F8-17;56F8-17	E			
Df(2R)AA21 56F9-17;57D11-12	*No further breakdown*		S			
Df(2R)59AD 59A1-3;59D1-4	*No further breakdown*					
Df(2R)bw-S46 59D8-11;60A7	*Df(2R)egl3*	59F1;59F5	/	*Takahe*	59D8-60B1	E
	Df(2R)egl2	59E;60A1	E	*tak[82-8]*		
				minus	59E1-2	/
				mi[1]		
				Abbreviated	59E2-F8	S
				abb[1]		
				Death caspase-1 Dcp-1[k05606];	5.90E+04	/
				Apontic, apt[k15608]	59F1-4	S
				Retained retn[RO44]	59F5	/
				Retained	59F5	/
				retn[02535]		
				egalitarian	59F7	/
				egl[1286]		
				Glassbottombo at gbb1	60A3-4	/

Table B.3 Break down of suppressive regions within Chromosome 2

Deficiency	Smaller deficiencies within suppressive region	Locus	Effect on *GMR;UA SDACK RE*	Gene (Allele) within suppressive regions	Locus	Effect on *GMR;UA SDACK RE*
				Glassbottombo at gbb4	60A3-4	/
				benign gonial cell neoplasm	60A4	E
				bgcn[1]		
				ken and barbie	60A6-7	/
				ken[02970]		
				gek[KG03105]	60B9-10	E
				genghis khan	60B9-10	/
				gek[09373]		
				enoki mushroom	60B10	/
				enok[1]		
				enoki mushroom	60B10	E
				enok[2]		
				Dopamine N acetyltransfer ase	60B12-C1	S>
				Dat[lo]		
				Spaghetti	60B12-13	S>
				spag[k12101]		
				ß-Tubulin at 60D	60C6	E
				betaTub60D[2]		
				pin	60C6-D1	/
				Pin[2]		
				piopio	60C6-D11	/
				pio[2R-16]		
				eyes closed	60D1-2	E
				eyc[04012b]		
Df(2R)106	*No further breakdown*					
60A3;60A7						
Df(2R)Px2	*No further breakdown*					
60C5-6;60D9-10						

Table B.4 Break down of suppressive regions within Chromosome 3

Deficiency	Smaller deficiencies within suppressive region	Locus	Effect on *GMR;UAS DACK RE*	Gene (Allele) within suppressive regions	Locus	Effect on *GMR;UAS DACK RE*
Df(3L)66C-G28	Df(3L)66C-I65	66C7-10	S	*N-myristoyl transferase*	66B10-11	/
66B8-9;66C9-10				*Nmt[j1C7]*		
Df(3L)Rdl-2, e[1]				*L(3)L0139[L0139]*	66C1-2	/
66F5				*pbl[09645]*	66A17-18	/
Df(3L)vin7				*Abdominal*	66D10-F5	/
68C8-11;69B4-5				*abd[2]*		
				Resistant to dieldrin	67A1	/
				Rdl[MD-RR]		
				Resistant to dieldrin	67A1	S
				Rdl[1]		
				P{ry[+t7.2]=PZ}l(3)05408[05408]	068C12-13	E
				lethal (3) 68Dc	68D3--6	/
				l(3)68Dc[2]		
				Cyclin A	6.80E+02	E
				CycA[03946]		
				Cyclin A	6.80E+02	E
				CycA[C8LR1]		
				rolling pebbles	68F1-68F3	E
				rols[08232]		
				L(3)j2D3[j2D3]	68F2-68F3	/
				Neurexin IV	68F6-68F7	E
				l(3)05088[05088]	69A1-3	E
				approximated	69A3-4	E
				app[61e]		
				Approximated app[1]	69A3-4	E
				Eyegone	69C2	E
Df(3L)BSC10				*eyg[1]*		
69D4-5;69F5-7				*sticky*	69C3-70F4	E
				sti[3]		

Table B.4 Break down of suppressive regions within Chromosome 3

Deficiency	Smaller deficiencies within suppressive region	Locus	Effect on *GMR;UAS DACK RE*	Gene (Allele) within suppressive regions	Locus	Effect on *GMR;UA SDACK RE*
				Autophagy-specific gene 1 Atg1[00305]	69E2-4	S
				Ribosomal protein S12 RpS12[s2783]	69F5-6	/
				Sneaky snky[1]	69F3-70C4	S
Df(3L)Ly				*Tartan*	70A1	E
70A2-3;70A5-6				*trn[S064117]*		
Df(3L)BK10				*l(3)71CDc*	71C-D	/
71C;71F				*l(3)71CDc[E7]*		
				l(3)71CDb	71C-D	E
				(3)71CDb[E36]		
				l(3)71CDb	71C-D	/
				l(3)71CDb[E65]		
				l(3)71CDa	71C-D	E
				l(3)71CDa[E3]		
				l(3)71CDa	71C-D	/
				l(3)71CDa[E71]		
				marionnettemrn [3]	71C3-E5	/
				drop out dop[1]	71C3-E5	S
				l(3)s1754	71D1-2	/
				l(3)s1754[s1754 Cyclic-AMP response element binding protein A CrebA[03576]	71D1-2	E
				RhoGAP71ERhoGAP71E[j6B9]	71E1-2	E
Df(3L)st-f13	Df(3L)st-e4	72D5-10;73A5-8	E	*thread th[1]*	72D1	E
72C1-D1;73A3-4				*thread th[4]*	72D1	/

Table B.4 Break down of suppressive regions within Chromosome 3

Deficiency	Smaller deficiencies within suppressive region	Locus	Effect on *GMR;UAS DACK RE*	Gene (Allele) within suppressive regions	Locus	Effect on *GMR;UA SDACK RE*
				Notum *Notum[72Da-1]*	72C3-D1	S
				Notum *Notum[I6]*	72C3-D1	/
				TBP-associated factor 4 *Taf4[1]*	72D7-8	S
				Zn72D *Zn72D[BG02677]*	72D6-7	S
				Phosphogluconate mutase *Pgm[nGB1]*	72D8	/
				Phosphogluconate mutase *Pgm[6tr]*	72D8	/
				male sterile (3) 72D *ms(3)72D[03957]*	72D1-72D12	E
				ascute *as[hg]*	72D12--73C4	S
				argos *argos[W11]*	73A2	S
				argos *argos [05845]*	73A2	E
				Argos[delta 7]	73A2	E
				bulge *bul[D]*	73A2	E
				bulge *bul[6d7]*	73A2	S
Df(3L)81k19 *73A3;74F*	Df(3L)st-j7	73A2;73B2	/			
	Df(3L)st7	73A3-4;74A3	S (good)			
Df(3L)W10 *75A6-7;75C1-2*	No further breakdown					
Df(3L)kto2 *76B1-2;76D5*	Df(3L)XS2182	76B;76F	S			

Table B.4 Break down of suppressive regions within Chromosome 3

Deficiency	Smaller deficiencies within suppressive region	Locus	Effect on *GMR;UAS DACK RE*	Gene (Allele) within suppressive regions	Locus	Effect on *GMR;UA SDACK RE*
Df(3L)XS533 *76B4;77B*						
Df(3L)ME107 *77F3;78C8-9*	Df(3L)Pc-MK	78A2;78C9	S>	*Integrin linked kinase* *Ilk[1]*	78C2	/
Df(3L)31A *78A;78E, 78D;79B*				*Skuld* *skd[L7062]*	78A2-5	E
Df(3L)HD1	Df(3L)Ten-m-AL1	79E1-4;79E3-8	S	*Rotund*	84D3	S>
79D3-E1;79F3-6	Df(3R)Dfd13	83E3;84A4-5	S	*rn[roe-1]*		
Df(3R)WIN11 *83E1-2;84A4-5*	Df(3R)p40	084E08-09;085B06, 064;090, 055;075	/	*Antennapedia* *Antp[18]*	84A6-B2	E
Df(3R)p-XT103 *85A2;85C1-2*	Df(3R)p25	85A3;85B1	E			
Df(3R)ea	Df(3R)red3l	87F12-14;88C1-3	S	*Aurora*	87A3	S
88E7-13;89A1	Df(3R)c(3)G-2	89A2;89A5	>	*aur[87Ac-3]*		
				l(3)L1231[L1231]	88C9-89C7	E
				supernova *spno[rev6]*	89A1	E
				supernova *spno[A42]*	89A1	E
				l(3)05057[05057]	89A1-2	/
				l(3)08724	89A1-B4	
Df(3R)P115 *89B7-8;89E7;20*	Df(3R)Spf	89B20-22;89D9-E1	S	*ms(3)08724;*	89B1-89B3;	E
Df(3R)Cha7	Df(3R)07280	91B2;91C1	/	*nanos*	91F7	S
90F1-F4;91F5	Df(3R)BX5	91B1-2;91D1-2	E	*nos[L7]*		

Table B.4 Break down of suppressive regions within Chromosome 3

Deficiency	Smaller deficiencies within suppressive region	Locus	Effect on *GMR;UAS DACK RE*	Gene (Allele) within suppressive regions	Locus	Effect on *GMR;UA SDACK RE*
	Df(3R)Dl-M2	91C7-D1;92A1	S			
	Df(3R)Dl-KX23	91C7-D3;92A5-8	E			
Df(3R)23D1 94A3-4;94D1-4	No further breakdown					
Df(3R)mbc-R1 95A5-7;95D6-11	Df(3R)06624	95C1;95C7	/			

Table B.5 Genetic interactions between components of the EGFR signaling pathway and DACK.

Gene	Allele	Allele Class	*GMRGal4; UAS WT-ACK*
Egfr	*egfr^{t1}bw 1*	Hypomorph	E
	egfr^{f24}	Amorph	S
	egfr^{f2}	loss of function, amorph	E
	egfr^{E1}PinYt	Hypomorph	/
	egfr^{JE1}	Amorph, loss of function	/
	egfr^{1F26}	Temperature sensitive	E
	CO(f24)	Amorph	V
	Df(2R)top18A		/
Argos	*argos^{delta7}*	Loss of function, amorph	/
	argos^{rlt}	-	/
	argos^{05846}	-	>MS
	argos^{w11}	Hypomorph	>S
spi	*Spi^{1}*	Loss of function	>S
	spi^{s3547}	-	/
star	*S^{1}*	-	E
	s^{IIN}	Amorph	E
	s^{k09530}	-	/
polehole	*ph1^{12}*	Hypomorph, loss of function	E
	ph1^{7}	Loss of function, amorph	E
	ph1^{G0475w67c23}	-	Varies
sos	*Sos^{34Ea-6} Adhn4*	-	/
	Sco7 AdhnB	-	>E
	w67c23;Sos^{k05224}	-	/
ksr	*ksr^{s-627}*	-	E
	w1118ksrj5E2	-	V

Table B. 6 Genetic interactions between DACK and components of the Dpp signaling pathway.

Gene	Alleles	Allele Class	*GMRGal4; UAS WT-ACK*	*GMRGal4; UAS KD-ACK*
Zipper	zip^{1}	-	/	/
	$Df(2R)gsb\ zip^{IIX62}$	-	E	/M >EF
	$W^{1118}\ DF(2R)$	-	S	/
Dpp	$dpp^{s4}\ dpp^{d\text{-}ho}$	Loss of function, hypomorph	/	/
	Dpp^{d6}	Hypomorph	/	/
	dpp^{hr27}	Hypomorph	>E	/
Medea	*Med 1*	-	/	>EF
	Med23	-		/
	Med3	-	/	/
Mad	*mad12FRT40A*	Amorph, loss of function	>E	
Dsmurf	*Dsmurf*		>E	/
Punt	*put135*	Hypomorph, amorph	/	>E

Table B.7 Genetic interactions between DACK and different alleles.

Stock #		Genotype of deficiency line	Results of Cross with: GMRGal4;UAS-WTACKZF
		nejire	
10102*		$w^{1118}P\{EP\}nej^{EP950}$	supp based on sz, same morph
5292*		$y^1nej^{Q7}v^1f^1/Dp(1;Y)FF1,y^+/C(1)DX$, $y^1\ w^1\ f^1$	same
3728*		w* P{lacW}nejP/FM7c	same
		shi	
1328*		shi^1	enhanced
2248*		shi^2	large, enhanced
7068*		w^{1118} shi^1/FM6	same
		Pros	
		pros 17/Tm6 Tbhu	sl.enh(sz var in balanced)
3128		Df(3R)M-Kx1/TM3, Sb^1 Ser^1	no RE
		wasp	
430		w^{1118}; Df(3R)3450/TM6B, Tb^1	same
		wsp^3(17)/Tm6 Tbhu	sup.(larger, bal all blk)
		w;$stewsp^1$/TM6 Tbhu	sl.sup
		Huntington	
	**	dhH #9(x)	same
	**	dhH #1(III)	same
		Longitudinals lacking	
10946		lola	same
		Starry night	
6967		$stan^{frz3}$	no change (same)
6969		$stan^{192}$	same to sl. Sup based on size
		Schnurri	
10478		shn^{k00401}	same
		Three rows	
3262		thr^1	same
6275		thr^3	same
10685		$thr^{k07805b}$	same

Table B.8 Genetic interactions between DACK and lab stocks

Gene/Deficiency	Effect on *GMRGal4; UAS WT-ACK*
shn	E
put135	S
DCIP4 (37-1)	/
17-1 UAS-LD14951(DCIP4)/cyo	/
pak6	/
insulin R	E
pnr	/
myoblastcity	/
w;src 42 a jp45/sm1	/
wjΔ17/Δ17 (src64b null)	<S
w;10h/TM3Sb (src64B Df)	/
5605 dl(6b)/tm6sb	S
(dock) k13421/cyo	/
11385 d(dock 04723)/cyo	/
ywcdc 42^2	/
ywcdc42^5 19afrt	S
3075 wt52	S
Df(3L)GN19/TM3Sb	<SF/EM
5603 d(1)(rf)/6ksb	S
w;(uas-alpha ps1, wt)3,5	<SF
su(h)^2/cyo	S
wt tyc 38 II	S
w;uasp52c 57wt/cyo	<S
ymysm^2f^369	E
wif B4 frt/fm7c	<E
ymys^g1 f^frt1ba/fm7c	S

Legend: S: suppression of *GMRGAL4;UASDACK* rough eye phenotype. E: enhancement. >: slight. /: no obvious difference detected. M: males. F: females.

Comments: This screen was conducted by myself and one accompanying undergraduate student each semester. All of the crosses were scored by both myself and a student. Therefore all of the phenotypes were assessed blindly by at least one of us. In most cases, the siblings from each cross that contained balancers and expressed DACK in the eye, were used as control. However, in some cases, the DACK rough eyed flies heterozygous for a mutation or deficiency were compared to both the parental and sibling (containing the balancer) rough eyed flies.

Other alleles that were tested that may not be represented here, including crosses to UAS-transgenes of particular genes, as well as ones for the Dpp and EGFR pathways. The result of such alleles that were separate from the Df screen can be found in the many books labelled "Df screen." In these books, description of each phenotype comparison

and details of each allele/deficiency tested can be found, as well as the crossing schemes and the Bloomington stock numbers. Helpful guides are the student reports on the Df screen. Many of the Df lines were rebalanced over *TM3Sb* or *CyO* using the lab balancer stocks before they were crossed to *GMR;DACK* flies. There also exists a complete excel file containing all of the different stocks used and their effect on the DACK induced rough eye. As well there is an incomplete schematic chromosome map showing regions of each chromosome that enhanced, suppressed, or had no effect on the DACK induced rough eye phenotype.

REFERENCE LIST

Abram, C. L. and Courtneidge, S. A. (2000). Src family tyrosine kinases and growth factor signalling. *Exp. Cell Res.* **254**, 1-13.

Adams, M. D. Celniker, S. E. Holt, R. A. Evans, C. A. Gocayne, J. D. Amanatides, P. G. Scherer, S. E. Li, P. W. Hoskins, R. A. Galle, R. F. et al. (2000). The genome sequence of Drosophila melanogaster. *Science* **287**, 2185-95.

Adams, M. D. and Sekelsky, J. J. (2002). From sequence to phenotype: reverse genetics in Drosophila melanogaster. *Nat Rev Genet* **3**, 189-98.

Adler, P. N., Liu, J. and Charlton, J. (2000). Cell size and the morphogenesis of wing hairs in Drosophila. *Genesis* **28**, 82-91.

Ahmed, I., Calle, Y., Sayed, M. A., Kamal, J. M., Rengaswamy, P., Manser, E., Meiners, S. and Nur, E. K. A. (2004). Cdc42-dependent nuclear translocation of non-receptor tyrosine kinase, ACK. *Biochem Biophys Res Commun* **314**, 571-9.

Arai, R. and Mabuchi, I. (2002). F-actin ring formation and the role of F-actin cables in the fission yeast Schizosaccharomyces pombe. *J Cell Sci* **115**, 887-98.

Araujo, H., Negreiros, E. and Bier, E. (2003). Integrins modulate Sog activity in the Drosophila wing. *Development* **130**, 3851-64.

Arquier, N., Perrin, L., Manfruelli, P. and Semeriva, M. (2001). The *Drosophila* tumor suppressor gene *lethal(2)giant larvae* is required for the emission of the Decapentaplegic signal. *Development* **128**, 2209-2220.

Ashburner, M. (1989). Drosophila: A Laboratory Manual. Cold Spring Harbor, NY: Cold Spring Harbor Laboratory Press.

Aspenstrom, P. (1997). A Cdc42 target protein with homology to the non-kinase domain of FER has a potential role in regulating the actin cytoskeleton. *Curr Biol* **7**, 479-87.

Barrios-Rodiles, M., Brown, K. R., Ozdamar, B., Bose, R., Liu, Z., Donovan, R. S., Shinjo, F., Liu, Y., Dembowy, J., Taylor, I. W. et al. (2005). High-throughput mapping of a dynamic signalling network in mammalian cells. *Science* **307**, 1621-5.

Bellen, H. J., Levis, R.W., Liao, G., He, Y., Carlson, J.W., Tsang, G., Evans-Holm, M., Hiesinger, P.R., Schulze, K.L., Rubin, G.M., Hoskins, R.A., and Spradling, A.C. (2004). The BDGP gene disruption project: single transposon insertions associated with 40% of Drosophila genes. *Genetics, in press.*

Blondel, M., Bach, S., Bamps, S., Dobbelaere, J., Wiget, P., Longaretti, C., Barral, Y., Meijer, L. and Peter, M. (2005). Degradation of Hof1 by SCF(Grr1) is important for actomyosin contraction during cytokinesis in yeast. *Embo J* **24**, 1440-52.

Bogdan, S., Grewe, O., Strunk, M., Mertens, A. and Klambt, C. (2004). Sra-1 interacts with Kette and Wasp and is required for neuronal and bristle development in Drosophila. *Development* **131**, 3981-9.

Bogdan, S., Stephan, R., Lobke, C., Mertens, A. and Klambt, C. (2005). Abi activates WASP to promote sensory organ development. *Nat Cell Biol* **7**, 977-84.

Brand, A. H. and Perrimon, N. (1993). Targeted gene expression as a means of altering cell fates and generating dominant phenotypes. *Development* **118**, 401-415.

Burbelo, P. D., Drechsel, D. and Hall, A. (1995). A conserved binding motif defines numerous candidate target proteins for both Cdc42 and Rac GTPases. *J Biol Chem* **270**, 29071-29074.

Carlier, M. F., Le Clainche, C., Wiesner, S. and Pantaloni, D. (2003). Actin-based motility: from molecules to movement. *Bioessays* **25**, 336-45.

Carnahan, R. H. and Gould, K. L. (2003). The PCH family protein, Cdc15p, recruits two F-actin nucleation pathways to coordinate cytokinetic actin ring formation in Schizosaccharomyces pombe. *J Cell Biol* **162**, 851-62.

Chitu, V., Pixley, F. J., Macaluso, F., Larson, D. R., Condeelis, J., Yeung, Y.-G. and Stanley, E. R. (2005). The PCH Family Member MAYP/PSTPIP2 Directly Regulates F-Actin Bundling and Enhances Filopodia Formation and Motility in Macrophages. *Mol. Biol. Cell* **16**, 2947-2959.

Clemens, J. C., Worby, C. A., Simonson-Leff, N., Muda, M., Maehama, T., Hemmings, B. A. and Dixon, J. E. (2000). Use of double-stranded RNA interference in Drosophila cell lines to dissect signal transduction pathways. *Proc Natl Acad Sci U S A* **97**, 6499-503.

Cooley, L. and Theurkauf, W. E. (1994). Cytoskeletal functions during Drosophila oogenesis. *Science* **266**, 590-6.

Cote, J. F., Chung, P. L., Theberge, J. F., Halle, M., Spencer, S., Lasky, L. A. and Tremblay, M. L. (2002). PSTPIP is a substrate of PTP-PEST and serves as a scaffold guiding PTP-PEST toward a specific dephosphorylation of WASP. *J Biol Chem* **277**, 2973-86.

Coyle, I. P., Koh, Y. H., Lee, W. C., Slind, J., Fergestad, T., Littleton, J. T. and Ganetzky, B. (2004). Nervous wreck, an SH3 adaptor protein that interacts with Wsp, regulates synaptic growth in Drosophila. *Neuron* **41**, 521-34.

Crawford, J. M., Harden, N., Leung, T., Lim, L. and Kiehart, D. P. (1998). Cellularization in Drosophila melanogaster is disrupted by the inhibition of rho activity and the activation of Cdc42 function. *Dev Biol* **204**, 151-64.

Das, P., Maduzia, L. L., Wang, H., Finelli, A. L., Cho, S. H., Smith, M. M. and Padgett, R. W. (1998). The Drosophila gene Medea demonstrates the requirement for different classes of Smads in dpp signalling. *Development* **125**, 1519-28.

Derynck, R. and Zhang, Y. E. (2003). Smad-dependent and Smad-independent pathways in TGF-beta family signalling. *Nature* **425**, 577-84.

Dobens, L. L. and Raftery, L. A. (2000). Integration of epithelial patterning and morphogenesis in *Drosophila* ovarian follicle cells. *Dev Dyn* **218**, 80-93.

Dorfman, R. and Shilo, B. (2001). Biphasic activation of the BMP pathway patterns the Drosophila embryonic dorsal region. *Development* **128**, 965-972.

Drysdale, R. A., Crosby, M.A. and the FlyBase Consortium. (2005). FlyBase: genes and gene models. *Nucleic Acids Res* **33**, D390-D395.

Eaton, S., Wepf, R. and Simons, K. (1996). Roles for Rac1 and Cdc42 in planar polarization and hair outgrowth in the wing of *Drosophila*. *J Cell Biol* **135**, 1277-89.

Echard, A., Hickson, G. R., Foley, E. and O'Farrell, P. H. (2004). Terminal cytokinesis events uncovered after an RNAi screen. *Curr Biol* **14**, 1685-93.

Edlund, S., Landstrom, M., Heldin, C.-H. and Aspenstrom, P. (2002). Transforming Growth Factor-beta -induced Mobilization of Actin Cytoskeleton Requires Signalling by Small GTPases Cdc42 and RhoA. *Mol. Biol. Cell* **13**, 902-914.

Edlund, S., Landstrom, M., Heldin, C.-H. and Aspenstrom, P. (2004). Smad7 is required for TGF-{beta}-induced activation of the small GTPase Cdc42. *J Cell Sci* **117**, 1835-1847.

Fankhauser, C., Reymond, A., Cerutti, L., Utzig, S., Hofmann, K. and Simanis, V. (1995). The S. pombe cdc15 gene is a key element in the reorganization of F-actin at mitosis. *Cell* **82**, 435-44.

Flynn, P., Mellor, H., Palmer, R., Panayotou, G. and Parker, P. J. (1998). Multiple interactions of PRK1 with RhoA. Functional assignment of the Hr1 repeat motif. *J Biol Chem* **273**, 2698-705.

Foe, V. E., Field, C. M. and Odell, G. M. (2000). Microtubules and mitotic cycle phase modulate spatiotemporal distributions of F-actin and myosin II in Drosophila syncytial blastoderm embryos. *Development* **127**, 1767-87.

Foe, V. E., Odell, G.M., and Edgar, B.A. (1993). Mitosis and Morphogenesis in the *Drosophila* embryo: Point and Counterpoint. In *The Development of Drosophila melanogaster*, vol. I (eds M. Bate and M. Martinez-Arias), pp. 149-300. Cold Spring Harbor.

Fuchs, U., Rehkamp, G., Haas, O. A., Slany, R., Konig, M., Bojesen, S., Bohle, R. M., Damm-Welk, C., Ludwig, W. D., Harbott, J. et al. (2001). The human formin-binding protein 17 (FBP17) interacts with sorting nexin, SNX2, and is an MLL-fusion partner in acute myelogeneous leukemia. *Proc Natl Acad Sci U S A* **98**, 8756-61.

Fujita, H., Katoh, H., Ishikawa, Y., Mori, K. and Negishi, M. (2002). Rapostlin is a novel effector of Rnd2 GTPase inducing neurite branching. *J Biol Chem* **277**, 45428-34.

Genova, J. L., Jong, S., Camp, J. T. and Fehon, R. G. (2000). Functional analysis of *Cdc42* in actin filament assembly, epithelial morphogenesis, and cell signalling during *Drosophila* development. *Dev Biol* **221**, 181-194.

Glise, B., Bourbon, H. and Noselli, S. (1995). *hemipterous* encodes a novel Drosophila MAP kinase kinase, required for epithelial cell sheet movement. *Cell* **83**, 451-461.

Glise, B. and Noselli, S. (1997). Coupling of Jun amino-terminal kinase and Decapentaplegic signalling pathways in *Drosophila* morphogenesis. *Genes Dev* **11**, 1738-1747.

Gonzalez-Gaitan, M. (2003). SIGNAL DISPERSAL AND TRANSDUCTION THROUGH THE ENDOCYTIC PATHWAY. *Nature Reviews Molecular Cell Biology* **4**, 213-224.

Greenspan, R. J. (1997). Fly Pushing,The Theory and Practice of *Drosophila* Genetics. Cold Spring Harbor laboratory.

Gutzeit, H. O. and Haas-Assenbaum, A. (1991). The somatic envelopes around the germ-line cells of polytrophic insect follicles: structural and functional aspects. *Tissue Cell* **23**, 853-65.

Harden, N. (2002). Signalling pathways directing the movement and fusion of epithelial sheets: lessons from dorsal closure in *Drosophila*. *Differentiation* **70**, 181-203.

Harden, N., Lee, J., Loh, H. Y., Ong, Y. M., Tan, I., Leung, T., Manser, E. and Lim, L. (1996). A *Drosophila* homolog of the Rac- and Cdc42-activated serine/threonine kinase PAK is a potential focal adhesion and focal complex protein that colocalizes with dynamic actin structures. *Mol Cell Biol* **16**, 1896-1908.

Harden, N., Ricos, M., Ong, Y. M., Chia, W. and Lim, L. (1999). Participation of small GTPases in dorsal closure of the *Drosophila* embryo: distinct roles for Rho subfamily proteins in epithelial morphogenesis. *J Cell Sci* **112**, 273-284.

Hawley, R. J. and Waring, G. L. (1988). Cloning and analysis of the dec-1 female-sterile locus, a gene required for proper assembly of the Drosophila eggshell. *Genes Dev* **2**, 341-9.

Hinz, U., Giebel, B. and Campos-Ortega, J. A. (1994). The basic-helix-loop-helix domain of Drosophila lethal of scute protein is sufficient for proneural function and activates neurogenic genes. *Cell* **76**, 77-87.

Ho, H. Y., Rohatgi, R., Lebensohn, A. M., Le, M., Li, J., Gygi, S. P. and Kirschner, M. W. (2004). Toca-1 mediates Cdc42-dependent actin nucleation by activating the N-WASP-WIP complex. *Cell* **118**, 203-16.

Holbert, S., Dedeoglu, A., Humbert, S., Saudou, F., Ferrante, R. J. and Neri, C. (2003). Cdc42-interacting protein 4 binds to huntingtin: neuropathologic and biological evidence for a role in Huntington's disease. *Proc Natl Acad Sci U S A* **100**, 2712-7.

Hoodless, P. A., Haerry, T., Abdollah, S., Stapleton, M., O'Connor, M. B., Attisano, L. and Wrana, J. L. (1996). MADR1, a MAD-related protein that functions in BMP2 signalling pathways. *Cell* **85**, 489-500.

Hopmann, R., Cooper, J. A. and Miller, K. G. (1996). Actin organization, bristle morphology, and viability are affected by actin capping protein mutations in Drosophila. *J Cell Biol* **133**, 1293-305.

Hopmann, R. and Miller, K. G. (2003). A balance of capping protein and profilin functions is required to regulate actin polymerization in Drosophila bristle. *Mol Biol Cell* **14**, 118-28.

Hutson, M. S., Tokutake, Y., Chang, M. S., Bloor, J. W., Venakides, S., Kiehart, D. P. and Edwards, G. S. (2003). Forces for morphogenesis investigated with laser microsurgery and quantitative modeling. *Science* **300**, 145-9.

Insall, R. H. and Machesky, L. M. (2004). Regulation of WASP: PIP2 Pipped by Toca-1? *Cell* **118**, 140-1.

Ip, Y. T. and Davis, R. J. (1998). Signal transduction by the c-Jun N-terminal kinase (JNK)--from inflammation to development. *Curr Opin Cell Biol* **10**, 205-19.

Jacinto, A., Wood, W., Balayo, T., Turmaine, M., Martinez-Arias, A. and Martin, P. (2000). Dynamic actin-based epithelial adhesion and cell matching during *Drosophila* dorsal closure. *Curr Biol* **10**, 1420-1426.

Jacinto, A., Wood, W., Woolner, S., Hiley, C., Turner, L., Wilson, C., Martinez-Arias, A. and Martin, P. (2002). Dynamic analysis of actin cable function during Drosophila dorsal closure. *Curr Biol* **12**, 1245-50.

Jackson, S. M. and Berg, C. A. (1999). Soma-to-germline interactions during Drosophila oogenesis are influenced by dose-sensitive interactions between cut and the genes cappuccino, ovarian tumor and agnostic. *Genetics* **153**, 289-303.

Johnson, D. I. (1999). Cdc42: An essential Rho-type GTPase controlling eukaryotic cell polarity. *Microbiol Mol Biol Rev* **63**, 54-105.

Joseph, B. D. (2002). GAL4 system in <I>drosophila</I>: A fly geneticist's swiss army knife. *Genesis* **34**, 1-15.

Kamioka, Y., Fukuhara, S., Sawa, H., Nagashima, K., Masuda, M., Matsuda, M. and Mochizuki, N. (2004). A Novel Dynamin-associating Molecule, Formin-binding Protein 17, Induces Tubular Membrane Invaginations and Participates in Endocytosis. *J Biol Chem* **279**, 40091-40099.

Kessels, M. M. and Qualmann, B. (2002). Syndapins integrate N-WASP in receptor-mediated endocytosis. *Embo J* **21**, 6083-94.

Kessels, M. M. and Qualmann, B. (2004). The syndapin protein family: linking membrane trafficking with the cytoskeleton. *J Cell Sci* **117**, 3077-3086.

Larocca, M. C., Shanks, R. A., Tian, L., Nelson, D. L., Stewart, D. M. and Goldenring, J. R. (2004). AKAP350 Interaction with cdc42 Interacting Protein 4 at the Golgi Apparatus. *Mol. Biol. Cell* **15**, 2771-2781.

Lecuit, T. (2004). Junctions and vesicular trafficking during Drosophila cellularization. *J Cell Sci* **117**, 3427-33.

Lee, W.-L., Bezanilla, M. and Pollard, T. D. (2000). Fission Yeast Myosin-I, Myo1p, Stimulates Actin Assembly by Arp2/3 Complex and Shares Functions with WASp. *J Cell Biol* **151**, 789-800.

Lin, Q., Lo, C. G., Cerione, R. A. and Yang, W. (2002). The Cdc42 target ACK2 interacts with sorting nexin 9 (SH3PX1) to regulate epidermal growth factor receptor degradation. *J Biol Chem* **277**, 10134-8. Epub 2002 Jan 17.

Lippincott, J. and Li, R. (2000). Involvement of PCH family proteins in cytokinesis and actin distribution. *Microsc Res Tech* **49**, 168-72.

Martin-Blanco, E., Gampel, A., Ring, J., Virdee, K., Kirov, N., Tolkovsky, A. M. and Martinez-Arias, A. (1998). *puckered* encodes a phosphatase that mediates a

feedback loop regulating JNK activity during dorsal closure in *Drosophila*. *Genes Dev* **12**, 557-570.

Martinez-Arias, A. (1993). Development and patterning of the larval epidermis of Drosophila. In *The Development of Drosophila melanogaster*, (eds M. Bate and M. Martinez-Arias). Cold Spring Harbor.: Cold Spring Harbor Laboratory Press.

Mazumdar, A. and Mazumdar, M. (2002). How one becomes many: blastoderm cellularization in Drosophila melanogaster. *Bioessays* **24**, 1012-22.

Misra, S., Crosby, M., Mungall, C., Matthews, B., Campbell, K., Hradecky, P., Huang, Y., Kaminker, J., Millburn, G., Prochnik, S. et al. (2002). Annotation of the Drosophila melanogaster euchromatic genome: a systematic review. *Genome Biology* **3**, research0083.1 - 0083.22.

Mlodzik, M. (1999). Planar polarity in the Drosophila eye: a multifaceted view of signalling specificity and cross-talk. *Embo J* **18**, 6873-9.

Modregger, J., DiProspero, N. A., Charles, V., Tagle, D. A. and Plomann, M. (2002). PACSIN 1 interacts with huntingtin and is absent from synaptic varicosities in presymptomatic Huntington's disease brains. *Hum Mol Genet* **11**, 2547-58.

Moon, S. Y. and Zheng, Y. (2003). Rho GTPase-activating proteins in cell regulation. *Trends Cell Biol* **13**, 13-22.

Morisato, D. and Anderson, K. V. (1995). Signalling pathways that establish the dorsal-ventral pattern of the *Drosophila* embryo. *Annu. Rev. Genet.* **29**, 371-399.

Murphy, A. M. and Montell, D. J. (1996). Cell type-specific roles for Cdc42, Rac, and RhoL in *Drosophila* oogenesis. *J Cell Biol* **133**, 617-630.

Naqvi, S. N., Feng, Q., Boulton, V. J., Zahn, R. and Munn, A. L. (2001). Vrp1p functions in both actomyosin ring-dependent and Hof1p-dependent pathways of cytokinesis. *Traffic* **2**, 189-201.

Newfeld, S. J., Wisotzkey, R. G. and Kumar, S. (1999). Molecular evolution of a developmental pathway: phylogenetic analyses of transforming growth factor-beta family ligands, receptors and Smad signal transducers. *Genetics* **152**, 783-95.

Nezis, I. P., Stravopodis, D. J., Papassideri, I., Robert-Nicoud, M. and Margaritis, L. H. (2000). Stage-specific apoptotic patterns during Drosophila oogenesis. *Eur J Cell Biol* **79**, 610-20.

O'Connor, M. and Chia, W. (1993). P Element-Mediated Germ-Line Transformation of *Drosophila*. In *Transgenesis Techniques: Priniciples and Protocols*, vol. 18 (eds D. Murphy and D. A. Carter), pp. 75-85. Totowa, NJ: Humana Press.

Ozdamar, B., Bose, R., Barrios-Rodiles, M., Wang, H. R., Zhang, Y. and Wrana, J. L. (2005). Regulation of the polarity protein Par6 by TGFbeta receptors controls epithelial cell plasticity. *Science* **307**, 1603-9.

Persson, U., Izumi, H., Souchelnytskyi, S., Itoh, S., Grimsby, S., Engstrom, U., Heldin, C. H., Funa, K. and ten Dijke, P. (1998). The L45 loop in type I receptors for TGF-beta family members is a critical determinant in specifying Smad isoform activation. *FEBS Lett* **434**, 83-7.

Preston, C. R., Sved, J. A. and Engels, W. R. (1996). Flanking duplications and deletions associated with P-induced male recombination in Drosophila. *Genetics* **144**, 1623-38.

Pufall, M. A. and Graves, B. J. (2002). AUTOINHIBITORY DOMAINS: Modular Effectors of Cellular Regulation. *Annual Review of Cell and Developmental Biology* **18**, 421-462.

Rechsteiner, M. and Rogers, S. W. (1996). PEST sequences and regulation by proteolysis. *Trends Biochem Sci* **21**, 267-71.

Ricos, M. G., Harden, N., Sem, K. P., Lim, L. and Chia, W. (1999). Dcdc42 acts in TGF-β signalling during *Drosophila* morphogenesis: distinct roles for the Drac1/JNK and Dcdc42/TGF-β cascades in cytoskeletal regulation. *J Cell Sci* **112**, 1225-1235.

Riesgo-Escovar, J. R. and Hafen, E. (1997). Common and distinct roles of DFos and DJun during *Drosophila* development. *Science* **278**, 669-672.

Riesgo-Escovar, J. R., Jenni, M., Fritz, A. and Hafen, E. (1996). The *Drosophila* Jun-N-terminal kinase is required for cell morphogenesis but not for DJun-dependent cell fate specification in the eye. *Genes Dev* **10**, 2759-2768.

Ring, J. M. and Martinez Arias, A. (1993). *puckered*, a gene involved in position-specific cell differentiation in the dorsal epidermis of the *Drosophila* larva. *Development Suppl.*, 251-259.

Roberts, D. B. (1998). *Drosophila*, A Practical Approach. New York: IRS press.

Rohatgi, R., Ho, H. Y. and Kirschner, M. W. (2000). Mechanism of N-WASP activation by CDC42 and phosphatidylinositol 4, 5-bisphosphate. *J Cell Biol* **150**, 1299-310.

Rorth, P. (1996). A modular misexpression screen in Drosophila detecting tissue-specific phenotypes. *Proc Natl Acad Sci U S A* **93**, 12418-22.

Rossman, K. L., Der, C. J. and Sondek, J. (2005). GEF means go: turning on RHO GTPases with guanine nucleotide-exchange factors. *Nat Rev Mol Cell Biol* **6**, 167-80.

Rubin, G. M., Hong, L., Brokstein, P., Evans-Holm, M., Frise, E., Stapleton, M. and Harvey, D. A. (2000). A Drosophila complementary DNA resource. *Science* **287**, 2222-4.

Sem, K. P., Zahedi, B., Tan, I., Deak, M., Lim, L. and Harden, N. (2002). ACK family tyrosine kinase activity is a component of Dcdc42 Signalling during dorsal closure in *Drosophila melanogaster. Mol Cell Biol* **22**, 3685-3697.

Shandala, T., Gregory, S. L., Dalton, H. E., Smallhorn, M. and Saint, R. (2004). Citron Kinase is an essential effector of the Pbl-activated Rho signalling pathway in Drosophila melanogaster. *Development* **131**, 5053-5063.

Shi, Y. and Massague, J. (2003). Mechanisms of TGF-beta signalling from cell membrane to the nucleus. *Cell* **113**, 685-700.

Sluss, H. K., Han, Z., Barrett, T., Davis, R. J. and Ip, Y. T. (1996). A JNK signal transduction pathway that mediates morphogenesis and an immune response in *Drosophila. Genes Dev* **10**, 2745-2758.

Sotillos, S. and Campuzano, S. (2000). DRacGAP, a novel Drosophila gene, inhibits EGFR/Ras signalling in the developing imaginal wing disc. *Development* **127**, 5427-38.

Soulard, A., Lechler, T., Spiridonov, V., Shevchenko, A., Shevchenko, A., Li, R. and Winsor, B. (2002). Saccharomyces cerevisiae Bzz1p is implicated with type I myosins in actin patch polarization and is able to recruit actin-polymerizing machinery in vitro. *Mol Cell Biol* **22**, 7889-906.

Spradling, A. C. (1993). Oogenesis. Cold Spring Harbor: Cold Spring Harbor Laboratory Press.

St Johnston, R. D., Hoffmann, F. M., Blackman, R. K., Segal, D., Grimaila, R., Padgett, R. W., Irick, H. A. and Gelbart, W. M. (1990). Molecular organization of the decapentaplegic gene in Drosophila melanogaster. *Genes Dev* **4**, 1114-27.

Stapleton, M., Liao, G., Brokstein, P., Hong, L., Carninci, P., Shiraki, T., Hayashizaki, Y., Champe, M., Pacleb, J., Wan, K. et al. (2002). The Drosophila Gene Collection: Identification of Putative Full-Length cDNAs for 70% of D. melanogaster Genes. *Genome Res.* **12**, 1294-1300.

Stark, K. A., Yee, G. H., Roote, C. E., Williams, E. L., Zusman, S. and Hynes, R. O. (1997). A novel alpha integrin subunit associates with βPS and functions in tissue morphogenesis and movement during *Drosophila* development. *Development* **124**, 4583-4594.

Strickland, L. I. and Burgess, D. R. (2004). Pathways for membrane trafficking during cytokinesis. *Trends Cell Biol* **14**, 115-8.

Tanentzapf, G., Smith, C., McGlade, J. and Tepass, U. (2000). Apical, lateral, and basal polarization cues contribute to the development of the follicular epithelium during *Drosophila* oogenesis. *J Cell Biol* **151**, 891-904.

Teo, M., Tan, L., Lim, L. and Manser, E. (2001). The tyrosine kinase ACK1 associates with clathrin-coated vesicles through a binding motif shared by arrestin and other adaptors. *J Biol Chem* **276**, 18392-8.

Thibault, S. T., Singer, M. A., Miyazaki, W. Y., Milash, B., Dompe, N. A., Singh, C. M., Buchholz, R., Demsky, M., Fawcett, R., Francis-Lang, H. L. et al. (2004). A complementary transposon tool kit for Drosophila melanogaster using P and piggyBac. *Nat Genet* **36**, 283-7.

Tian, L., Nelson, D. L. and Stewart, D. M. (2000). Cdc42-interacting protein 4 mediates binding of the Wiskott-Aldrich syndrome protein to microtubules. *J Biol Chem* **275**, 7854-61.

Van Aelst, L. and D'Souza-Schorey, C. (1997). Rho GTPases and signalling networks. *Genes Dev* **11**, 2295-2322.

Verheyen, E. and Cooley, L. (1994a). Looking at oogenesis. *Methods Cell Biol* **44**, 545-61.

Verheyen, E. M. and Cooley, L. (1994b). Profilin mutations disrupt multiple actin-dependent processes during Drosophila development. *Development* **120**, 717-28.

Virca, G. D., Northemann, W., Shiels, B. R., Widera, G. and Broome, S. (1990). Simplified northern blot hybridization using 5% sodium dodecyl sulfate. *Biotechniques* **8**, 370-1.

Wharton, K. A., Ray, R. P. and Gelbart, W. M. (1993). An activity gradient of decapentaplegic is necessary for the specification of dorsal pattern elements in the Drosophila embryo. *Development* **117**, 807-22.

Wilkes, M. C., Murphy, S. J., Garamszegi, N. and Leof, E. B. (2003). Cell-Type-Specific Activation of PAK2 by Transforming Growth Factor {beta} Independent of Smad2 and Smad3. *Mol Cell Biol* **23**, 8878-8889.

Wodarz, A., Hinz, U., Engelbert, M. and Knust, E. (1995). Expression of Crumbs confers apical character on plasma membrane domains of ectodermal epithelia of Drosophila. *Cell* **82**, 67-76.

Worby, C. A., Simonson-Leff, N., Clemens, J. C., Huddler, D., Jr., Muda, M. and Dixon, J. E. (2002). Drosophila Ack targets its substrate, the sorting nexin DSH3PX1, to

a protein complex involved in axonal guidance. *J Biol Chem* **277**, 9422-8. Epub 2001 Dec 28.

Xia, Y. and Karin, M. (2004). The control of cell motility and epithelial morphogenesis by Jun kinases. *Trends Cell Biol* **14**, 94-101.

Yang, W. and Cerione, R. A. (1997). Cloning and characterization of a novel Cdc42-associated tyrosine kinase, ACK-2, from bovine brain. *J Biol Chem* **272**, 24819-24.

Yang, W., Lin, Q., Guan, J. L. and Cerione, R. A. (1999). Activation of the Cdc42-associated tyrosine kinase-2 (ACK-2) by cell adhesion via integrin β_1. *J Biol Chem* **274**, 8524-30.

Yang, W., Lin, Q., Zhao, J., Guan, J. L. and Cerione, R. A. (2001a). The nonreceptor tyrosine kinase ACK2, a specific target for Cdc42 and a negative regulator of cell growth and focal adhesion complexes. *J Biol Chem* **276**, 43987-93.

Yang, W., Lo, C. G., Dispenza, T. and Cerione, R. A. (2001b). The Cdc42 target ACK2 directly interacts with clathrin and influences clathrin assembly. *J Biol Chem* **276**, 17468-73.

Yeung, Y. G., Soldera, S. and Stanley, E. R. (1998). A novel macrophage actin-associated protein (MAYP) is tyrosine-phosphorylated following colony stimulating factor-1 stimulation. *J Biol Chem* **273**, 30638-42.

Zeitlinger, J., Kockel, L., Peverali, F. A., Jackson, D. B., Mlodzik, M. and Bohmann, D. (1997). Defective dorsal closure and loss of epidermal *decapentaplegic* expression in *Drosophila fos* mutants. *Embo J* **16**, 7393-7401.